Chem Soc Rev

REVIEW ARTICLE

View Article Online
View Journal | View Issue

Anion receptor chemistry: highlights from 2011 and 2012

Cite this: *Chem. Soc. Rev.*, 2014, **43**, 205

Received 31st August 2013

DOI: 10.1039/c3cs60316d

www.rsc.org/csr

Philip A. Gale,* Nathalie Busschaert, Cally J. E. Haynes, Louise E. Karagiannidis and Isabelle L. Kirby

This review covers advances in anion complexation in the years 2011 and 2012. The review covers both organic and inorganic systems and also highlights the applications to which anion receptors can be applied such as self-assembly and molecular architecture, sensing, catalysis and anion transport.

Introduction

This review is the latest in a series covering recent advances in anion complexation.[1–4] It highlights the developments during 2011 and 2012 in the field of new receptors, modes of binding, transport and extraction of anions, and sensing mechanisms. It is not intended to be a comprehensive overview of the area. The structure of the review is primarily according to the dominant functional group used to complex the anion and by the potential applications of these systems. Many receptors use more than one functional group to bind anions or have various applications and the organisation of this review should be

Chemistry, University of Southampton, Southampton, SO17 1BJ, UK. E-mail: philip.gale@soton.ac.uk; Fax: +44 (0)23 8059 6805; Tel: +44 (0)23 8059 3332

Nathalie Busschaert, Cally Haynes, Phil Gale, Louise Karagiannidis and Isabelle Kirby

Phil Gale is Professor of Supramolecular Chemistry and Head of Chemistry at the University of Southampton. His research has recently focused on understanding transmembrane lipid bilayer anion transport processes mediated by small molecules with the goal of applying anion transporters to the future treatment of diseases such as cancer and cystic fibrosis. He has won a number of research awards including the Corday Morgan medal and prize from the RSC (2005) and a Royal Society Wolfson Research Merit Award (2013–2018). He is currently the chair of the editorial board of Chemical Society Reviews.

*Nathalie Busschaert completed a BSc in chemistry at the K. U. Leuven, Belgium, and continued studying for an MSc in chemistry at the same university. She then moved to the University to Southampton in 2010 to undertake a PhD under the supervision of Professor Philip A. Gale, with research stays at A*STAR, Singapore, and the University of Ljubljana, Slovenia. She is currently working as a post doctoral researcher in the group of Phil Gale. Her research interests are anion coordination chemistry, transmembrane anion transport and medicinal applications of supramolecular systems.*

Cally J. E. Haynes completed a masters degree in chemistry at Wadham College, Oxford in 2008 and went on to study for a PhD under the supervision of Professor Philip Gale at the University of Southampton from 2009–2011. She continued post doctoral work in the group of Phil Gale until 2013, and is currently working as a publishing editor at the Royal Society of Chemistry. Her research interests are in supramolecular chemistry, focusing on the coordination and membrane transport of anions.

Louise E. Karagiannidis completed her masters degree in chemistry at the University of Southampton in 2011. She is currently in the third year of her PhD studies, under the supervision of Professor Philip A. Gale at the University of Southampton. Her research focuses on supramolecular chemistry, in particular the influence of receptor structure on the transmembrane transport of small anions.

Isabelle L. Kirby graduated with a masters degree in chemistry from the University of Southampton in 2010. She is currently completing her PhD studies under the joint supervision of Professor Philip Gale and Dr Simon Coles in Southampton focusing on the molecular recognition of anions and the characterisation of non-covalent interactions in the solid-state.

regarded as a flexible guide to the classification of these systems.

Ammonium-based receptors

As anions are inherently negatively charged, an intuitive way of achieving anion binding is by the employment of positively charged species and ammonium groups have been widely used for this purpose. Bencini, Lippolis and co-workers have studied the effect of the aromatic linker between two [9]aneN$_3$ ammonium units in receptors **1–3**.[5] In aqueous solutions the two [9]aneN$_3$ units are protonated and have the potential to interact with anions *via* hydrogen bonding and electrostatic interactions. Using potentiometric, ^{1}H NMR and ^{31}P NMR measurements it was found that **1** selectively binds triphosphate over di- and monophosphate, while **2** selectively binds diphosphate and **3** monophosphate in aqueous solutions over a wide pH range, an order that correlates well with the distance between the two [9]aneN$_3$ units in **1–3**. Furthermore, **1** and **2** also preferentially interact with the nucleotides ATP (adenosine triphosphate) and ADP (adenosine diphosphate) over inorganic phosphate species, with the highest associations observed for receptor **1** with ATP and ADP. This can be attributed to the presence of π-stacking and hydrophobic interactions between the adenine units of the guest and the aromatic linker in **1** and **2**, an effect that is more pronounced for the larger phenanthroline spacer in receptor **1**. In a subsequent paper, the groups of Bencini and Lippolis reported the anion binding properties of terpyridine analog **4**.[6] Potentiometric titrations and ^{1}H NMR and fluorescence spectra in water showed that receptor **4** is only able to selectively bind and sense diphosphate over mono- and triphosphate after the addition of Zn^{2+} leads to a conformational change from *trans–trans* to *cis–cis* to create a convergent binding site that has optimal dimensional fitting for diphosphate (Scheme 1).

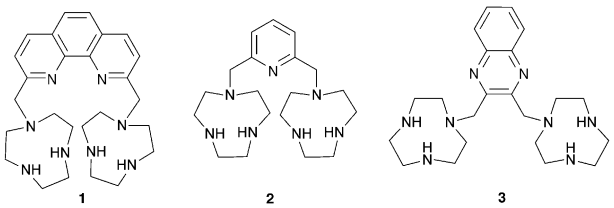

Continuing their work on [9]aneN$_3$ based receptors, Bencini, Lippolis, Pasini and co-workers have reported the synthesis of chiral ditopic polyammonium receptor **5** based on a (*S*)-BINOL scaffold capable of selectively binding (*S,S*)-tartaric acid in water over its (*R,R*) or *meso*-forms and over other carboxylates such as (*S*)/(*R*)-malate, (*S*)/(*R*)-lactate, maleate, fumarate and succinate (Fig. 1a).[7] Potentiometric, ^{1}H NMR and fluorescence titrations were used to probe the interaction of **5** with carboxylates at a range of pH values. The compound was shown to interact selectively with (*S,S*)-tartrate over a range of pH values. The authors attribute the selectivity to the configuration of the stereocentres and the possibility of hydrogen bonding between the –OH groups of (*S,S*)-tartrate and both tertiary amine groups of receptor **5** (Fig. 1b).

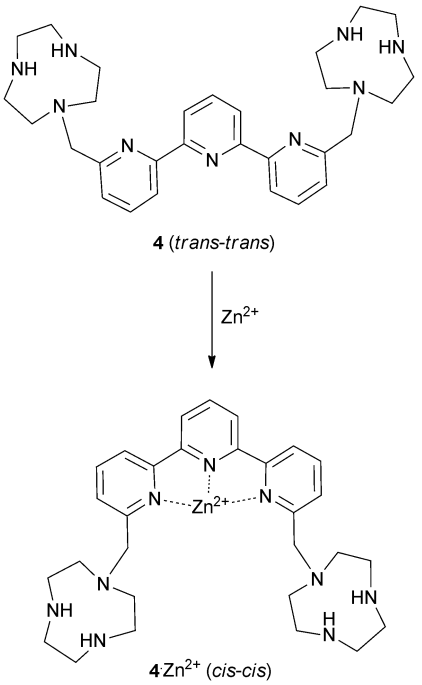

Scheme 1 Zn^{2+} induced conformational change of the terpyridine unit in receptor **4**.

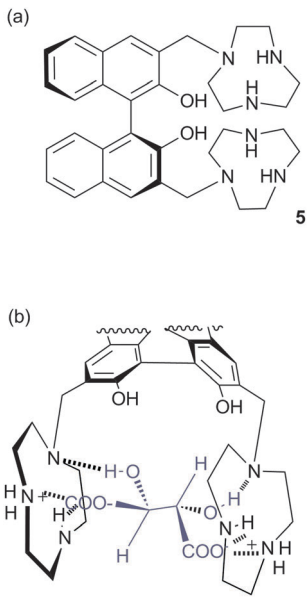

Fig. 1 (a) Structure of receptor **5**. (b) The proposed interaction mode between (*S,S*)-tartrate and $(H_2\mathbf{5})^{2+}$.

Bowman-James and co-workers have studied the role of charge on anion affinity in mixed amide–amine based macrocyclic anion receptor systems using NMR and X-ray crystallography.[8] Proton NMR titrations in DMSO-d_6 showed that the quaternised receptors **9**, **10** and **11** showed significantly higher affinity for anions than the neutral precursors **6**, **7** and **8** (Table 1). The NMR titration curves obtained predominantly fitted 1 : 1 binding stoichiometry apart from those for dihydrogen phosphate and

Table 1 Binding constants K_a/M^{-1} of compounds **6–11** in DMSO-d_6 at 25 °C. Compounds **9**, **10** and **11** are in the form of BPh_4^- salts

Anions	6	7	8	9^{2+}	10^{2+}	11^{2+}
Cl^-	25	490	20	1700	56 230	130
Br^-	20	515	<10	140	23 990	>10
I^-	<10	<10	<10	100	160	>10
$H_2PO_4^-$	830	10 960	100	10 960	208 900[b]	900
HSO_4^-	795	107	<10	[a]	7945	1500
NO_3^-	<10	<10	<10	45	210	<10
ClO_4^-	<10	<10	<10	40	250	<10

[a] Calculation complicated due to peak broadening after the addition of anion. [b] At the upper limits for NMR determination.

hydrogen sulfate. In the former case slow exchange was observed upon addition of this anion to **10** and the stability constant was calculated by integration of the proton resonances of the free and bound receptor. Addition of HSO_4^- to **9** caused significant broadening in the host's NMR resonances precluding the determination of a stability constant by this method. The results show that the pyridine containing receptors have a higher affinity in general than the compounds containing *m*-xylyl or thiophene spacers. This may, in part, be due to the pre-organising influence of the pyridine group on the amide NH protons forming a cavity suitable for anion complexation. This was confirmed by X-ray crystallography whereby the crystal structures of **9**·Cl and **9**·HSO_4 showed the anions located outside the macrocycle, with one amide NH coordinating to one anion, while the crystal structure of **10**·I showed that iodide was bound *via* two convergent amide NH groups around the pyridine spacer (Fig. 2).

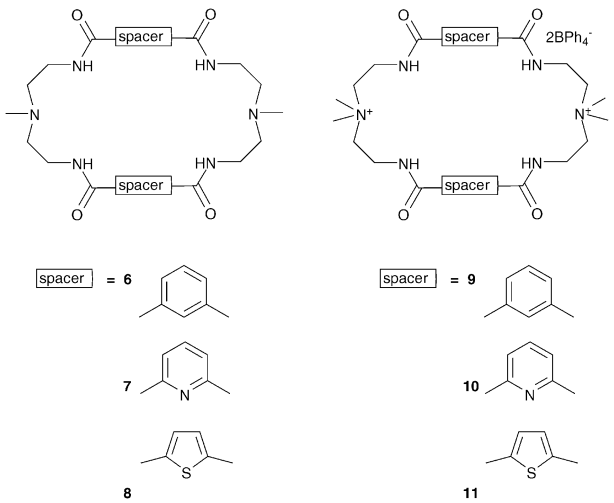

Another ammonium based macrocycle is cyclobis(paraquat-*p*-phenylene) ($CBQT^{4+}$) **12**, which is often studied as the ring component of [2]catenanes and [2]rotaxanes with π-electron donating guests,[9] but the role of the counteranions on the host–guest properties of this ammonium macrocycle is less well explored. Flood, Jeppesen and co-workers have investigated the effect of different sized counterions PF_6^- and $TRISPHAT^-$ on the binding of **12** with various tetrathiafulvalene guests **13–15** and naphthalene guest **16**.[10] UV/Vis dilution experiments in MeCN at 298 K revealed that the association between **12**·4TRISPHAT and **13–15** is nearly twice as strong as between **12**·4PF_6 and **13–15**.

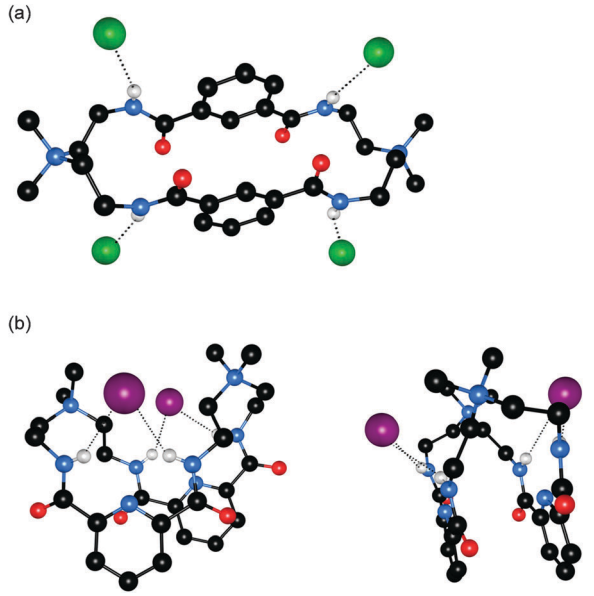

Fig. 2 (a) Crystal structure of $9^{2+}\cdot 2Cl^-\cdot 2.66H_2O$ (b) two views on the crystal structure of $10^{2+}\cdot 2I^-\cdot 2H_2O$. Hydrogen bonds are shown as dashed lines; solvent molecules and non-coordinating hydrogens are omitted for clarity; chloride is represented in green spacefill; iodide in purple spacefill and the receptors are shown in ball-and-stick.

The authors explain this observation by the larger size of the $TRISPHAT^-$ anion, leading to an increased distance between **12** and the anion, and hence stronger π-electron acceptor ability of **12**. It was also shown that the opposite was true for naphthalene guest **16**, where **12**·4PF_6 binds **16** more strongly (K_a = 2000 M^{-1}) than **12**·4TRISPHAT (K_a < 10 M^{-1}), presumably because the interaction between **12** and **16** is governed by CH···π interactions and not by donor–acceptor interactions.

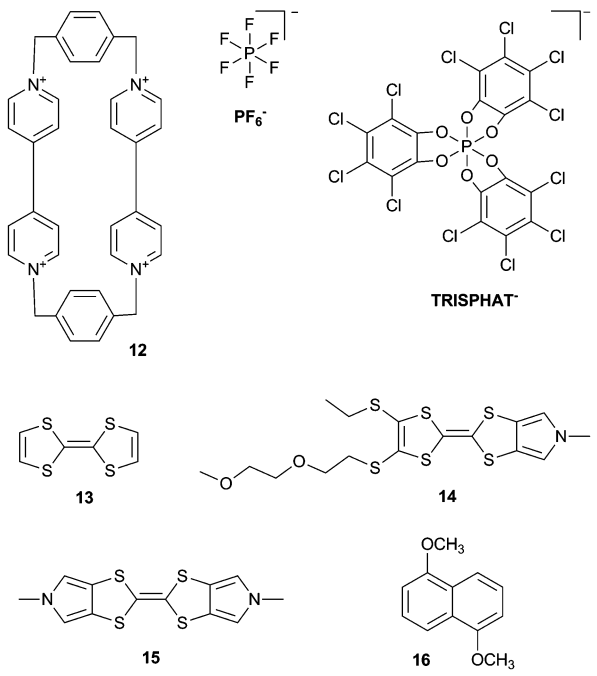

Amide-, urea-, thiourea- and squaramide-based anion receptors

Due to their facile synthesis and easily tunable NH acidity, amides, ureas and thioureas are probably the most widely employed hydrogen bond donor groups in anion receptor systems, and this has not changed during 2011 and 2012. Recently Beer and co-workers have used anion coordination by amide groups in the fabrication of core@shell bimetallic metal nanoparticles (Scheme 2).[11] Beer's method involves coating a nanoparticle in hydrogen bond donor groups that can form complexes with chlorometallate anions. Upon reduction the anions coat the nanoparticle with a second metal. Au@Pd, Pd@Au, Pt@Pd and Pd@Pt nanoparticles were synthesised using this methodology (Scheme 2) employing imidazole (to bind to the core nanoparticle) functionalised with an alkylamide group as the hydrogen bond donor. Beer demonstrated the reduction of 2-chloronitrobenzene using Au@Pd nanoparticles produced using this methodology and showed that small nanoparticles (<5 nm) can be produced using this method.

Acylhydrazone groups are similar to amide groups in terms of NH hydrogen bonding, but the reversible nature of this group allows it to be used in dynamic combinatorial chemistry. Beeren and Sanders have employed this strategy to develop a powerful receptor for dihydrogen phosphate.[12] A dynamic combinatorial library of hydrazone linked ferrocene-based macrocycles and linear oligomers was generated and it was found that the addition of tetrabutylammonium dihydrogen phosphate ($TBAH_2PO_4$) led to the amplification of linear receptor **17**, at the expense of the macrocyclic compounds. UV/Vis and NMR titrations in 94 : 6 chloroform : methanol with $TBAH_2PO_4$ showed that **17** binds $H_2PO_4^-$ in a 2 : 1 binding mode with positive cooperativity (K_1K_2 = 800 000 M^{-2}). Using NOESY NMR and CD (circular dichroism) experiments the authors were able

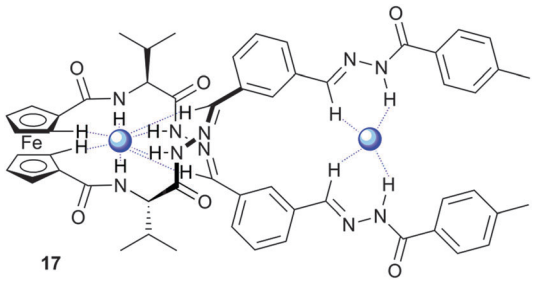

Fig. 3 Representation of helical linear receptor **17** binding two $H_2PO_4^-$ anions (blue spheres) using hydrogen bonding (blue dashed lines).

to show that the complex of **17** with $H_2PO_4^-$ adopts a helical conformation with two $H_2PO_4^-$ anions bound by various combinations of imine CH, cyclopentyl CH and hydrazone NH hydrogen bonds (Fig. 3).

Ureas and thioureas possess two NH hydrogen bond donors and are therefore often used to coordinate anions *via* multiple hydrogen bonds. Johnson, Haley and co-workers have continued their work on bis(anilinoethynyl)pyridine derivatives containing urea groups and showed that these compounds can show switchable ON–OFF and OFF–ON fluorescence responses to anions.[13] During previous studies it was noted that the fluorescence of compounds **18** and **19** was quenched upon protonation in chloroform, concurrently with a change in the colour of the solution from colourless to yellow.[14] Derivatives of compound **19** containing either electron donating methoxy- (**20a**) or electron withdrawing nitro- (**20b**) groups were synthesised in addition to methoxy- (**21a**) and nitro- (**21b**) functionalised sulfonamide derivatives. The colour and fluorescence changes of the compounds upon exposure to acid are illustrated in Fig. 4. The solutions of the compounds go from colourless to yellow in the presence of HCl. For the compounds with electron donating methoxy substituents fluorescence is switched off in the presence

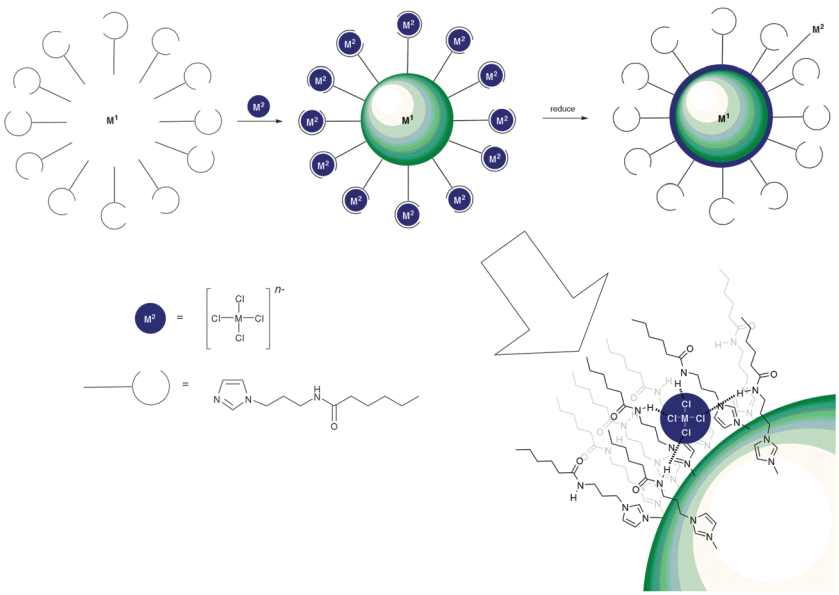

Scheme 2 A diagrammatic representation of the synthesis of core@shell bimetallic nanoparticles using anion coordination.

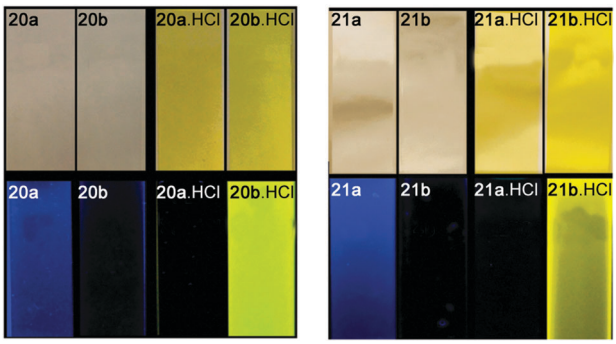

Fig. 4 Colourless solutions of neutral compounds in $CHCl_3$ turn yellow upon protonation (top); fluorescence (excitation 365 nm) is quenched in electron-rich compounds **20a**, **21a** and is 'turned on' in electron poor compounds **20b**, **21b** (bottom). Reproduced with permission from *Chem. Commun.* 2011, **47**, 5539–5541 © Royal Society of Chemistry.

of HCl, while for those with electron withdrawing nitro groups fluorescence is switched on. Using Frontier molecular orbital calculations, the authors show that in compounds **20a** and **21a** the electron density remains near the alkynyl groups resulting in radiative de-excitation and hence fluorescence. In the compounds containing nitro substituents (**20b** and **21b**) a charge-transfer fluorescent state is formed resulting in quenched fluorescence. This gives rise to an ON–OFF fluorescence response for **20a** and **21a**, and an OFF–ON response for **20b** and **21b** upon the addition of acid, and the magnitude of the response depends on the nature

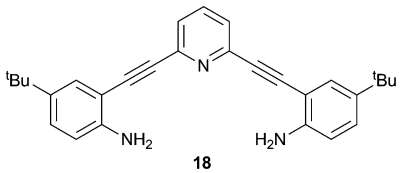

18

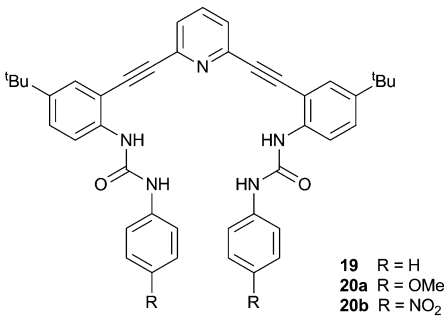

19 R = H
20a R = OMe
20b R = NO_2

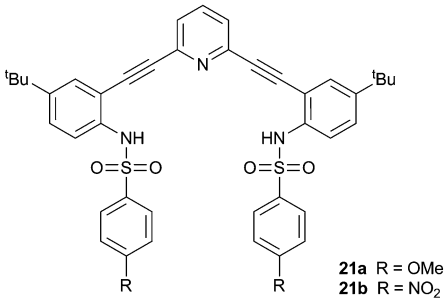

21a R = OMe
21b R = NO_2

of the acid (anion) with a larger response seen for HCl than for CF_3COOH. Subsequent studies on derivatives of **19** containing various functionalities, revealed that the presence of electron withdrawing groups in 2,6-bis-(anilinoethynyl)pyridine bisureas in general transforms this class of compounds into "switch on" fluorescent chloride sensors.[15]

Chao and co-workers have reported the anion sensing ability of a series of mononuclear gold(I) acetylide complexes containing a urea group (*e.g.* **22**).[16] These complexes exhibit intense luminescence in the solid state and in THF solutions, which was assigned to the $^3(\pi\pi^*)$ excited state of the acetylide ligands. The authors found that changing the urea substituent could modify the anion binding strength in THF, with electron withdrawing groups (such as $-NO_2$ in **22**) resulting in the strongest anion binding due to the increased acidity of the urea NH groups. UV/Vis titrations showed that receptor **22** forms a strong 1 : 1 complex with F^- ($\log K_a$ = 6.44) in THF. The anion complexation was signalled by a decrease in the intensity of bands at 263, 276, 288, 301 and 345 nm, with the gradual appearance of bands at 292, 308 and 375 nm. In DMSO, receptor **22** was found to undergo a colour change from colourless to yellow upon the addition of F^-. Analysis of the UV/Vis titration data revealed that this colour change is due to the deprotonation of the receptor by the anion, allowing for the straightforward naked eye detection of F^- anions.

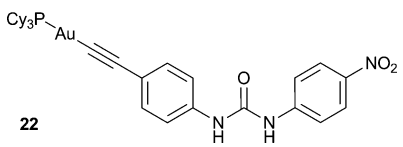

22

Allen, Sargent and colleagues have reported a fluorescent phospholipid analogue containing a urea group (**23**).[17] The fluorescence of this system derives from the diarylacetylene spacer, which separates the urea group from the phosphocholine (PC) lipid head group. Consequently, the receptor forms a "head-to-tail" dimer in dichloromethane at concentrations above 2×10^{-5} M, in which the urea group of one receptor forms hydrogen bonds to the PC group of a second receptor and *vice versa*. The dimeric complex was identified by electrospray ionization MS in acetonitrile–water, and by ^{1}H NMR in CD_3CN, and was predicted by DFT analysis. Fluorescence experiments in dichloromethane indicated that, at high concentrations of **23** (2.6×10^{-5} M) the addition of a large excess of Cl^- or NO_3^- did not produce a significant fluorescence response, while the addition of HCO_3^- or $H_2PO_4^-$ anions led to significant fluorescence quenching. However, at lower receptor concentrations ($\leq 5 \times 10^{-6}$ M) the addition of all of these anions was found to induce suppression of the emission intensity. This indicates that at lower receptor concentrations the dimeric species is not formed and anion binding does not compete with self-association.

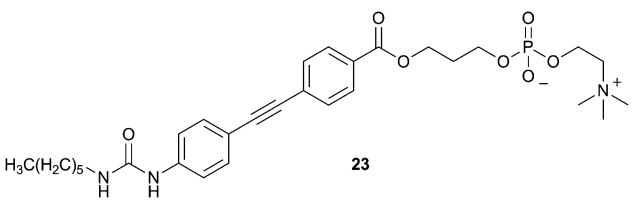

23

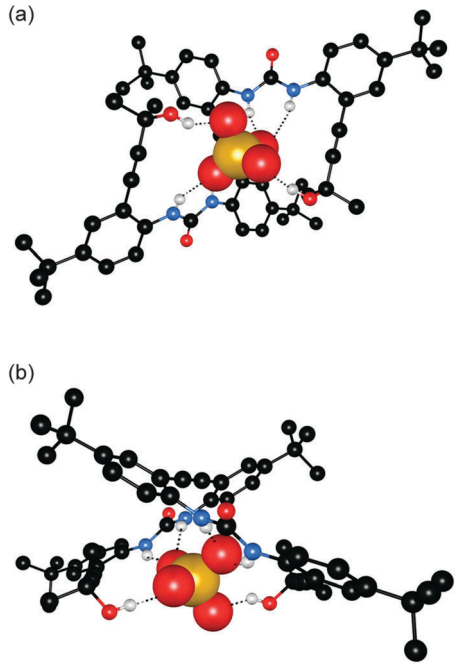

Fig. 5 Two views of the crystal structure for complex **25**·$(Bu_4N)_2SO_4$. Hydrogen bonds are marked by dashed lines, non-coordinating hydrogen atoms and TBA counterions are omitted for clarity. The receptor is shown as ball-and-stick and the anion as spacefill.

Jeong and co-workers have reported a series of diphenylureas **24–28** that form foldamer complexes with chloride and sulfate.[18] The solution phase sulfate binding properties were investigated by ^{1}H NMR titration in 20% and 40% CD_3OH–DMSO-d_6. In both cases the sulfate binding strength was found to increase with increasing chain length from **24–28** by approximately 4 orders of magnitude. In contrast, chloride binding studies in 15% CD_3OH–acetone-d_6 indicated that the binding strength reached a plateau after receptor **26** (K_a = 1340 M^{-1}). The authors attributed this difference to the greater hydrogen bond acceptor ability of sulfate, with the tetrahedral array of oxygen atoms allowing the formation of up to 12 hydrogen bonds, whereas chloride can be coordinatively saturated by fewer urea groups. The crystal structure of **25**·$(Bu_4N)_2SO_4$ confirmed the encapsulation of a single SO_4^{2-} anion in a 1:1 foldamer complex with each anion coordinated by four hydrogen bonds from two urea groups, and a further two hydrogen bonds from peripheral OH groups (Fig. 5).

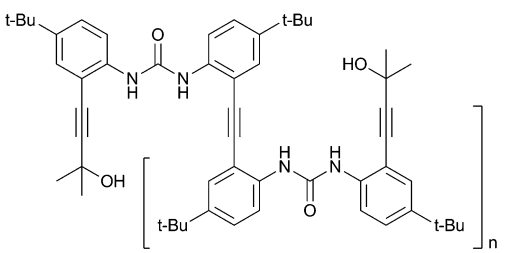

n = 0 (**24**), 1 (**25**), 2 (**26**), 3 (**27**) or 4 (**28**)

Gunnlaugsson and co-workers have reported the synthesis of a variety of pyridine-2,6-dicarboxamide-based receptors such as compound **29** (including systems containing two of these units linked *via* a glycol chain).[19] The glycol chain confers solubility in polar solvents allowing the response of these systems to a variety of inorganic and biologically relevant organic anions to be measured in water : ethanol or methanol mixtures, or in DMSO-d_6. Using UV/Vis titrations they found that receptors based on structure **29** were found to interact with AcO^-, F^- and $H_2PO_4^-$, resulting in an increase in the ICT transition of the receptor in the presence of the anions. The data obtained in the competitive 1:1 EtOH : H_2O solvent system fitted best to a 1:1 receptor : anion binding model, whereas higher order complexes were observed in titrations in DMSO : H_2O and pure EtOH or MeOH solution. The authors suggested that this could be due to the formation of a hydrophobic cleft in the more strongly coordinating environment, which favours the formation of the 1:1 complex. The authors also investigated the binding of some biologically relevant phosphate anions under the same conditions. They found that AMP and ADP formed a 1:1 hydrogen bonded complex with these receptors, with binding of AMP slightly favoured over ADP. In contrast, the titration of these receptors with $HP_2O_7^{3-}$ and ATP appeared to result in the deprotonation of the receptor by the anion, as indicated by a large change in the pH of the system determined by spectroscopic pH titrations.

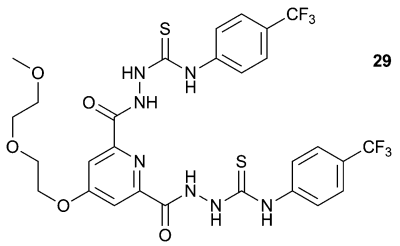

29

Sada and co-workers have incorporated a *p*-nitro-phenylthiourea group into a polymer gel network that shows selective colour change and swelling behaviour in the presence of certain anions.[20] Cross-linked poly(octadecyl acrylate) containing a small number of thiourea groups (**31**) was prepared by radical co-polymerization gelation from the relevant monomers in a benzene : methanol mixture using azobis-isobutyronitrile (AIBN) as an initiator. The solvent was removed from the resulting gel, which was then transferred into a THF solution of the tetrabutylammonium (TBA) salts of a number of anions for 48 hours. The authors found that incubation in the presence of F^- or AcO^- anions leads to a significant swelling of the gel as a result of anion complexation causing the countercations to become entrapped in the gel network. This was accompanied by a colour change of the gel from pale yellow to red (F^-) or yellow-green (AcO^-), while other anions did not induce a colour change. Less strongly coordinating anions such as Cl^- and PF_6^- induced a much smaller swelling effect. The F^- induced swelling was found to be reversible, as immersion in THF : methanol (8:2) for 48 hours resulted in the collapse of the swelled gel. UV/Vis titration experiments in MeCN with the thiourea monomer **30** confirmed that F^- and AcO^- were complexed more strongly than

the other anions tested, with binding constants of 3.7×10^3 M^{-1} and 9.2×10^3 M^{-1} respectively.

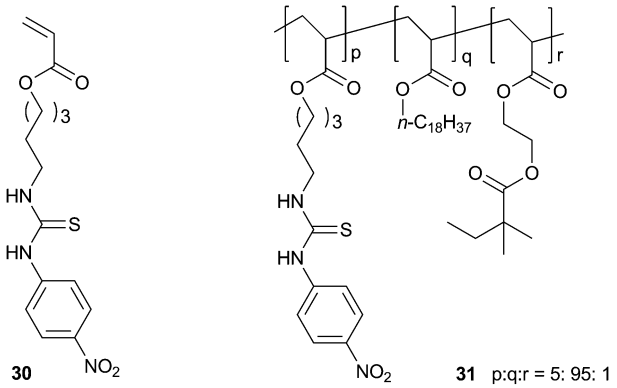

Wu and co-workers have reported a simple pyridylurea ligand **32** that assembles into a hexameric capsule, directed by the coordination of six copper(II) ions, which can encapsulate sulfate anions with six urea groups.[21] The sulfate inclusion complex was generated by the reaction of $CuSO_4 \cdot 5H_2O$ with 3 equivalents of the free ligand **32** in DMF. The resulting complex provided single crystals suitable for X-ray analysis. The authors found that the structure contains two kinds of copper(II) environment, designated [Cu^1] and [Cu^2]. The [Cu^1] moieties are octahedrally coordinated by six ligand molecules forming two opposing, inversion related C_3-symmetric clefts. The sulfate anion is positioned within a cavity formed by two such complex units and coordinated by six urea groups, and the capsules further extend into a 1D chain (Fig. 6). Meanwhile, the [Cu^2] moieties are chelated by two ligands and two DMF molecules, and adopt a Jahn–Teller distorted octahedral geometry.

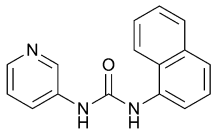

Similarly, Custelcean *et al.* have synthesised symmetrical bipyridine substituted urea ligand **33** to construct a M_4L_6 cage using zinc(II) coordination.[22] The authors hoped that the M_4L_6 cage would favour the coordination of tetrahedral anions within the cavity. The formation of complexes in solution was monitored using NMR techniques. The addition of zinc nitrate to a solution of **33** in 2 : 1 $CD_3OD : D_2O$ revealed that a low-symmetry coordination complex or mixture of complexes was formed between 6 ligands and 4 zinc(II) cations within minutes.

Subsequently, the addition of a number of EO_4^{2-} anions (E = S, Se, Cr, Mo, W, P) resulted in the formation of a new set of sharp NMR resonances, consistent with the formation of the desired Zn_4L_6 cage. The tetrahedral geometry of the templating anion proved to be crucial, as the complex was not formed in the presence of F^-, Cl^-, Br^-, I^-, NO_3^-, BF_4^-, PF_6^-, AcO^- or $CF_3SO_3^-$. Additionally, the divalent charge of the tetrahedral anions was important, as no complex formation was observed using ClO_4^- or ReO_4^-, whilst the non-tetrahedral divalent anions CO_3^{2-}, SeO_3^{2-} and SO_3^{2-} also did not result in complex formation. Although the cages were found to not persist in the

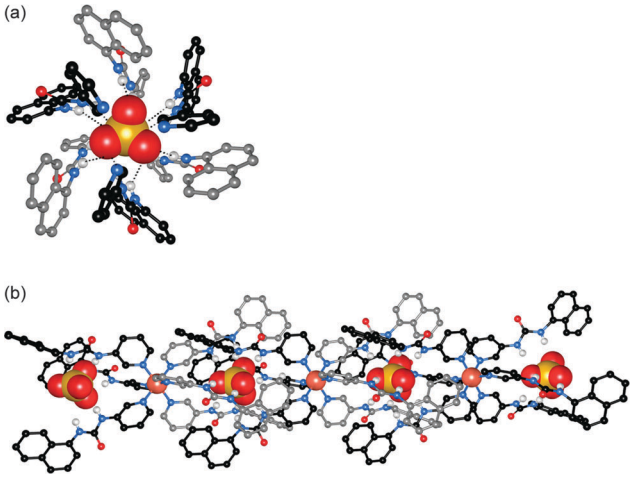

Fig. 6 Crystal structure of the [Cu^1] fragment in $CuSO_4$ complex of **32**. Sulfate and copper ions are shown as spacefill, while the receptor is shown as ball-and-stick. Hydrogen bonds are represented by dashed lines. (a) Sulfate encapsulation by multiple hydrogen bonds from six urea groups in the $[SO_4(\mathbf{32})_6]^{2-}$ capsule (copper ions are omitted for clarity). (b) Infinite 1D hydrogen bonded chain linked by sulfate encapsulation and copper coordination.

absence of the encapsulated anions, the authors were able to perform competitive binding experiments in 2 : 1 $CD_3OD : D_2O$ using ^{77}Se NMR to identify encapsulated and free $^{77}SeO_4^{2-}$. The cages were prepared encapsulating $^{77}SeO_4^{2-}$, and one or two equivalents of Na_2EO_4 (E = S, Cr, Mo and W) were added. These experiments were used to calculate EO_4^{2-}/SeO_4^{2-} exchange constants (K_{ex}), with CrO_4^{2-}complexed the strongest (K_{ex} = 40.10) and selectivity in the order $CrO_4^{2-} > SO_4^{2-} > SeO_4^{2-} > MoO_4^{2-} > WO_4^{2-}$. With the exception of CrO_4^{2-}, this represents anti-Hofmeister selectivity. The authors also noted that CrO_4^{2-}, which is the anion that does not fit the anti-Hofmeister bias, is the most basic anion, which could explain why it is bound the strongest. The crystal structures of the $[Zn_4(\mathbf{33})_6(EO_4)](NO_3)_6$ complexes (E = S (Fig. 7), Cr and Mo) were found to be isomorphous, with each EO_4^{2-} anion encapsulated by twelve hydrogen bonds from six urea groups. The hydrogen bonding parameters are very similar across these three structures despite the varying anion size, indicating that the cage is flexible and can accommodate anions of different sizes.

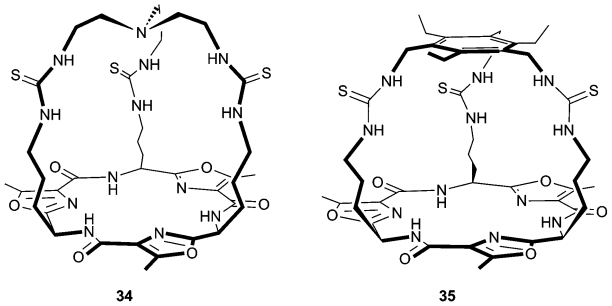

Jolliffe and co-workers have reported the synthesis of thiourea cryptands **34** and **35**, based on a rigid cyclic peptide scaffold.[23] They found that the yield in the final cyclisation of

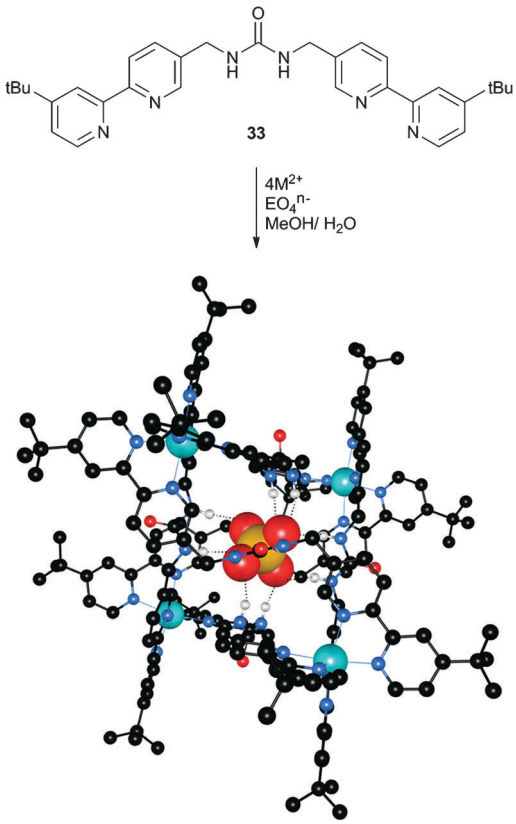

Fig. 7 The assembly of an M_4L_6 cage templated by tetrahedral EO_4^{n-} anions. The figure represents the crystal structure where M^{2+} = Zn^{2+} (turquoise spheres) and EO_4^{n-} = SO_4^{2-}. Hydrogen bonds are represented by dashed lines and non-coordinating hydrogen atoms and solvent molecules are omitted for clarity. Sulfate is bound by six urea groups and the four Zn^{2+} cations form a distorted tetrahedron.

34 and **35** was improved if the cyclopeptide precursor was added as the hydrogen bromide salt, implying that this procedure may be anion templated. The interaction of the cryptands with a range of monovalent anions was investigated by ^{1}H NMR titrations in DMSO-d_6–H_2O 0.5%. Receptor **34** was found to interact strongly with a range of anions including F^-, Cl^- and AcO^- (all with $K_a > 10^4$ M^{-1}), while receptor **35** only showed a strong interaction with AcO^- ($K_a > 10^4$ M^{-1}), which was at least three times higher than any other anion studied. The authors suggested that the higher anion selectivity of **35** was due to the increased rigidity inferred by the 1,3,5-triethylbenzene cap, whereas the tren-capped cryptand **34** is more flexible, allowing it to interact strongly with a wider range of anions.

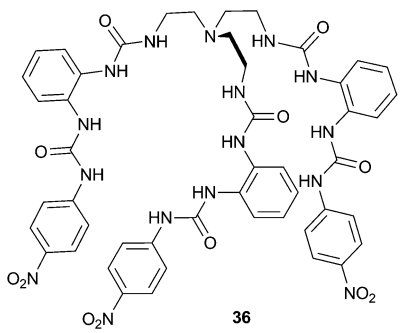

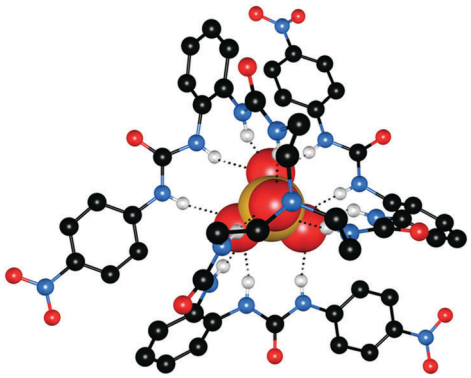

Fig. 8 Crystal structure of the sulfate complex of receptor **36** (top view). The anion is shown as spacefill and the receptor as ball-and-stick; hydrogen bonds are represented by dashed lines; non-coordinating hydrogen atoms, solvent and countercations (TBA) are omitted for clarity.

Wu and co-workers have published the strong sulfate binding and extraction properties of tripodal hexaurea **36**.[24] In the solid state, the authors found that a single sulfate anion could be encapsulated by 12 hydrogen bonds to the six urea groups, making **36** the first organic receptor reported to show saturated coordination of a sulfate anion by a single host. In this structure the complex forms a tetrahedral cage, with each of the three terminal arms folded along an edge of the bottom triangular face and each urea group chelating an edge of the tetrahedron (Fig. 8). The authors also investigated the solution phase anion binding properties by a number of techniques, and using ^{1}H NMR titration estimated a sulfate binding strength of $K_a > 10^4$ M^{-1} in the highly competitive DMSO-d_6–H_2O 25%. Using NMR techniques receptor **36** was also found to be capable of efficiently extracting sulfate anions from aqueous $NaNO_3$–Na_2SO_4 solutions into $CDCl_3$ (containing tetrabutylammonium chloride for solubility purposes).

Continuing their work on receptors containing multiple urea groups, Wu and co-workers have also reported tetra- and hexa-urea ligands **37**[25] and **38**[26] incorporating repeating bis-urea units. In the solid state, receptor **37** was found to form a fascinating dinuclear triple helix structure on coordination of phosphate anions, in which three ligands are wrapped around two PO_4^{3-} centres (Fig. 9a). Each phosphate anion is bound by six urea groups from three different receptors through twelve hydrogen bonds. The interaction of **37** with PO_4^{3-} anions was also investigated in solution by ^{1}H NMR titration in DMSO-d_6–H_2O 5%. This analysis revealed that the major species in solution was also a 3 : 2 receptor : anion aggregate. Meanwhile, hexaurea **38** was found to form a range of interesting structures in the solid state on complexation with a number of different chloride and bromide salts. The treatment of **38** with tetraethylammonium chloride (TEACl) resulted in a 'molecular barrel' complex (Fig. 9b). Two receptors dimerise by weak CH···O_2N– hydrogen bonding interactions, and two of these associated dimers encapsulate three TEA^+ cations. The urea NH groups face out of the cavity, and consequently a number of Cl^- anions are associated with the outside of the barrel. When tetrapropylammonium chloride (TPACl) was used a similar

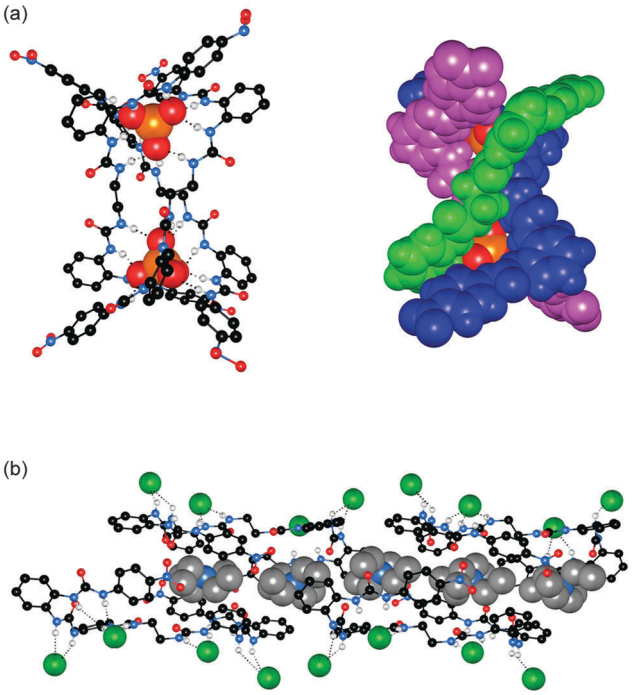

Fig. 9 Crystal structure of (a) triple helix formed by receptor **37** and PO_4^{3-} shown in ball-and stick (left) and spacefill (right). $[K(18\text{-crown-6})]^+$ counterion has been omitted for clarity; (b) molecular barrel formed by receptor **38** and TEACl. Solvent molecules and non-coordinating hydrogen atoms have been omitted for clarity. Hydrogen bonds are represented by dashed lines.

barrel-like structure resulted, which encapsulates two TPA^+ cations. As a result of encapsulating two TPA^+ *vs.* three TEA^+ cations, the diameter of the barrel is wider and the length is shorter. However, moving to tetrabutylammonium chloride (TBACl) a helical foldamer-type structure was formed, in which

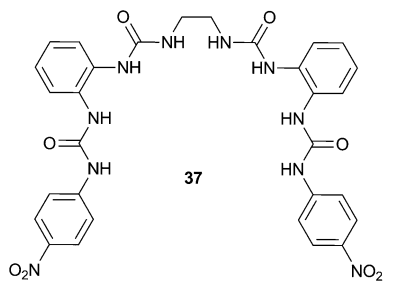

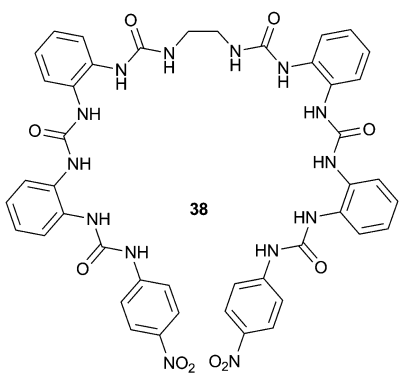

one receptor molecule is threaded around two chloride anions. One Cl^- accepts six hydrogen bonds from urea NH groups while the other receives four NH···Cl and two CH···Cl contacts with the cation and solvent molecules. A variety of interesting arrays were also formed using tetraalkylammonium bromide salts.

Wu *et al.* have also reported a series of oligourea receptors including **39** and **40** that coordinate chloride anions in either a mononuclear assembly or a dinuclear foldamer depending on the number of urea groups present.[27] Single crystal X-ray crystallography revealed that short chain receptor **39** was found to wrap around a single chloride anion, forming mononuclear crescents. The chloride anion was complexed *via* four hydrogen bonds to the two peripheral urea groups, while the middle urea formed an intermolecular hydrogen bond, which connects adjacent complexes into an infinite ribbon. Longer chain analogues such as **40** form dinuclear foldamer complexes with chloride, in which two chloride anions are encapsulated within a helix. The crystal structure of $[\mathbf{40}\cdot Cl^-]$ is shown in Fig. 10. Each chloride anion is bound by four hydrogen bonds from two alternating urea groups. The Cl···Cl distance measures 3.613(9) Å, which is unusually short given that the sum of the ionic radii is 3.62 Å, indicating that a large amount of electrostatic repulsion has been overcome in the formation of this complex.

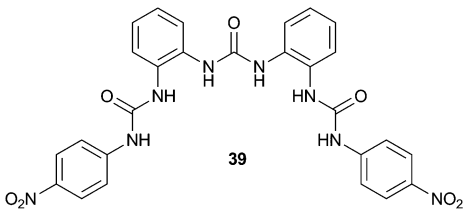

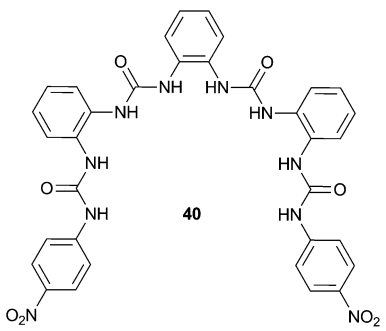

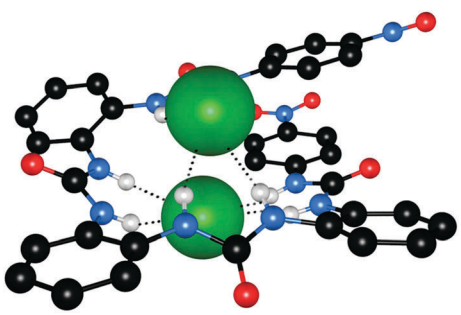

Fig. 10 Crystal structure of the complex of receptor **40** with TBACl. The chloride anions are shown in spacefill, with the receptor in ball-and-stick, and hydrogen bonds are represented by dashed lines. Non-coordinating hydrogen atoms and countercations are omitted for clarity.

Squaramides are becoming a popular isostere for urea or thiourea anion binding sites. Taylor and co-workers have reported the synthesis of poly(squaramide) **41** by Lewis acid catalysed condensation.[28] The anion complexation properties of this polymer were investigated by fluorescence spectroscopy in the competitive 10% water–NMP medium by comparison to mono-squaramide **42**. The authors found that both systems showed a "turn-on" increase in fluorescence intensity on the addition of $H_2PO_4^-$. However, monosquaramide **42** also displayed a significant response on the addition of F^- anions, while polymer **41** was found to be completely selective for $H_2PO_4^-$. Hill plot analysis also indicated that $H_2PO_4^-$ binding by polymer **41** was cooperative. The authors suggested that the high affinity and selectivity of the polymer system was the result of the interplay between anion binding and polymer aggregation, which was observed by GPC analysis (gel permeation chromatography), temperature dependent UV/Vis spectroscopy and transmission electron microscopy (TEM). Dynamic light scattering (DLS) indicated that the addition of phosphate anions to a heterogeneously distributed solution of **41** in DMF causes the formation of well-defined aggregates. This work highlights that the aggregation of this class of materials can be beneficial towards achieving highly selective anion sensing.

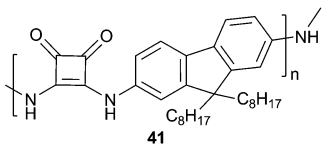

41

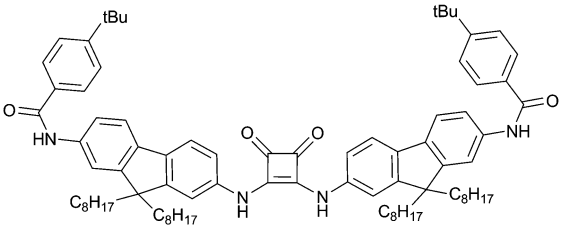

42

Pyrrole and indole based anion receptors

Unlike amides, (thio)ureas and squaramides, pyrrole- and indole-based anion receptors have the advantage that they do not possess any hydrogen bond acceptor moieties, avoiding aggregation and competition for hydrogen bond donor sites, rendering pyrroles and indoles popular anion binding motives. Sokkalingam *et al.* have employed the anion binding ability of modified calix[4]-pyrrole **43** to develop a selective sensor for fluoride using a fluorescent dye displacement assay (FDDA).[29] When the fluorescent dye chromenolate **44** is bound to **43**, the fluorescence of the dye is completely quenched. Subsequent addition of F^- results in the recovery of the fluorescence. As no change in fluorescence was observed upon the addition of Cl^-, Br^-, I^-, CN^-, SCN^-, AcO^-, NO_3^-, $PhCO_2^-$, PF_6^-, $HP_2O_7^{3-}$, HSO_4^- and $H_2PO_4^-$, the assembly consisting of **43** and **44** is a powerful and selective fluoride sensor. ITC (isothermal titration calorimetry) and UV/Vis titrations confirmed the fluoride sensing ability of the **43–44** assembly, with the affinity constant for $[\mathbf{43}\cdot F]^-$ ($K_a = 5.69 \times 10^6\ M^{-1}$) being slightly higher than for $[\mathbf{43}\cdot\mathbf{44}]^-$ ($K_a = 4.69 \times 10^6\ M^{-1}$). Furthermore, the addition of Li^+ to the fluorescent mixture of $[\mathbf{43}\cdot F]^-$ and **44**, led to a "switch off" of the fluorescence, presumably due to the removal of F^- from **43** by Li^+ and the formation of the original non-fluorescent $[\mathbf{43}\cdot\mathbf{44}]^-$ assembly.

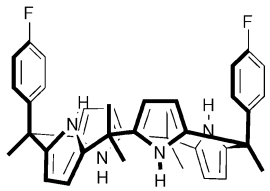

43

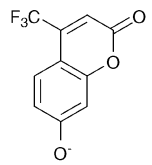

44

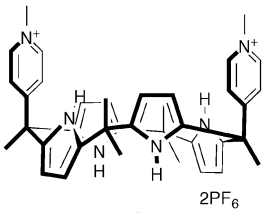

45

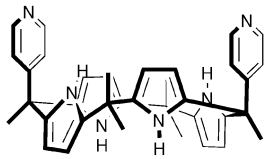

46

In a subsequent paper, Sokkalingam *et al.* have reported bis-pyridinium substituted calix[4]pyrrole **45** as a selective pyrophosphate sensor using a similar fluorescent dye displacement assay.[30] The receptor was shown to form a non-fluorescent 1:1 complex with the fluorescent chromenolate anion **44** in acetonitrile (Scheme 3), with an affinity constant of $7.25 \times 10^6\ M^{-1}$. The original fluorescence was shown to fully recover upon the addition of $HP_2O_7^{3-}$, while negligible or small enhancements of fluorescence were observed upon the addition of other anions, such as HSO_4^-, Br^-, F^-, $H_2PO_4^-$, CH_3COO^- and Cl^-. This selectivity towards $HP_2O_7^{3-}$ over other anions such as F^- and $H_2PO_4^-$ was even more pronounced when 30% aqueous acetonitrile was used as the solvent. The formation of a 1:1 receptor:$HP_2O_7^{3-}$ complex was further supported by ^1H NMR and MALDI-TOF MS experiments. The authors attribute the exceptionally high affinity for $HP_2O_7^{3-}$ ($K_a = 2.55 \times 10^7\ M^{-1}$) to the cationic charge of receptor **45**, as the affinity for neutral bipyridine receptor **46** was found to be much lower ($K_a = 5.25 \times 10^5\ M^{-1}$), although hydrogen bonding and anion$\cdots\pi$ interactions were also found to contribute to $HP_2O_7^{3-}$ binding.

Sessler and co-workers have reported the ion-controlled thermal electron transfer from tetrathiafulvene calix[4]pyrroles **47** and **48** to

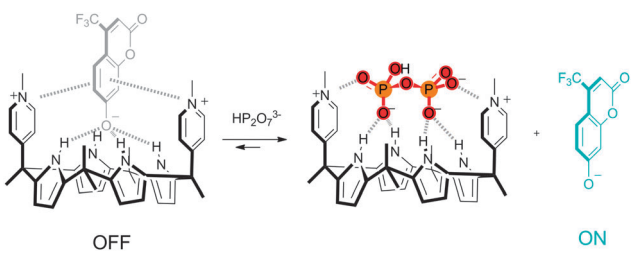

Scheme 3 Proposed Fluorescent Dye Displacement Assay (FDDA) detection of pyrophosphate anion by **45**.

$Li^+@C_{60}$ in benzonitrile, consisting of an electron transfer switched *on* by addition of tetra-*n*-hexylammonium (THA) chloride and *off* by the addition of tetraethylammonium (TEA) chloride.[31] THA chloride was shown to bind to **47** and **48** in benzonitrile with affinity constants of 1.9×10^4 M^{-1} and 1.7×10^4 M^{-1} respectively. The binding of Cl^- presumably causes a conformational change of the calix[4]pyrrole to the "cone" conformation, which stabilises the close association of the $Li^+@C_{60}^{\bullet-}$ radical ion pair inside the cavity of the cone. This close association of the radical ion pair was suggested by NIR absorption and EPR spectra, DFT calculations and X-ray crystallography, which showed an overall neutral 1 : 1 : 1 binding stoichiometry of chloride and the $Li^+@C_{60}^{\bullet-}$ radical ion pair to **47**. The authors also showed that the addition of TEACl to the electron transfer product obtained from **47**/**48**, THACl and $Li^+@C_{60}$ in benzonitrile results in a back-electron-transfer to form the original species. It is thought that TEA^+ is more effectively bound in the calix[4]pyrrole cavity, thus repelling the $Li^+@C60^{\bullet-}$ radical and reversing the electron transfer process.

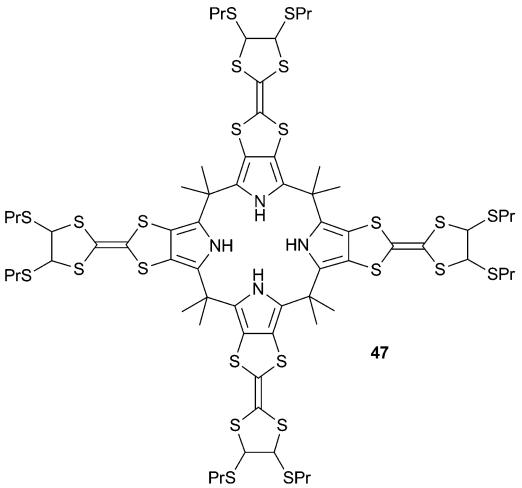

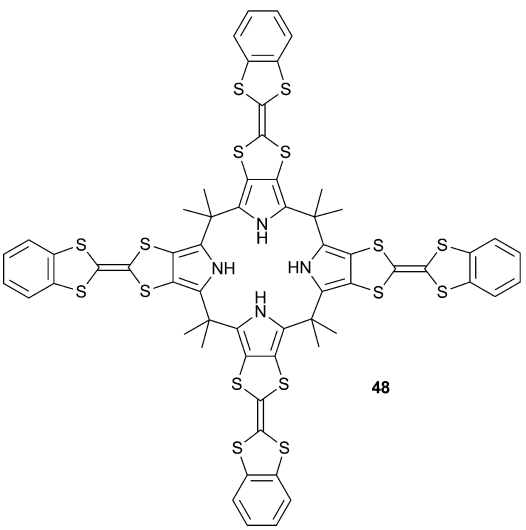

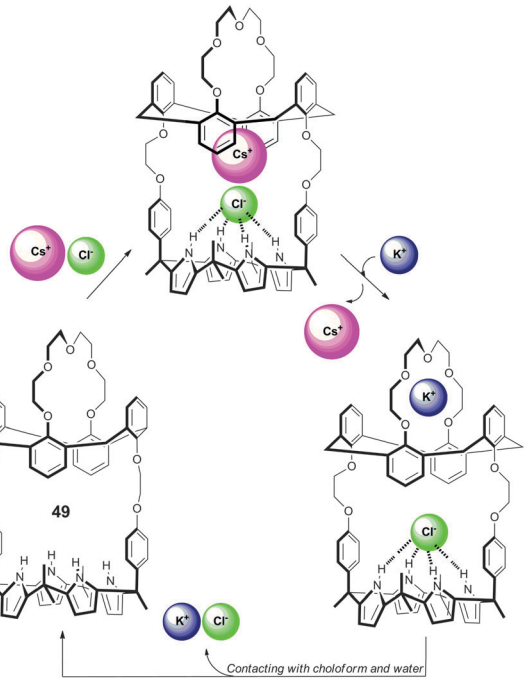

Scheme 4 Design concept underlying ion pair receptor **49** and its cation metathesis abilities.

Sessler and co-workers have also reported the controlled recognition and cation metathesis properties of ion pair receptor **49** based on the anion binding calix[4]pyrrole unit appended with multiple cation binding sites.[32] Proton NMR studies in 10% CD_3OD : $CDCl_3$, as well as gas phase energy-minimisation studies and X-ray crystallography suggest that the receptor forms stable 1 : 1 complexes with CsCl and $CsNO_3$. However, the stronger association between the receptor and potassium means that the addition of $KClO_4$ results in cation metathesis from bound caesium to bound potassium (Scheme 4). Proton NMR and radiotracer measurements showed that the receptor was able to extract CsCl and $CsNO_3$ from D_2O into nitrobenzene with the caesium cation released by contacting an aqueous $KClO_4$ solution with the nitrobenzene phase. Recovery of the free receptor was promoted by exposure to $CHCl_3$, suggesting the reusability of the receptor.

Maeda and co-workers have studied the anion recognition properties of π-conjugated dipyrrolyldiketone based anion receptors, including the anion-induced changes in the chiroptical properties of a series of chiral BINOL-boron substituted π-conjugated receptors such as receptors **50a–c**.[33] CD experiments suggest that the chiral boron substitution patterns (**50b–c**) lead to enantiomerically distorted *M*-like conformations. X-ray crystal structures, ^1H NMR and nuclear Overhauser effect spectroscopy (NOESY) indicated that a conformational change occurs upon anion binding with the inversion of the two pyrrole rings (Fig. 11). UV/Vis titration studies in CH_2Cl_2 with TBA salts of acetate and chloride give binding affinities for **50c** of 51 000 and 8200 M^{-1} respectively. Anion complexation of receptors **50a–c** was also shown to mediate changes to the CD, UV/Vis absorption and fluorescence spectra and result in an increased circularly

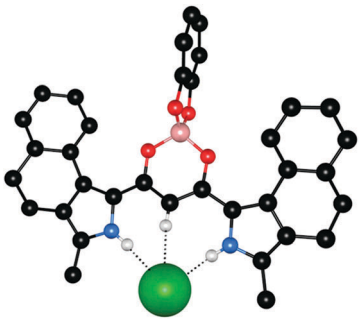

Fig. 11 X-ray crystal structure of **50a**·TBACl, non-coordinating hydrogen atoms and TBA counterions are omitted for clarity and hydrogen bonds are shown as dashed lines, the receptor is shown in ball-and-stick with the chloride anion in spacefill.

polarized luminescence (CPL), with β-dihydronapthopyrrole **50c** found to be most efficient at anion-driven CPL enhancement.

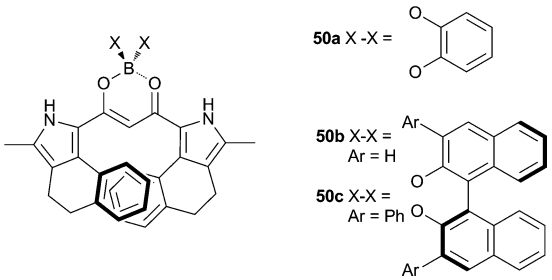

Maeda *et al.* have also shown that the anion recognition properties of these boron-appended dipyrrolyldiketones can lead to the formation of soft materials through the introduction of different anion modules.[34] Replacing spherical halide anions with aliphatic gallic carboxylate derivatives **52-*n*** (as TBA salts) in complexes with the acyclic anion receptors **51a,b** promoted the formation of ordered lamellar assemblies through the electrostatic interactions between the charged components. The binding mode between the receptor and anions was elucidated by ^{1}H NMR, UV/Vis and DFT studies, and X-ray diffraction measurements highlighted the lamellar nature of the materials. Differential scanning calorimetry (DSC) and polarised optical microscopy (POM) suggested the presence of mesophases with properties modulated by the length of the anion's alkyl chains. Flash-photolysis time-resolved microwave conductivity (FP-TRMC) measurements were used characterise the electrical conductivity of these materials.

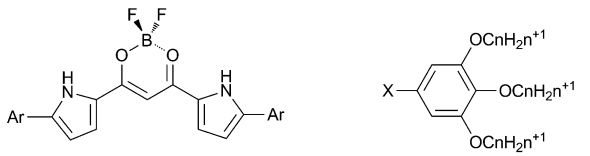

Maeda and Terashima have also reported that the incorporation of amide groups into the dipyrrolyldiketone BF_2 based anion receptors (**53a–c**) can lead to the formation of various solvent-dependent supramolecular assemblies based on the hydrogen bonding properties of the amides.[35] This solvent

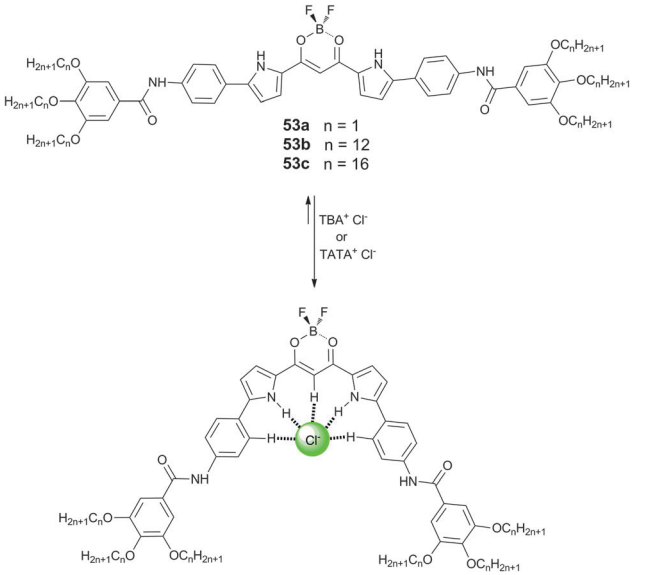

Scheme 5 Structures of dipyrrolyldiketone BF_2 complexes **53a–c** and the chloride-induced pyrrole inversion.

dependence is due to the balance of hydrogen bonding, π···π interactions and van der Waals interactions in these systems. In octane, receptors **53a–c** were shown to form soluble H-aggregates, while supra-molecular gels were formed in CH_2Cl_2, $CHCl_3$ and 1,4-dioxane. UV/Vis and IR spectroscopic studies suggested this was due to the different preferences for π···π stacking in the assemblies. Octane prefers to interact with the aliphatic side chains of the receptors and leads to tight π···π stacking between the receptors forming H-aggregates, while CH_2Cl_2, $CHCl_3$ and 1,4-dioxane prefer the π-planes over the alkyl chains and hence these assemblies lack strong π···π interactions and form gels. The resulting gels were studied by scanning electron microscopy (SEM) and X-ray diffraction and were shown to be responsive to anions, with addition of both TBA and TATA (4,8,12-tripropyl-4,8,12-triazatriangulenium) salts of chloride promoting a gel–solution transition. The authors suggest that pyrrole inversion upon anion binding prevents the effective hydrogen bonding between the amide groups and hence causes a gel–solution transition upon the addition of the appropriate anion (Scheme 5).

Incorporation of an anionic moiety to the π-conjugated pyrrole based scaffold has been shown by Maeda and co-workers to lead to the formation of anion binding self-assemblies.[36] The neutral receptor **54** displays high affinity for carboxylates, with UV/Vis studies giving a K_a of 47 000 M^{-1} in CH_2Cl_2 for the 1 : 1 binding stoichiometry of the receptor with acetate. Substitution of the receptor with a carboxylate at the *para* (**55a**) or *meta* (**55b**) position led to the formation of self-complementary dimers (Fig. 12), as evidenced by ESI-TOF-MS in MeCN and ^{1}H NMR titration studies in $CDCl_3$. DFT studies highlighted the difference in geometries of the dimers depending on the position of the carboxylate group and this was shown to lead to narcissistic self-sorting behaviour where mixing of the two dimers **55a** and **55b** in $CDCl_3$ did not result in the formation of any mixed dimers, due to the higher stability of

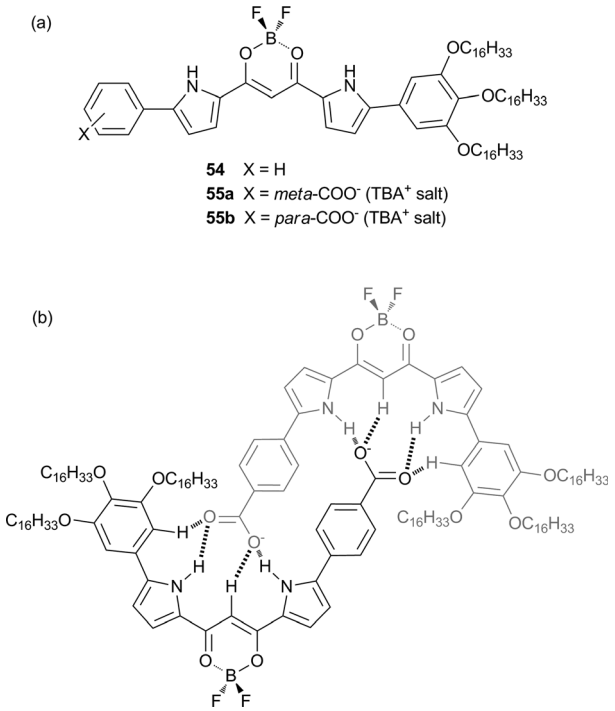

Fig. 12 (a) Structure of receptors **54** and **55a,b**; (b) proposed dimeric structure of **55b**·**55b**.

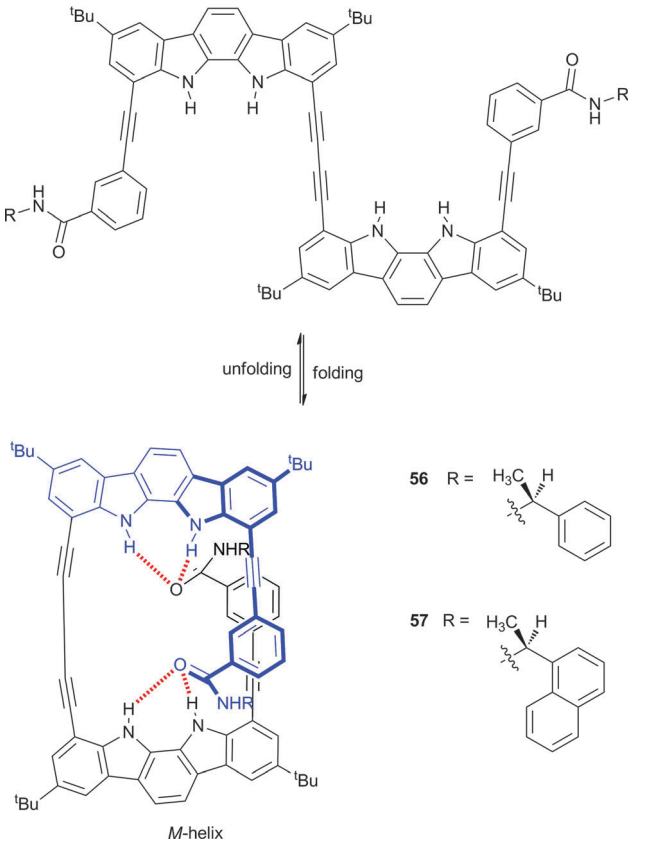

Scheme 6 Chiral indolocarbazole dimers **56** and **57** displaying unfolding and folding behaviour.

one self-complementary dimer over the other. Protic solvents were shown to induce dissociation of the self-assembled dimers due to their ability to solvate the hydrogen bond donor and acceptor groups of the receptor.

Indoles, carbazoles and indolocarbazoles are the π-extended analogues of pyrrole and have therefore been widely used in anion-responsive foldamers. Jeong and co-workers have reported indolocarbazole dimers substituted with chiral (*S*)-arylethylamido groups (**56** and **57**), which lead to the preferential formation of one helical isomer over the other.[37] The incorporation of the butadiynyl spacer promotes the formation of a helix *via* hydrogen bonding interactions between the indole and amide groups (Scheme 6). This folding was shown to be solvent dependent with ^{1}H NMR confirming that the folded conformation exists in a 5% $CD_3CN:CD_2Cl_2$ solvent mix, while the unfolded form is present in DMSO-d_6. CD spectroscopy and polarimetry implied the formation of a left-handed (*M*) helix with optical rotation dependent on the solvent. The reversed chirality of the helix was observed when the amides were altered from the (*S*)- to the (*R*)-isomers, confirming that the terminal chiral units determine the helical sense. Strong association between **56** and sulfate was observed by UV/Vis titration, with an affinity constant for TBA_2SO_4 of 2.2 × 10^5 M^{-1} in 5% $MeOH:CH_3CN$ and binding of sulfate was shown to switch the helical sense. The sulfate dimer complex was assigned as a *P*-helix by CD spectroscopy, polarimetry and crystallography. The crystal structures of **56**·SO_4^{2-} and **57**·SO_4^{2-} show that the sulfate anion is situated within the cavity, stabilised by strong indole-sulfate NH···O hydrogen bonds complemented by weaker aromatic CH···O or amide NH···O hydrogen bonds. The switching from one helical sense to the other was shown to be reversible and cyclic, as demonstrated by the CD spectral changes upon the sequential addition of a sulfate sequestering agent and sulfate.

Suk, Kim and Jeong have also demonstrated the use of chiral anions to induce chirally biased helices.[38] Indolocarbazole trimer **58** had previously been shown to exhibit enantiomeric helix formation upon the binding of sulfate within the cavity.[39] On the other hand, CD and NMR spectroscopy in dichloromethane show that chiral camphorsulfonates promote preferential *M*- or *P*-helix formation depending upon the enantiomer added. Strong affinity between the chiral adenosine 3′,5′-cyclic monophosphate (cAMP) and **58** (K_a = 1.1 × 10^4 M^{-1}), was also observed by ^{1}H NMR titration studies in a 1:9:90 $H_2O:CD_2Cl_2:CD_3CN$ solvent mix. CD spectroscopy in MeCN (containing 1% water) showed that the helix formed between **58** and cAMP was dissociated by the addition of CF_3COOH due to

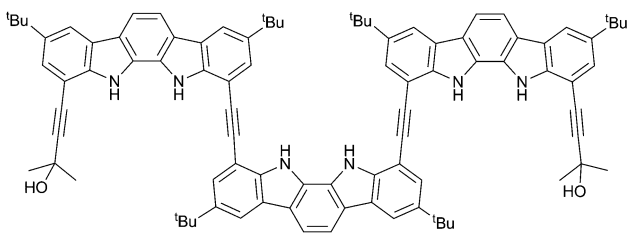

58

protonation of the phosphate group and that this dissociation could be reversed by the addition of the base DABCO, which regenerated cAMP phosphate. This cyclic and CD observable acid–base control of helix formation offers a possibility for the development of responsive chiroptical molecular switches.

Anion receptors containing CH hydrogen bond donors

As shown in the previous sections, the majority of hydrogen bonding anion receptors employ NH functionalities as hydrogen bond donors. However, in recent years OH and CH hydrogen bond donors have also become popular. Cao *et al.* have reported the anion-binding and electrochemical recognition properties of ferrocene appended aryl 1,2,3-triazole **59**.[40] ^{1}H NMR titration studies in CD_2Cl_2 showed that the binding affinities for 1 : 1 complexes follow the trend of $Cl^- > HP_2O_7^{3-} > H_2PO_4^-$. However, these titration studies and DFT calculations suggest that in the case of Cl^- only the aryl CH bonds of the triazole and phenyl groups are involved in hydrogen bonding to the anion, while in $H_2PO_4^-$ and $HP_2O_7^{3-}$ the cyclopentadienyl α-protons of the ferrocene groups also contribute to the binding between the anion and the receptor. Cyclic (CV) and differential pulse voltammetry showed that this conferred electrochemical recognition selectivity of **59** for phosphate ions. Electrochemical recognition studies showed that 2.0 equivalents of $H_2PO_4^-$ and $HP_2O_7^{3-}$ resulted in full saturation to the 1 : 1 receptor : phosphate anion complex with an associated cathodic shift in the CV spectrum, but no change was observed when testing the TBA salts of F^-, Cl^-, Br^-, I^-, PF_6^-, ClO_4^-, HSO_4^- and CH_3COO^-.

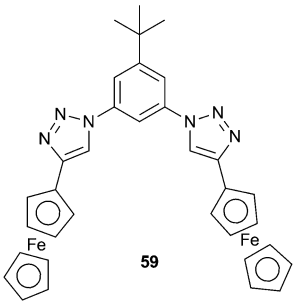

59

Ganguly, Das and co-workers have incorporated $^+PPh_3$ groups into an anthraquinone based receptor (**60**) in order to obtain an optical anion sensor through the activation of the methylene protons as C–H hydrogen bond donors that can bind anions.[41] The anion binding properties of the receptor with a range of TBA salts in acetonitrile were studied by ^{1}H and ^{31}P NMR, electronic spectroscopy and supported by DFT calculations. Weak interactions were observed for chloride, bromide and hydrogen sulphate, with much stronger interactions detected for dihydrogen phosphate and fluoride, where the binding stoichiometry was shown to be 1 : 2 receptor : anion and the formation constants $K_f = 2.24 \times 10^6$ M^{-1} for F^- and $K_f = 8.98 \times 10^4$ M^{-1} for $H_2PO_4^-$. The association of these anions and the receptor was accompanied by significant changes in the electronic spectra of the receptor and a distinct colour change, most noticeable in the case of fluoride. The receptor was shown to be highly effective at extracting fluoride from aqueous solutions, with an extraction efficiency of 99.3% and effective at concentrations of F^- as low as 0.06 ppm.

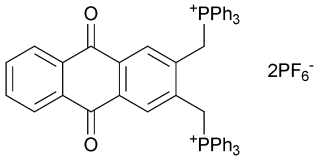

60

Kim and co-authors have described the use of imidazolium-anthracene based cyclophane **61** for the detection of guanosine-5′-triphosphate (GTP) and iodide in aqueous solutions at physiological pH with detection limits of 4.8×10^{-7} M and 8×10^{-5} M respectively.[42] Fluorescence spectroscopy studies in 100% aqueous solution at pH 7.4 with 100 equivalents of the TBA anion salts revealed the receptor's high selectivity for iodide and a range of phosphates, most significantly GTP, with the observation of chelation-enhanced fluorescence quenching (CHEQ) of excimer emission. Different binding modes were observed between the two anions with a 2 : 1 and 1 : 1 receptor : anion stoichiometry and affinity constants of $1.1 \times 10^3/2.1 \times 10^6$ M^{-1} and 1.3×10^4 M^{-1} for GTP and I^- respectively. ^{1}H NMR titration experiments and DFT calculations suggest that this altered binding mode is due to GTP being bound by two receptors through imidazolium CH$^+\cdots$O interactions while I^- is bound within the cavity through both imidazolium CH$^+\cdots$anion and anthracene CH$\cdots$anion interactions.

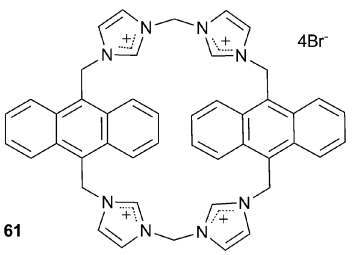

61

Flood and co-workers have been interested in the anion binding properties of aryl-triazole containing receptors (triazolophanes, *e.g.* **62**). These triazolophanes display high binding affinity for Cl^- (> 10^6 M^{-1} in CH_2Cl_2), due to pre-organisation (macrocyclic effect), the presence of CH hydrogen bond donor groups and size complementarity of the receptor and chloride. The properties of these triazolophanes have been recently review by Flood and co-workers.[43] In 2011, this research group also studied a variety of chloride : triazolophane complexes with varying degrees of conformational freedom (**62–64**) to verify the importance of structural rigidity as a pre-organisation factor paying the enthalpic cost of bringing together the electropositive CH hydrogen bond donor groups in the triazolophanes.[44] Computational studies were supplemented by ^{1}H NMR titrations to calculate the binding affinities and preparation free energies (the energy difference between the observed and ideal binding energies) for three triazolophanes (Scheme 7): a "strongly" preorganised macrocycle (**62**), a "partially" preorganised macrocycle (**63**) and a "poorly" preorganised macrocycle (**64**).

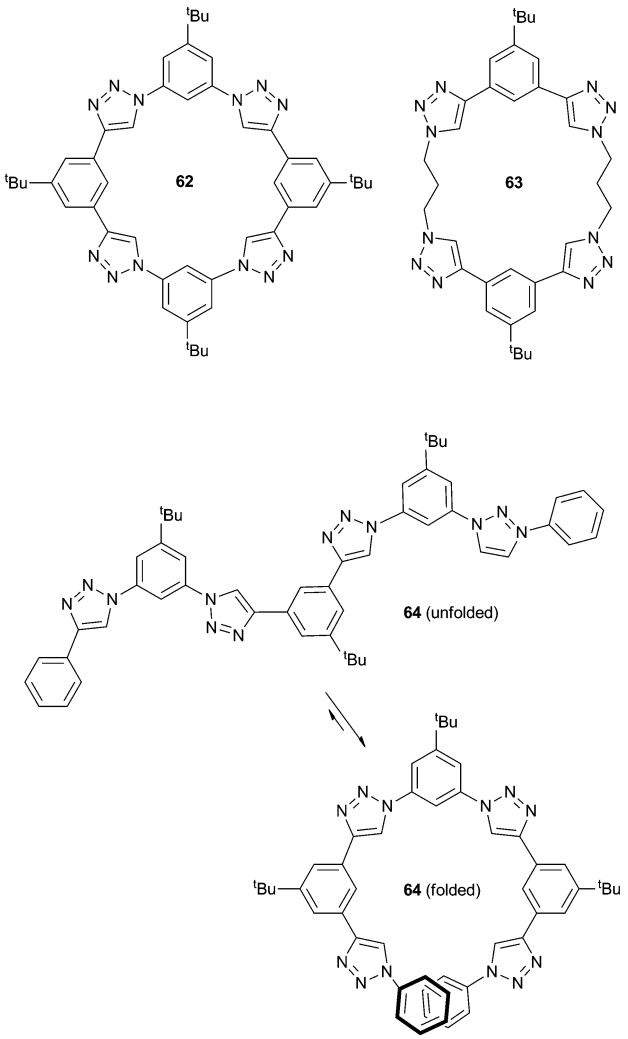

Scheme 7 Structure of triazolophanes **62–64** with various degrees of rigidity, and the folded and unfolded conformation of **64**.

These studies show that high rigidity (in combination with the macrocyclic effect) prevents the relaxation of close H···H contacts and retains the preorganised nature of the CH triazole hydrogen bond donors in **62** to maximise the strength of the receptor···anion interactions.

In a separate manuscript, Flood and co-workers have used the triazolophane scaffold to compare the strength of aromatic and aliphatic C–H hydrogen bond donors by replacing one of the phenylene groups in receptor **62** with a propylene linker in receptor **65**.[45] Gas phase computational studies showed that the length of the CH···Cl distance in the propylene based triazophane **65** was greater for the aliphatic (3.02 Å) than the aromatic (2.96 Å) CH donor, supporting its classification as a weaker interaction. The gas phase studies also suggested that the free energy of binding decreased from −194 to −182 kJ mol^{-1} upon substitution of the phenylene to a propylene unit and that the propylene unit interacts with chloride *via* a single CH···Cl hydrogen bond. ESI-MS and diffusion NMR spectroscopy were used to quantify all of the possible complexes present in solution, namely a 1:1 receptor:anion complex, a 2:1 sandwich complex and ion pairing (TBA^+Cl^- and $TBA^+[\mathbf{65}\cdot Cl]^-$). This allowed the deconvolution of the ion pairing events from chloride:receptor binding and hence the calculation of accurate 1:1 equilibrium binding constants for each receptor by ^{1}H NMR and UV/Vis titrations in CH_2Cl_2. The free energies of binding for each receptor were shown to be within experimental error (−38 ± 2 kJ mol^{-1} for **62** and −39 ± 2 kJ mol^{-1} for **65**), suggesting that the difference in CH···Cl hydrogen bond strength between aromatic and aliphatic donors can only be distinguished when they are competing within the same receptor.

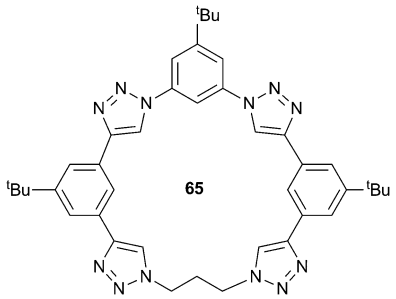

McDonald *et al.* have shown that the 1,8-napthalimide unit is an effective CH hydrogen bond donor in studies on receptor **66**, and quantified the strength of the anion binding from this interaction by comparison to an analogous receptor where the naphthalimide is substituted by 4-*tert*-butyl benzene (**67**).[46] UV/Vis and ^{1}H NMR titration studies in CD_2Cl_2 with a series of TBA salts demonstrate the high affinity of naphthalimide substituted receptor **66** for halide anions. Shifts in the ^{1}H NMR signals for the two CH naphthalene protons (H_d and H_g, Scheme 8) support their involvement in CH···anion hydrogen

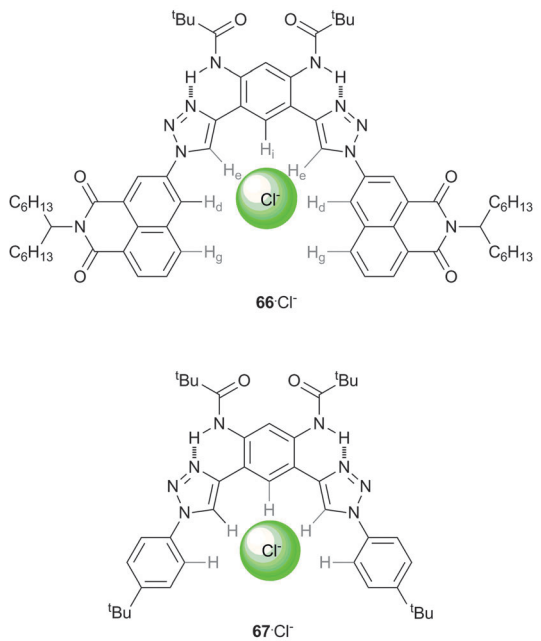

Scheme 8 Structures of receptors **66** and **67**, with the coordinating CH hydrogen atoms labelled in **66**, and showing the chloride binding site.

Table 2 Association constants K_a (M^{-1}) for **66–67** obtained *via* UV/Vis titrations with TBA salts in CH_2Cl_2 and changes in chemical shift $\Delta\delta$ (ppm) during NMR titrations of receptor **66** in CD_2Cl_2

Anion	K_a (**66**)	K_a (**67**)	$\Delta\delta$ (H_e)	$\Delta\delta$ (H_d)
Cl^-	$1.4 \pm 0.2 \times 10^5$	$4.2 \pm 0.2 \times 10^4$	2.2	0.7
Br^-	$3.9 \pm 0.5 \times 10^4$	$1.1 \pm 0.1 \times 10^4$	1.9	0.9
I^-	$7.8 \pm 2 \times 10^3$	$<10^3$	1.6	1.0

bonding interactions. As the size of the halide anion increases, the contribution of the CH···anion interaction of the napthalimide unit (H_d and H_g) to the binding increases, while the contribution of the triazole unit (H_e) decreases (Table 2). DFT calculations show that the CH···Cl^- distances increase from triazole (H_e) < napthalamide (H_d) < phenylene (H_i) and support a bifurcated CH···anion interaction of the napthalimide unit, analogous to that of urea, which gives an electronic binding energy greater than that of the triazole (ΔE of −80 kJ mol^{-1} *vs.* −64 kJ mol^{-1}). All these results suggest that naphthalimides possess strongly polarised CH donors suitable for anion binding.

Anion receptors employing halogen bonding, anion–π interactions and hydrophobic effects

The majority of anion receptors use electrostatic interactions or hydrogen bonding to bind anions, but in recent years more unconventional interactions such as halogen bonding, anion–π interactions and solvophobic effects have become popular. Out of these binding modes, halogen bonding, *i.e.* the non-covalent interaction between an electron-deficient halogen compound (Lewis acid) and a neutral or anionic Lewis base, is being increasingly exploited as an alternative to the commonly applied hydrogen bonding. Beer and co-authors have reported the anion binding properties of preorganised bidentate bromoimidazoliophane receptor **68**.[47] Two conformers of the receptor exist, the *syn* (**68a**) and *anti* (**68b**) forms, and they were found to exhibit different anion recognition behaviour in both solution and solid state. X-ray crystal structures of the bromide salts of the receptors show that the bromoimidazolium groups in the *anti* conformer **68b** each bind a bromide, while in the *syn* conformer **68a** the bromoimidazolium groups chelate a bromide to form a calix-like structure with the second bromide involved in hydrogen bonding interactions to a MeOH solvent molecule (Fig. 13). The sterics of the *syn*-conformer lead to a less linear halogen bonding interaction, 166.8° compared to 174° in the *anti*-conformer, and the increase in C–Br bond distance of the bromoimidazolium group from the *anti*- to *syn*-conformer suggests an increase in halogen bonding strength following the same trend. Proton NMR titration studies in 9 : 1 CD_3OD : D_2O found no significant binding of TBA halides in solution for the *anti* conformer, however, the *syn* conformer was shown to form 1 : 1 complexes with affinity constants of 889 M^{-1}, 184 M^{-1}, 184 M^{-1} and <10 M^{-1} for bromide, iodide, chloride and fluoride respectively. This high selectivity for bromide was not observed in the protic version of the receptor, **69**,

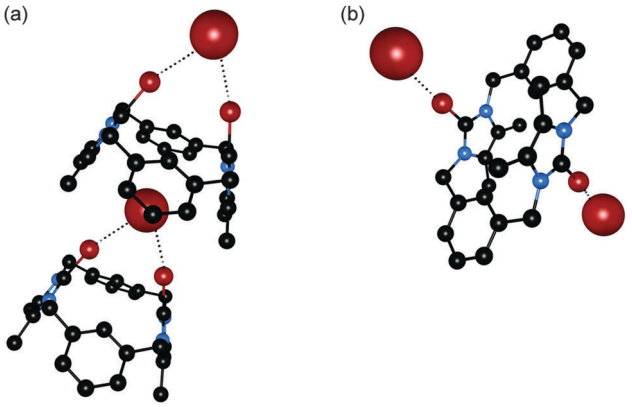

Fig. 13 Crystal structures of (a) **68a**·2Br (non-coordinating bromide ion is omitted for clarity) and (b) **68b**·2Br. Hydrogen atoms and solvent molecules are omitted for clarity; halogen bonds are represented by dashed lines; the coordinated bromide anion is shown in spacefill, with the receptor in ball-and-stick.

with moderate binding of ~100 M^{-1} observed for chloride, bromide and iodide. This suggests that substitution of halogen atoms into hydrogen bond receptors can alter both the electronic and geometric features of the receptor and hence the exhibited anion recognition properties.

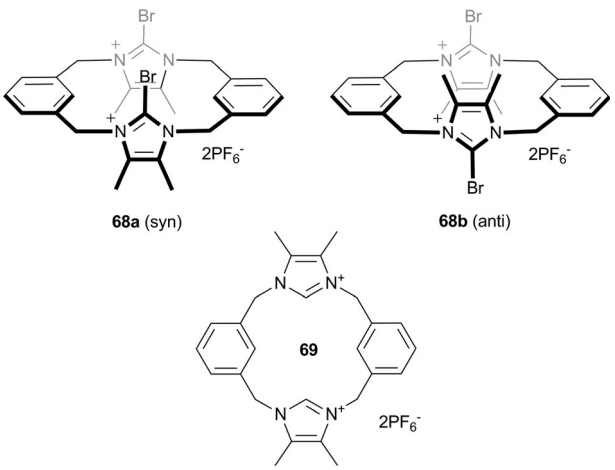

Beer and co-workers have also incorporated the bromoimidazolium motif into catenane **70**, which was synthesised *via* bromide anion templation.[48] The receptor was designed to give a linear arrangement of the two halogen bond donor groups, resulting in cooperative halogen bonding interactions with anions. The incorporation of the naphthalene spacer allowed for the optical sensing of anions by fluorescence spectroscopy, with studies showing that while no change was observed for corresponding macrocycle **71** with the TBA salts of fluoride, chloride, bromide, iodide, acetate, dihydrogen phosphate, nitrate and the TEA salt of bicarbonate, catenane **70** displayed selective recognition of chloride and bromide, with no optical changes observed for the remaining anions. This suggests that the 1 : 1 binding of chloride and bromide by the catenane, with affinity constants of 3.71×10^6 M^{-1} and 1.48×10^5 M^{-1} respectively, was achieved through size

complementary recognition and the preorganised cooperative nature of the halogen bond donor groups.

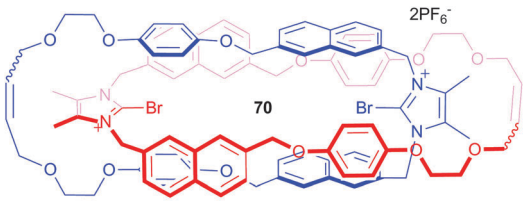

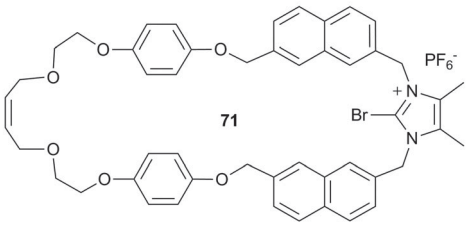

Taylor and co-workers have studied a series of urea based receptors incorporating iodoperfluorobenzoate groups (**72a,b**, **73a,b**, **74a,b**, **75a,b** and **76a,b**) in an attempt to use hydrogen bonding and halogen bonding in concert to bind anions.[49]

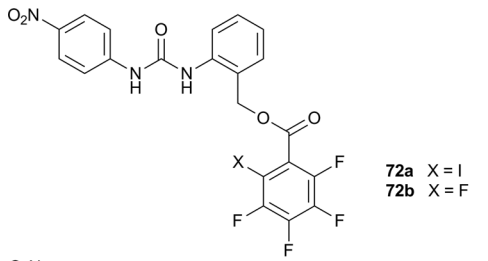

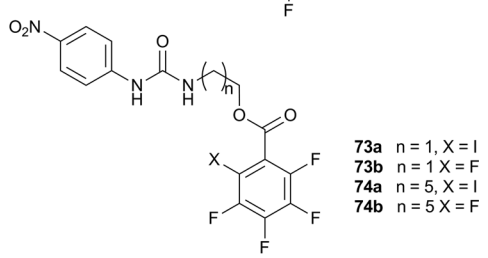

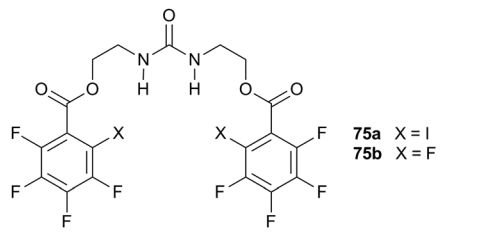

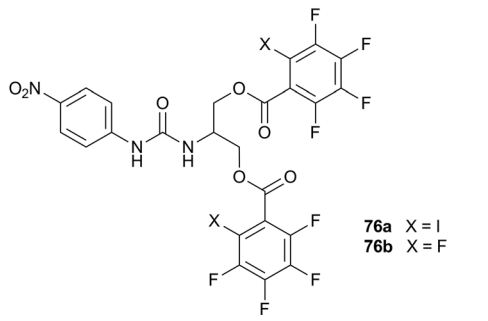

Solution state UV/Vis, ^{1}H NMR and ^{19}F NMR titration studies characterised the binding strength between the urea receptors and TBA salts of halides and oxoanions in CD_3CN and suggested a 1 : 1 binding stoichiometry for all receptor : anion complexes. The results demonstrate that hydrogen bonding and halogen bonding can occur simultaneously and show that incorporating halogen bond donor groups into urea based systems confers halide selectivity to receptors that have high affinity for Y-shaped anions, without negating the strength of the interactions with oxoanions. Incorporation of perfluorinated benzoates into the scaffolds as controls that do not participate in halogen bonding (**72b**, **73b**, **74b**, **75b** and **76b**) allowed the quantification of the halogen bond contribution to the overall anion binding. For example in the symmetrical urea receptor **75a** the affinity constant for the binding of halides was 30 times greater than observed with **75b**, where no halogen bond donor group is present. Computational studies supported the observed dependence of halogen bond contribution to anion binding on the length of the linker, with receptors where the linker results in a more linear XB···anion interaction shown to give a greater halogen bonding contribution to the overall anion binding, illustrating the strong preference for linear geometry in halogen bonding. The contribution of the halogen bond to the overall thermodynamics of anion binding was found to be negligible for the majority of oxoanions, NO_3^-, HSO_4^-, TsO^- (<0.2 kcal mol^{-1}), small for BzO^- and $H_2PO_4^-$ (0.3 and 0.4 kcal mol^{-1}) and significant for the halides (approaching 1 kcal mol^{-1}).

Anion···π interactions, the non-covalent interactions between an anion and an electron deficient π-system, are far less common than their cation···π counterparts but have received recent attention. Giese *et al.* have reported the anion binding properties of phenylbenzamide derivatives **77–80** in both the solid and solution state.[50] In the crystal structure of tetraethylammonium (TEA) bromide with pentafluorobenzamide **77** an interaction between the aromatic pentafluorophenyl ring and the bromide anion was observed, with a Br···centroid distance of 3.67 Å. The bromide anion is offset from the centre of the ring due to the additional NH···Br interaction (3.431 Å) (Fig. 14). The effect of the electron withdrawing C_6F_5 group to promote cooperative NH···anion and anion···π binding interactions by acidifying the NH bond and providing an electron poor arene ring for increased strength anion···π interactions was further investigated in solution by ^{1}H and ^{19}F NMR titration studies of *N*-phenylbenzamides **78–80**

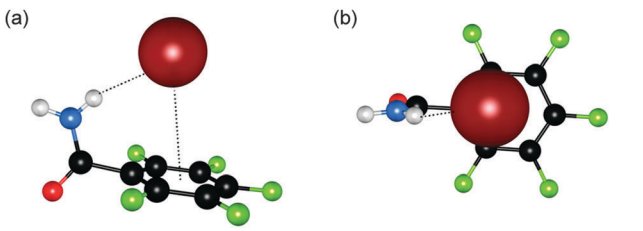

Fig. 14 Two views (a and b) on the crystal structure of pentafluorobenzamide **77** and TEA bromide. The bromide anion is shown in spacefill with the receptor in ball-and-stick; hydrogen bonds and anion···π interactions are shown as dashed lines.

with the TBA salts of Cl^-, Br^-, I^-, BF_4^- and PF_6^-. Titrations of **78** and **79** were performed in $CDCl_3$ while solubility issues meant the titrations of **80** were conducted in CD_3CN. A 1 : 1 stoichiometry was confirmed for the receptors with all anions except PF_6^- where ambiguity between 1 : 1 and 2 : 1 receptor : anion complexation was observed. Affinity constants suggest that the strength of anion binding increases from $I^- < Br^- < Cl^-$, with the binding constants for each receptor calculated from the shifts in the amide NH signals. The increase in anion binding strength from **79** < **78** < **80** was attributed to the electron-withdrawing effect of the C_6F_5 unit and the presence of two amide NH donor groups in **80**. Low temperature NMR and computational studies suggest that anion receptor complex **80** exists as the symmetric conformer.

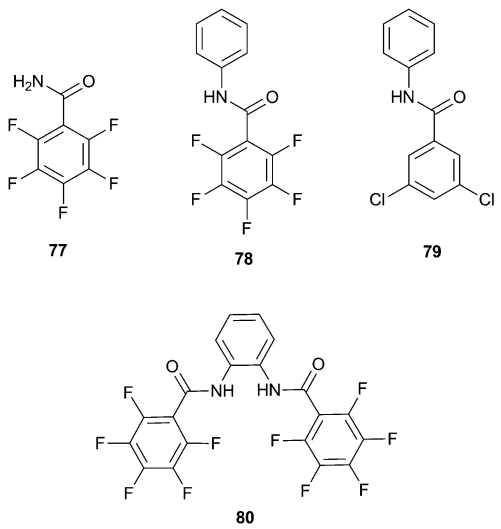

Saha and co-workers have characterised the range of interactions that can occur between electron deficient naphthalene-diimides (NDIs) and a variety of anions.[51] By altering a NDI scaffold by substituting either the core with electron withdrawing substituents (**81**) or the nitrogen centres with various electron donating or electron withdrawing groups (**82–90**) they were able to control the π-acidity of the NDIs. Electrochemical studies showed that core substitution enhances π-acidity more dramatically than substitution at the nitrogen centres. The interactions of the NDIs with the TBA and TEA salts of decreasing Lewis bases $OH^- > F^- > CN^- > AcO^- > H_2PO_4^- > Cl^- > Br^- > I^- > PF_6^-$ were probed using ESI-MS and ITC (in 1,2-dichlorobenzene) and 1 : 1 anion : receptor complexes were observed with affinity constants shown to decrease as the π-acidity of the NDI decreased and as the Lewis basicity of the anion decreased. The interaction was shown to be dependent on the electron donor–acceptor strengths and not on CH···anion interactions, as NMR titrations showed that iodo- and fluoro-substituted NDIs **82**, **83** and **87**, with no possible CH donors, have higher binding affinities. This was complemented by computational studies where electrostatic potentials suggest that the imide rings of the NDIs are the most electron-deficient. The strength of the interaction was shown to be controlled by the strength of both the anion and NDI basicity. With the strongly π-acidic NDI **81** thermal electron transfer (ET) to form both $NDI^{\bullet-}$ and NDI^{2-} was observed with OH^-, F^- and CN^- in CD_3CN in the dark. The method of transfer was confirmed by UV/Vis, EPR spectroscopy, ^{19}F NMR and XPS, which provided no evidence of C–F bond formation but the sequential formation of the $F^{\bullet}$, $NDI^{\bullet-}$ and NDI^{2-} radical species. Switching on thermal anion-to-NDI ET was shown to be possible by maximising the π-acidity of the receptor and basicity of the anion. Moderately basic anions were shown to result in light induced PET (photo-induced electron transfer), while for the weakly basic anions such as I^- and less electron deficient NDIs no ET was suggested and only anion···π interactions were observed. The basicity of the solvent was also shown to affect the interactions between the anion and NDI with higher solvation of anions in polar solvents hindering their electron donating ability.

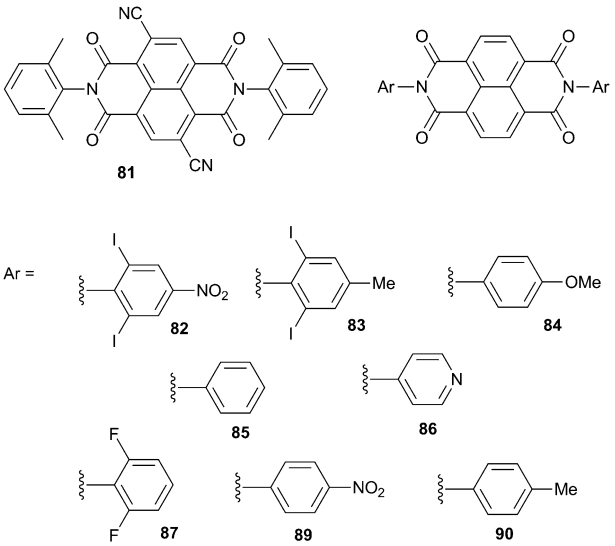

Solvophobic effects (usually hydrophobic) play an important role in supramolecular chemistry, but are often overlooked. Gibb and Gibb have studied the curved amphiphile **91** (based on the calixarene structure) with a water soluble outer coat comprised of 8 carboxylic acids, and a 8 Å × 8 Å hydrophobic pocket capable of binding a range of hydrophobic guests including adamantane carboxylic acid.[52] ^1H NMR titration studies in 10 mM phosphate buffer at pH 11.3 with the sodium salts of a range of anions, showed that the amphiphile displays Hofmeister selectivity, with no association observed for strongly and moderately solvated anions (F^-, SO_4^{2-}, AcO^-, Cl^-, and Br^-) while for the weaker solvated anions the signals of the benzyl protons at the base of the hydrophobic cavity were observed to shift downfield upon increasing concentration of anion. Fitting of the isotherms suggested a 1 : 1 ratio of anion : **91**, with association constants increasing across the Hofmeister series from $NaNO_3$, $<1\ M^{-1}$; $NaClO_3$, $3\ M^{-1}$; NaI, $11\ M^{-1}$; NaSCN, $33\ M^{-1}$; to $NaClO_4$, $95\ M^{-1}$. *In silico* studies suggest that the perchlorate anion moves from solvation by eight waters to three or four waters upon binding within the hydrophobic cavity, supporting the hypothesis that the observed anion selectivities are related to the adaptability of the anion's solvation shell, with strongly solvated anions unable to reorganise or lose part of their solvation shell, meaning they cannot be

accommodated within the cavity of the amphiphilic host. ITC experiments in 10 mM phosphate buffer at pH 11.3 in the presence of adamantane carboxylic acid show that chlorate, iodide, thiocyanate and perchlorate are able to compete with the hydrophobic guest and weaken the hydrophobic effect, with the binding of adamantane carboxylic acid 1.5 kcal mol^{-1} lower in the presence of perchlorate than in the presence of fluoride (the free energy of binding for adamantane carboxylic acid and **91** in the absence of salts is 9.1 kcal mol^{-1}).

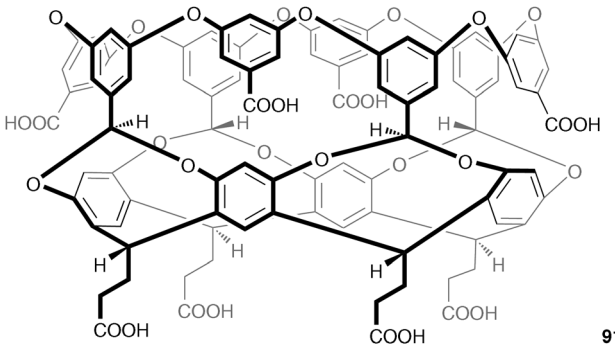

91

Metal and Lewis acid containing anion receptors

Metal and Lewis acid containing anion receptors have also remained popular during 2011 and 2012. Yam and co-workers have reported highly luminescent bifunctional receptor **92** containing a 1,3-alternate calix[4]-crown-5 moiety for potassium binding and Lewis acidic borane centres for the coordination of fluoride anions.[53] The free receptor was found to display an intense electronic absorption band at 342 nm and bright blue fluorescence in dichloromethane. The emission was attributed to an excited state caused by intramolecular charge transfer from the phenolic oxygen atoms to the boron centres *via* the conjugation of the alkynyl spacers. UV/Vis and fluorescence titrations were performed with a range of anions in dichloromethane. Receptor **92** was found to interact strongly and selectively with F^- by complexation through the Lewis acidic boron centres. This interaction caused significant fluorescence quenching as a result of the destruction of the intramolecular charge transfer. The binding constant for this process was determined as $\log K_a = 4.46 \pm 0.1$. Additionally, the complexation of K^+ cations was observed by similar means in 1 : 1 dichloromethane : methanol, and induced a blue shift with

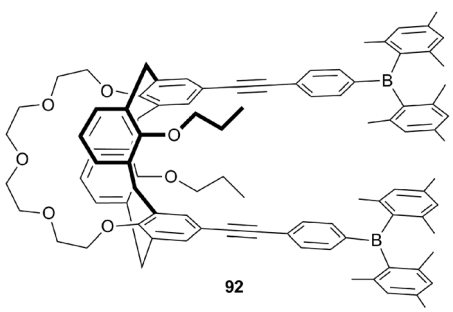

92

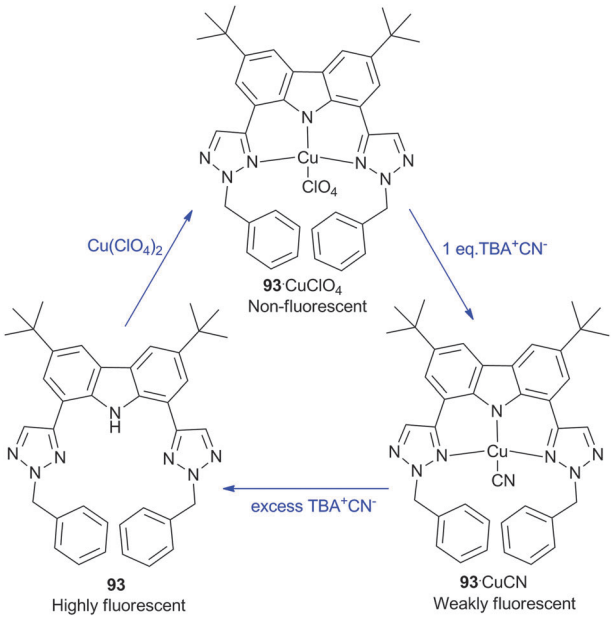

Scheme 9 The proposed mechanism of CN^- sensing by the **93**–Cu(II) complex.

enhancement in the absorbance and extensive fluorescence quenching.

Jang and co-workers have reported the CN^- sensing properties of the copper(II) complex of ligand **93**.[54] The free ligand was found to exhibit strong absorptions around 300 and 370 nm and fluorescence emission around 385 nm in MeCN. On the addition of copper(II)perchlorate, the fluorescence emission at 385 nm almost completely disappeared after the addition of 1 equivalent of copper(II). The authors then investigated the response to the addition of tetrabutylammonium cyanide (TBA^+CN^-). UV/Vis and fluorescence titrations indicated the presence of two areas of spectral change; on the addition of up to 1 equivalent of CN^- the absorptions around 360 and 408 nm were found to gradually increase, with an accompanying linear increase in fluorescence intensity. When further amounts of CN^- were added the fluorescence intensity increased much faster, and by the addition of 10 equivalents of anion the fluorescence of the free ligand had been largely recovered. This was attributed to the de-metallation of the **93**-Cu complex in the presence of excess CN^- (Scheme 9). However, the authors noted that up to the addition of 1 equivalent of cyanide this system could also be used to accurately determine micromolar concentrations of CN^-.

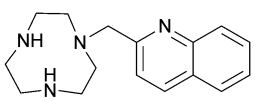

94

Caltagirone and Lippolis have reported the anion complexation properties of the copper(II) complex of ligand **94**.[55] This ligand had been previously reported as a fluorescent sensor for zinc(II) ions,[56] and the authors reasoned that the analogous copper(II) complex would be coordinatively unsaturated and therefore suitable for anion complexation. The solution phase

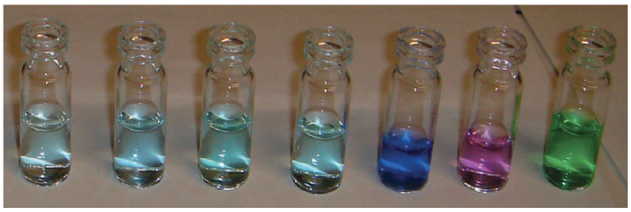

Fig. 15 Colour change of [Cu(**94**)](BF$_4$)$_2$·MeCN (10^{-3} M) upon the addition of different anions in MeCN. From left to right: free receptor; +1 eq. F$^-$; +1 eq. Cl$^-$; +1 eq. Br$^-$; +1 eq. CN$^-$; +2 eq. CN$^-$; +1 eq. I$^-$. Reproduced with permission from *Chem. Commun.* 2011, **47**, 3805–3807. © Royal Society of Chemistry.

response of [Cu(**94**)](BF$_4$)$_2$·MeCN to a range of anions was investigated in MeCN and H$_2$O by UV/Vis titration. The authors found that only the addition of CN$^-$ and I$^-$ anions produced a significant response. The interaction with I$^-$ was found to follow a 1 : 1 binding stoichiometry and gave a binding constant of $\log K_a = 4.8 \pm 0.1$ in MeCN, with weaker binding observed in H$_2$O ($\log K_a = 2.4 \pm 0.1$). The interaction with CN$^-$ was found to be more complex in MeCN, with the formation of stable 1 : 1 and 2 : 1 anion : receptor complexes, while in H$_2$O the formation of the 1 : 1 CN$^-$ complex was significantly more favourable than the I$^-$ complex ($\log K_a > 7$). Remarkably, the spectral changes upon the addition of these anions allowed for the naked eye detection of I$^-$ in MeCN only and CN$^-$ in both MeCN and H$_2$O (Fig. 15). In MeCN the formation of two different **94**·CN$^-$ complexes is evident to the naked eye with a colour change from cyan (no anion) to dark blue (1 equivalent of CN$^-$) to pink (2 equivalents of CN$^-$). Crucially, this report represents the first example of CN$^-$ sensing by a Cu(II) complex without removal of the Cu(II) centre from the receptor complex.

Lindoy and co-workers have previously reported the formation of a [Fe$_4$L$_6$]$^{8+}$ cage (L = **95**) which has been used for the encapsulation of anionic guests such as BF$_4^-$ and PF$_6^-$, with selectivity for the latter guest.[57] The BF$_4^-$ inclusion complex could be generated by forming the cage from a mixture of ligand **95** and Fe(BF$_4$)$_2$·6H$_2$O in MeCN. In a recent study the same authors have reported that attempts to form the cage using FeCl$_2$·5H$_2$O as a source of iron(II) in MeCN followed by anion exchange with KPF$_6$ yielded an unprecedented complex in which the encapsulated anionic species was [Fe^{III}Cl$_4$]$^-$.[58] Microanalysis confirmed that the stoichiometry of the deep red product was Fe$_4$L$_6$·(FeCl$_4$)·(PF$_6$)$_7$·CH$_3$OH (with L = **95**) and the structure of this complex was elucidated by single crystal X-ray diffraction (Fig. 16). The encapsulated [FeCl$_4$]$^-$ anion was found to have perfect tetrahedral symmetry with Fe–Cl bond lengths in the expected range for this species (2.1994(17) Å). Given that this anion is not displaced by PF$_6^-$ during the purification process (when this host had previously shown good selectivity for PF$_6^-$ over BF$_4^-$) the authors reasoned that the size, shape and symmetry of the [FeCl$_4$]$^-$ guest must be highly complementary to the cavity of this cage.

Nitschke and co-workers have continued their work on self-assembled tetrahedral cages, including a report on face-capped tetrahedral Fe$_4$L$_4$ cages of different sizes that can encapsulate a

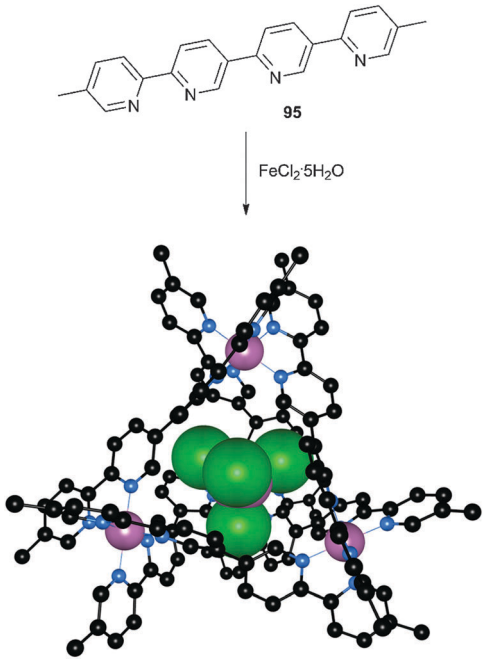

Fig. 16 The encapsulation of [FeCl$_4$]$^-$ within a Fe$_4$(**95**)$_6$ cage, along with the crystal structure of Fe$_4$(**95**)$_6$·(FeCl$_4$)·(PF$_6$)$_7$·CH$_3$OH. Iron and [FeCl$_4$]$^-$ ions are shown in spacefill with ligand **95** in ball-and-stick (iron: purple, chloride: green, nitrogen: blue, carbon: black). Hydrogen atoms, solvent molecules and counterions are omitted for clarity.

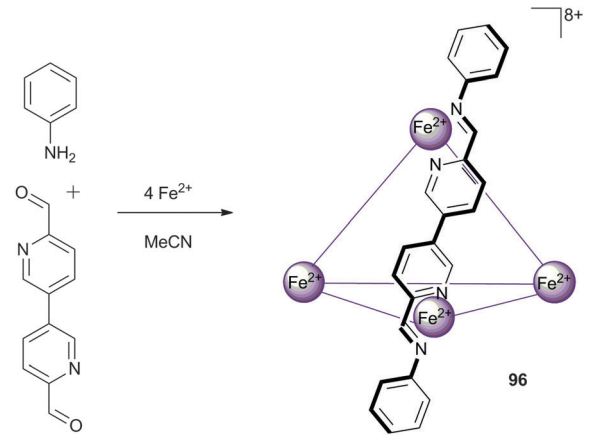

Scheme 10 The construction of Nitschke's M$_4$L$_6$ cages with reconfigurable exterior.

variety of neutral guests (depending on the size of the cage),[59] and a report on a series of M$_4$L$_6$ cages of the form **96** in which the exterior framework of the cage is exchangeable.[60] In the latter, the cage is constructed by the generation of the ligands *in situ* as shown in Scheme 10. As the ligand synthesis is reversible, the addition of alternative anilines into the system can lead to displacement of the original aniline and the generation of a new cage structure in a dynamic process. In general, anilines substituted with electron donating substituents appeared to be favoured; thus, the addition of *p*-methoxyaniline into a cage formed from *p*-chloroaniline resulted in the quantitative displacement of the *p*-chloroaniline residues, as observed by

^{1}H NMR. If the electronic properties of the anilines used had greater similarity, a mixture of products was observed by ESI-MS analysis with varying degrees of substitution. The cages were all found to encapsulate BF_4^- and PF_6^- counteranions from the reaction media, which were difficult to remove from the cavity causing difficulties in investigating the anion binding properties of the free host. Consequently, cage **96** was synthesised with a trifluoromethanesulfonamide counteranion, which is too large to be contained within the cage, thus enabling anion complexation studies. Using NMR titration techniques in CD_3CN, the authors found that BF_4^- and OTf^- were suitable guests, with binding constants determined as $K_a = 2.3 \times 10^4$ M^{-1} and 5.2×10^4 M^{-1} respectively. The binding of PF_6^- was found to be exceptionally strong, with a binding constant of $K_a = 1.3 \times 10^6$ M^{-1} estimated by competitive binding experiments with BF_4^- and OTf^-, representing the strongest example of host–guest binding for a metal–organic host that can be isolated in the absence of a guest.

Self-assembled and anion templated molecular architectures

In the previous sections there have already been some examples of self-assembled structures, but in most of those cases it was the metal ion that drove the self-assembly. Cases where the anion functions as a template for the self-assembled structure or where the anion influences the architecture *via* allosteric effects are less common. Nitschke and co-workers have described a dynamic system where the addition of one anion (perchlorate) triggers a structural reorganisation to obtain a new structure with a high affinity for another anion (chloride).[61] A dynamic library **97** containing a mix of coordinated complexes was created from the reaction between *p*-toluidine, 6,6′-diformyl-3,3′-bipyridine and cobalt(II)triflimide hydrate in MeCN. The addition of KPF_6 or NaOTf to this library leads to the formation of tetrahedral $Co_4L_6^{8+}$ cage **98** as the only observed species in ^{1}H NMR and ESI-MS spectroscopy, with the anions (PF_6^- or OTf^-) encapsulated within the tetrahedral cage. Interestingly, the addition of $LiClO_4$ to these tetrahedral cages or to the original dynamic library leads to the transformation into a pentagonal prism $Co_{10}L_{15}^{20+}$ (**99**) as the unique species observed by ^{1}H NMR and ESI-MS spectroscopy (Scheme 11). Single crystal X-ray crystallography of **99** revealed that it forms a "barrel-like" structure formed by 60 chemical species and that the ligands form five anion binding pockets on the outside of the barrel, ideally suited for the ClO_4^- anions that occupy these sites, and one binding pocket on the inside of the barrel, ideally suited for the Cl^- anion that occupies this site (Fig. 17). As no chloride was added to the mixture, the authors postulate that the chloride anions were scavenged from the glassware and thus that the affinity of the $Co_{10}L_{15}^{20+}$ pentagonal prism **99** for chloride must be extremely high. When specifically added during formation, other anions such as F^-, Br^-, N_3^-, OCN^- and SCN^- could also be bound inside the cavity of the $Co_{10}L_{15}^{20+}$ pentagonal prism (but not HF_2^-, CN^-, $SeCN^-$, acetylene or CO_2). A pentagonal prism with an empty central pocket could be obtained by

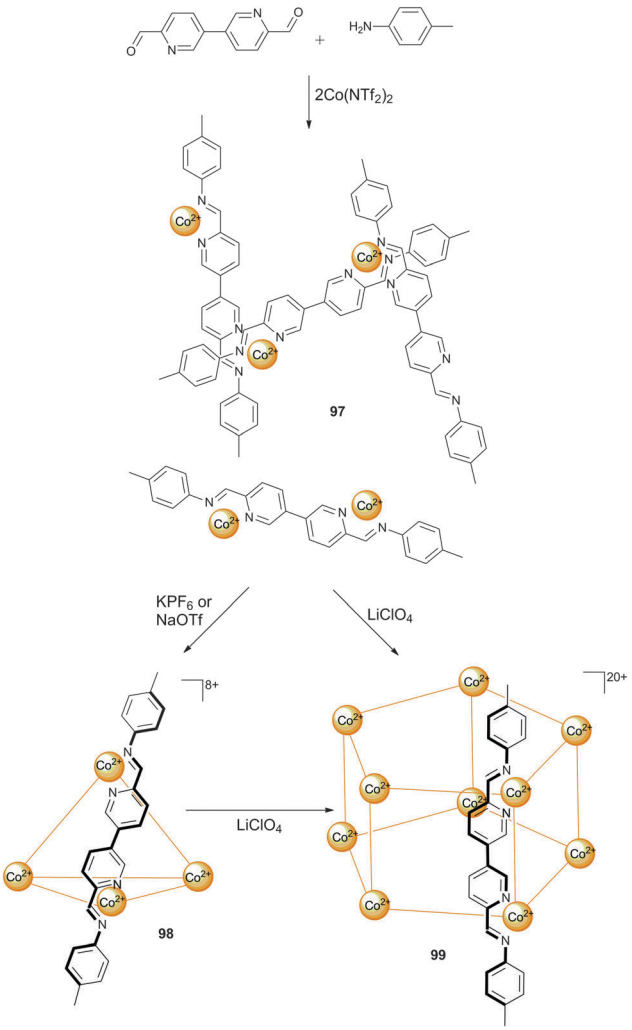

Scheme 11 Formation of dynamic library **97**, tetrahedral cage **98** or pentagonal prism **99**.

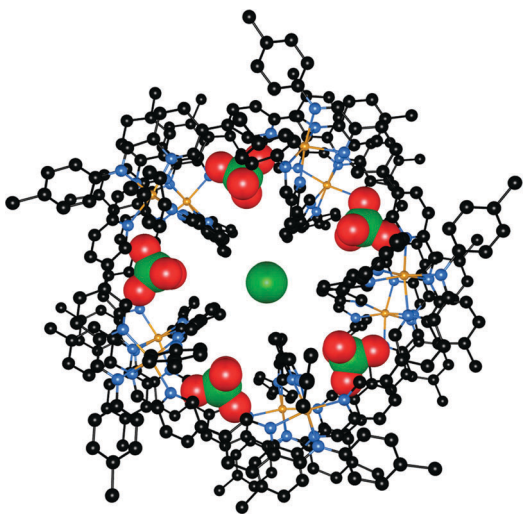

Fig. 17 Crystal structure of **99**·ClO_4·Cl (top view). Perchlorate and chloride anions are in spacefill, with the ligands and cobalt ions (gold) in ball-and-stick. Hydrogen atoms and non-coordinated counterions are omitted for clarity.

replacing *p*-toluidine with 4-hydroxyaniline during formation, indicating that only the peripheral perchlorate anions are necessary to template the formation of the pentagonal prism, while the central anion is not required as a template but is merely bound with high affinity. The authors also note that a similar pentagonal prism could be obtained from the PF_6^- adduct of tetrahedral cage **98** after heating the sample for a prolonged period of time.

Sessler and co-workers have reported tetracationic macrocycle **100** that is able to form ''molecular boxes'', environmentally responsive pseudorotaxanes, or metal-linked supramolecular polyrotaxanes, depending on the anion used and the external stimuli provided.[62] The authors have previously reported that macrocycle **100** can bind terephthalate dianion **101** on the outside of the macrocycle.[63] Alternatively, when receptor **100** is exposed to the larger dianion **102** a pseudorotaxane is formed with a 2 : 3 host : guest stoichiometry (pseudodimeric species of the pseudorotaxane), as confirmed by ^{1}H NMR titrations, NOESY NMR and Job plot analysis in DMSO-d_6 and ESI-MS. Furthermore, the addition of related dianion **103** to **100** results in the formation of a pure 1 : 1 pseudorotaxane, as confirmed by ^{1}H NMR titrations and NOESY NMR experiments. The different supramolecular architectures that were obtained from macrocycle **100** with the varying anions **101–103** are represented by their crystal structures shown in Fig. 18a–c. The authors also showed that not only the nature of the anionic guest influences the obtained supramolecular architecture and stoichiometry, but also temperature, pH and $Ag(I)^+$ cations. Variable temperature ^{1}H NMR showed that increased temperature leads to de-threading of the pseudorotaxanes, while pH-dependent ^{1}H NMR studies showed that lower pH (upon addition of CF_3COOD) can also lead to de-threading and the regeneration of free **100** due to the formation of the neutral dicarboxylic acid forms of the anions (pseudorotaxane formation was still observed for the monoprotonated forms of the dianions **101–103**). Subsequent addition of base (triethyl-amine) converts the acids back to their dianionic form and hence results in the formation of pseudorotaxanes and this cycle of threading and de-threading can be repeated several times by the addition of acid and base. Interestingly, the addition of Ag(I) (as a PF_6^- or NO_3^- salt) to a mixture of **100** and **103** leads to the formation of a polyrotaxane whereby the monomers are the individual 1 : 1 pseudorotaxanes **100**·**103** held together in a 1D supramolecular polymer *via* Ag(I) cation bridges, as observed by single crystal X-ray diffraction (Fig. 18d).

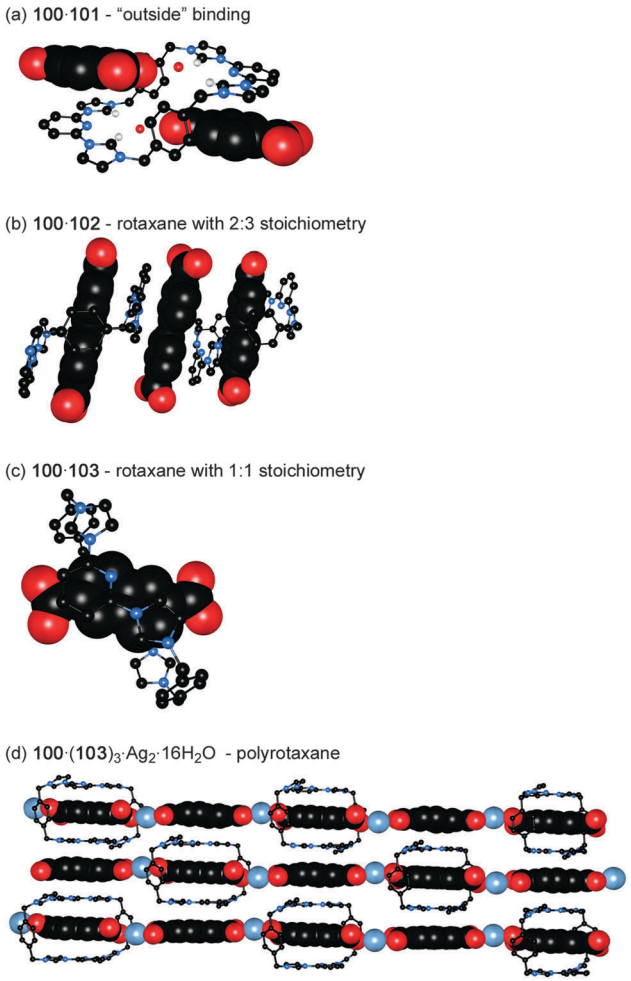

Fig. 18 Crystal structures of Sessler's tetracationic macrocycle with various dianions. Hydrogen atoms, solvent molecules and counterions have been omitted for clarity; the dianions are shown in spacefill with the macrocycle in ball-and-stick. (a) $[\mathbf{100}\cdot\mathbf{101}]^{2+}$ showing that the dianion is bound outside the macrocycle (no threading); (b) $[\mathbf{100}\cdot\mathbf{102}]^{2+}$ showing rotaxane formation with 2 : 3 stoichiometry; (c) $[\mathbf{100}\cdot\mathbf{103}]^{2+}$ showing rotaxane formation with 1 : 1 stoichiometry; (d) $\mathbf{100}\cdot(\mathbf{103})_3\cdot Ag_2\cdot 16H_2O$ showing polyrotaxane formation upon the addition of Ag(I).

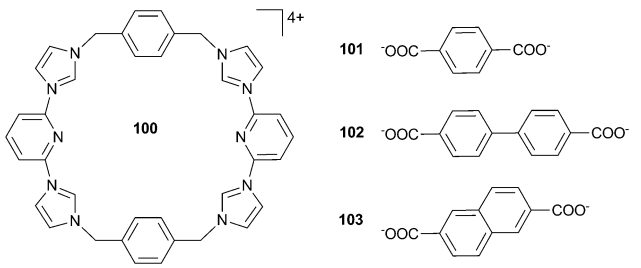

Singh and Sun have reported the solvent-dependent reversible nitrate binding and self-assembly properties of tripodal receptor **104**.[64] The HNO_3 complex of **104** was observed as the sole species when nitric acid was added to a methanol suspension of **104** and the structure of **104**·HNO_3 was confirmed using single crystal X-ray diffraction. However, it was found that when nitric acid in aqueous methanol was added to a chloroform solution of **104**, two species were observed in ^{1}H NMR and ESI-MS experiments, namely the HNO_3 adducts of **104** and of its nitro substituted analogue **105**. On the other hand, when nitric acid was added to a MeCN solution of **104**, the HNO_3 complex of **105** was observed as the sole species, as confirmed by ^{1}H, COSY, HSQC, HMBC and ROESY NMR and ESI-MS. Furthermore, when $CHCl_3$ was added to a DMSO solution of the HNO_3 complex of **105**, the formation of self-assembled dimer $(\mathbf{105})_2$ was observed using ^{1}H NMR and ESI-MS techniques. Thus, chloroform caused the release of the bound nitric acid and the subsequent formation of homodimer $(\mathbf{105})_2$ *via* hydrogen bonding between the amide NHs and the *ortho* nitro substituents, and this was found to be reversible as the evaporation of

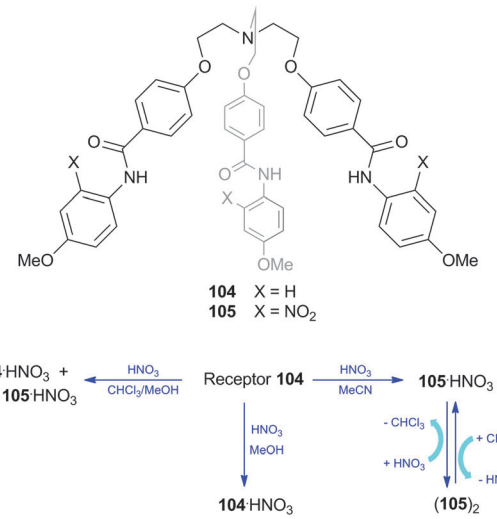

Scheme 12 Structure of receptor **104** and the nitro analogue **105** produced upon addition of HNO_3, along with the various solvent-dependent conversions between receptor and complexes and dimers.

chloroform from this solution resulted back in the formation of **105**·HNO_3. The various solvent-dependent conversions between **104**, the nitrated analogue **105**, HNO_3 adducts of the receptors and homodimer $(\mathbf{105})_2$ are shown in Scheme 12.

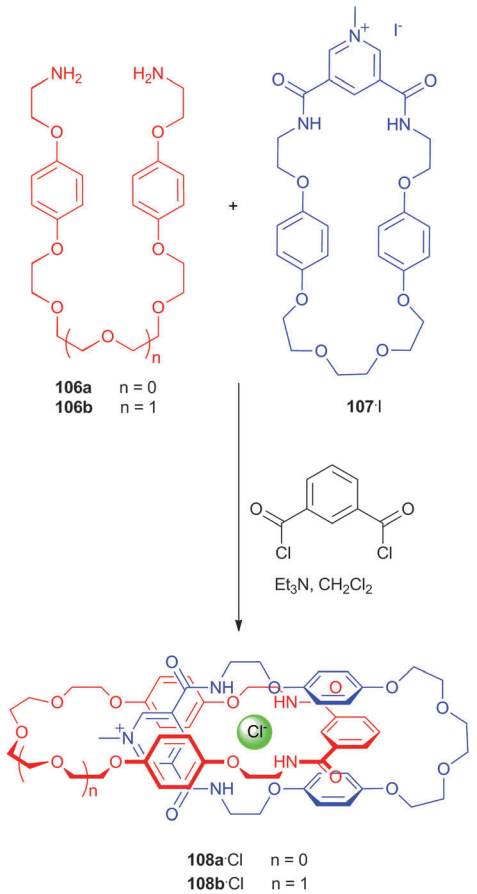

Scheme 13 Chloride templated synthesis of [2]catenanes **108a** and **108b** by Beer and co-workers.

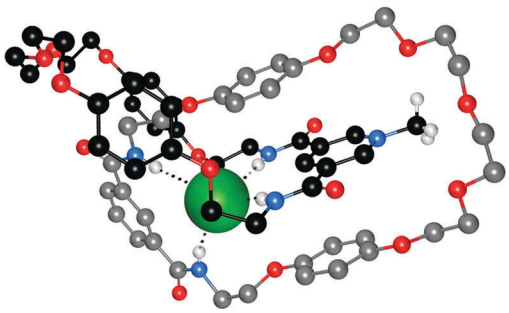

Fig. 19 Crystal structure of **108a**·Cl. The chloride anion is shown in spacefill with the macrocycles in ball-and-stick (one macrocycle is shown in a lighter shade of grey for clarity); non-coordinating hydrogen atoms, disorder and solvent molecules are omitted for clarity; hydrogen bonds with the chloride anion are represented by dashed lines.

Beer and co-workers have continued their work on anion templated catenanes. In a 2011 communication they reported a new synthetic pathway for preparing [2]catenanes (*e.g.* **108a,b**), based upon the association between an acyclic flexible bis-amine with a positively charged macrocycle, followed by a ring-closure reaction with an appropriate bis-acid chloride mediated by chloride anion templation (Scheme 13).[65] The new catenanes thus obtained (**108a** and **108b**) were characterized using ^{1}H NMR, ^{13}C NMR, 2D ^{1}H ROESY NMR and ESI-MS and the interlocked structure of **108b** was also confirmed *via* single crystal X-ray diffraction (Fig. 19). These experiments also showed that the chloride : catenane complexes are stabilized through hydrogen bonding interactions between chloride and the amides, π–π donor–acceptor interactions between the pyridinium surface and the hydroquinone rings and hydrogen bonding between the pyridinium methyl protons and the polyether oxygens of the neutral macrocycle. In order to determine anion binding affinities, the templating chloride anion in **108a** and **108b** was exchanged for the non-coordinating PF_6^- anion. ^{1}H NMR titrations in 1 : 1 $CDCl_3$: CD_3OD revealed that 1 : 1 anion : receptor complexes were formed in the case of Cl^-, Br^-, $H_2PO_4^-$ and OAc^- (as TBA^+ salts), with the strongest interactions seen for Cl^-, presumably due to the complementary size and geometry of chloride and the catenane binding cavity.

Employing a similar chloride templated synthetic strategy, Beer and colleagues have also reported the synthesis and properties of redox-active, ferrocene-containing [2]catenane **109** and the self-assembled monolayer of analogous surface-confined catenane **110**.[66] ^{1}H NMR, HRMS, ROESY NMR and X-ray crystallography were used to characterise the [2]catenanes and show that the chloride anion is bound inside the cavity *via* hydrogen bonding and that the structure is further stabilised through π–π interactions and hydrogen bonding between the macrocycles, in a similar fashion to the previously reported catenanes **108a** and **108b**. The anion binding properties of the PF_6^- salt of catenane **109** were determined using ^{1}H NMR titrations in 1 : 1 $CDCl_3$: CD_3OD and *via* cyclic and square wave voltammetry in 0.1 M $TBAPF_6$ 1 : 1 CH_2Cl_2 : CH_3CN. The NMR results revealed that chloride was bound more strongly than oxo-anions OBz^-, $H_2PO_4^-$ and HSO_4^-, while the voltammetry

experiments showed only measurable cathodic shifts of the Fc/Fc^+ redox couple for Cl^- and $H_2PO_4^-$, with chloride bound more strongly. The surface-confined catenane **110** was prepared from a pseudo-rotaxane containing a bis-thiol functionalised thread to allow absorption onto a gold electrode. Unfortunately, the bound chloride anion of this interesting surface-confined catenane could not be exchanged for PF_6^- and anion binding properties could therefore not be determined.

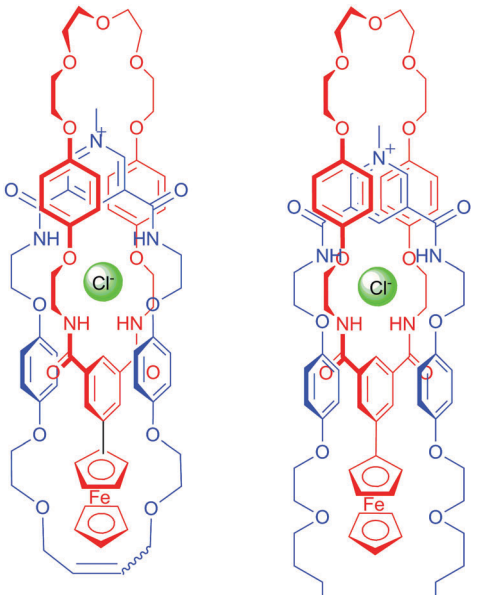

109·Cl **110**·Cl·Au

Beer and co-workers have also used chloride templated synthesis to prepare heteroditopic [2]catenanes **111** and **112**.[67] These catenanes contain a calix[4]diquinone unit able to bind cations, as well as an anion binding site used for templation. The chloride complexed catenanes obtained during synthesis were characterised by ^{1}H NMR, COSY, HSQC and ESI-MS spectroscopy and X-ray diffraction and showed that both catenanes adopt the same conformation, indicating that the benzyl group does not cause rotation of the pyridinium in the calix[4]diquinone cavity and does not affect the anion binding site. After exchanging Cl^- with PF_6^-, 1 : 1 cation complexation was observed for Na^+, K^+, NH_4^+ and Ba^{2+} using ^{1}H NMR and UV/Vis titration in 4 : 1 dichloromethane : acetonitrile. It was observed that the addition of $Ba(ClO_4)_2$ leads to desymmetrisation of the catenane structure and the authors suggest that the electrostatic repulsion between

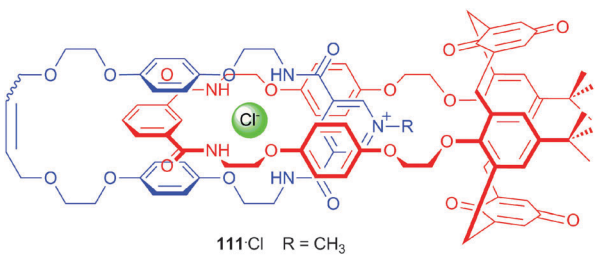

111·Cl R = CH_3
112·Cl R = CH_2Ph

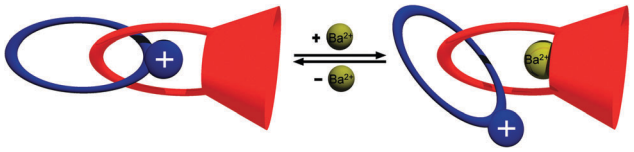

Fig. 20 Molecular rotation in [2]catenane **111** driven by cation–cation repulsion proposed by Beer and co-workers.

Ba^{2+} and the positively charge pyridinium group causes an intra-ring co-conformational rotation between the two macrocycles (Fig. 20). The original symmetric catenane could subsequently be re-obtained *via* the addition of TBA_2SO_4 through decomplexation of Ba^{2+} and precipitation of $BaSO_4$.

Ballester and co-workers have reported an exclusive self-sorting system that involves the formation of a heterodimeric assembly from tolyl calix[4]arene **113** and benzyl calix[4]pyrrole **114** in the presence of a neutral guest (trimethylamine-*N*-oxide) in CH_2Cl_2.[68] This capsule is held together *via* hydrogen bonding between the urea functionalities of both macrocycles and the interactions with both the encapsulated guest (*via* calix[4]pyrrole **114**) and the co-encapsulated solvent molecule (*via* calix[4]arene **113**). Based on this information, the same group has subsequently reported the synthesis and properties of [2]catenane **117** consisting of a tetraurea calix[4]pyrrole and a tetraurea calix[4]arene.[69] Bis-loop calix[4]arene **116** was synthesized according to known procedures and was mixed with calix[4]pyrrole **115** and trimethylamine-*N*-oxide to obtain the heterodimeric pseudo-rotaxane **115**·**116**, according to their previous heterodimer experiments. Subsequent ring-closure metathesis and hydrogenation yielded [2]catenane **117** as a racemic mixture that was separated by HPLC chromatography with a chiral stationary phase. Using ^{1}H NMR and GOESY NMR experiments, the authors were able to show that **117** can encapsulate *N*-oxides **118** and **119** along with a $CHCl_3$ molecule to fill the void, while *N*-oxide **120** was large enough to be encapsulated without the additional $CHCl_3$. Furthermore, ^{1}H NMR experiments in $CDCl_3$ revealed that **117** is able to accommodate ion pairs tetramethylammonium chloride, tetramethyl phosphonium chloride and tetraethyl phosphonium chloride, whereby the chloride anion is bound to the calix[4]pyrrole through hydrogen bonding and the cation sits in the calix[4]arene unit stabilised by cation$\cdots\pi$ and CH$\cdots\pi$ interactions (further confirmed through ^{31}P NMR and ^{1}H DOSY NMR for tetramethyl phosphonium chloride).

Ballester and co-workers have also described the anion binding properties of a pseudo-rotaxane consisting of bis(calix[4]pyrrole) **121** and bis(amidepyridyl-*N*-oxide) **122**.[70] This assembly is held together by hydrogen bonds between the pyrroles and the oxygen atom of the *N*-oxide functionality and forms a binding site containing six convergent hydrogen bond donors for anion complexation. ^{1}H NMR experiments with TBA^+OCN^-, $TBA^+N_3^-$, TBA^+SCN^- and $TBA^+NO_3^-$ in $CDCl_3$ revealed that the anion is bound inside the cavity *via* hydrogen bonding, while the TBA^+ counterion was bound in the shallow external cavity defined by calix[4]pyrrole. This ion pair complexation forming a 4-component pseudo-rotaxane was further

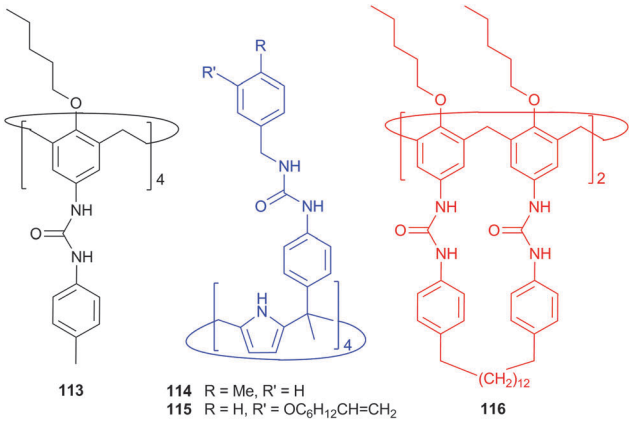

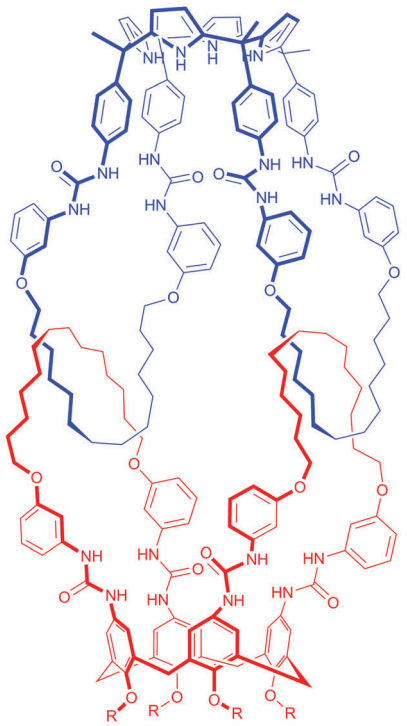

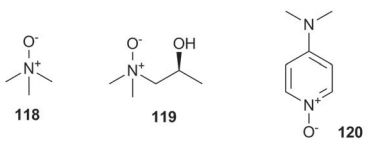

confirmed using ROESY and DOSY NMR, ITC and X-ray crystallography (Fig. 21).

Leigh and co-workers have reported the self-assembly of five bis-aldehydes, five bis-amines, five metal cations and one chloride anion to form a 160-atom covalent pentafoil knot.[71] The authors first described that the reaction of bis-aldehyde **123** and a series of amines (**124a–j**) in the presence of $FeCl_2$ in DMSO at 60 °C forms a symmetric and cyclic pentafoil knot, as confirmed by ^{1}H NMR and ESI-MS spectroscopy. It was found that anilines (**124j**) and amines with two substituents on the

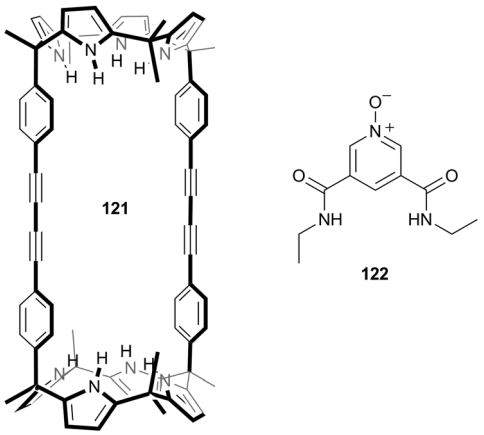

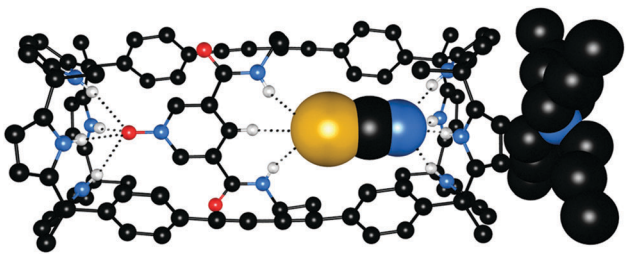

Fig. 21 Crystal structure of the 4-component pseudo-rotaxane formed of **121**, **122** and TBA^+SCN^-; the ion pair is shown in spacefill with the receptor assembly in ball-and-stick; non-coordinating hydrogen atoms are omitted for clarity and hydrogen bonds are shown as dashed lines.

amine-bearing carbon atom (**124h,i**) could not form pentafoil knots with **123** and $FeCl_2$, but all other amines tested did. Interestingly, CD spectra showed that the use of chiral amines (*S*)-**124g** or (*R*)-**124g** led to the formation of the cyclic pentafoil helicate with complete diastereoselectivity, with the handedness of the cyclic helicate determined by the enantiomer used. The authors then tried to obtain a similar, fully covalent pentafoil knot using various diamines (**125a–c** and **126**), but only diamine **126** led to the formation of the desired cyclic pentafoil helicate. This was attributed to the preference for antiperiplanar arrangement of carbon atoms, preventing a full carbon chain (*e.g.* **125a–c**) folding back to form a loop, whereas heteroatoms are known to induce loops (*e.g.* **126**). The structure of the pentafoil knot formed by **123**, **126** and $FeCl_2$ was further characterised by ^{1}H NMR, ESI-MS and X-ray crystallography, showing that a chloride anion is bound in the centre of the knot by ten CH···Cl^- hydrogen bonds (Fig. 22). An empty cavity analogue of the pentafoil knot could be generated by the addition of $AgPF_6$ in MeCN and the subsequent addition of TBACl, TBABr and TBAI showed that only the chloride anion can be bound inside the cavity and hence probably templates the formation of the pentafoil knot.

Yashima and co-workers have studied the chiral amplification properties of positively charged amidine oligomers during the formation of double stranded helices with achiral anionic carboxylate oligomers.[72] A series of chiral amidine strands were synthesised composed of (*R*)- or (*S*)-1-phenylethyl and/or achiral isopropyl amidine units, having either an all-chiral (**127**), edge-chiral (**128**)

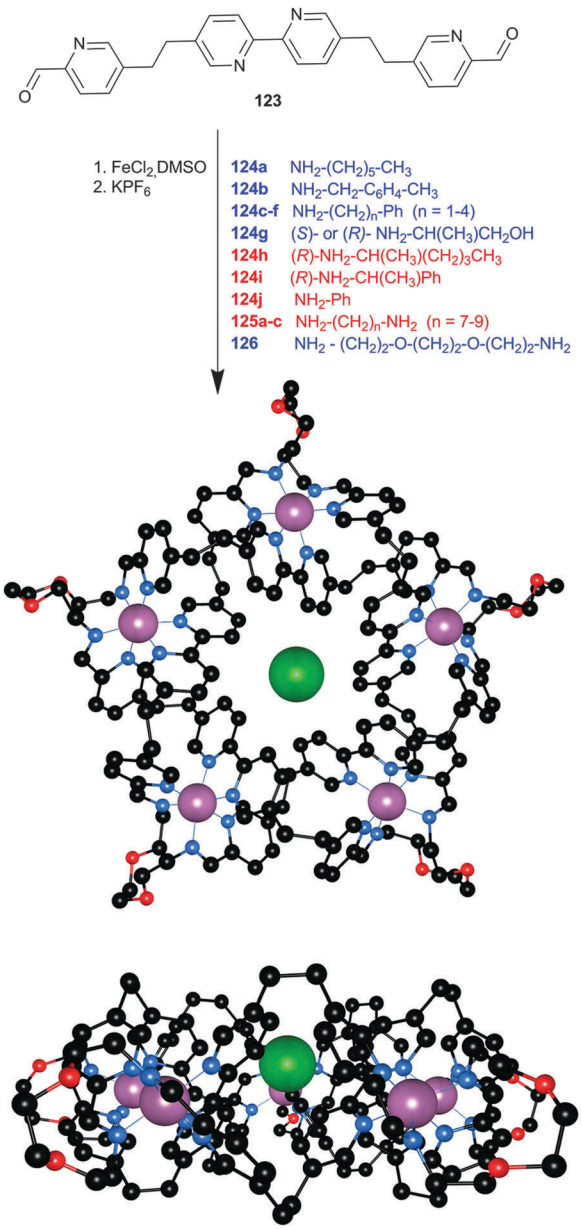

Fig. 22 (top) Self-assembly of a pentafoil knot from aldehyde **123**, $FeCl_2$ and amines **124–126**. The amines capable of forming a pentafoil knot are shown in blue, with the other amines in red. (below) Two views of the crystal structure of the knot formed between **123** and **126**; hydrogen atoms, counterions and solvent molecules are omitted for clarity; chloride and iron(II) ions are shown in spacefill with the rest of the knot shown in ball-and-stick.

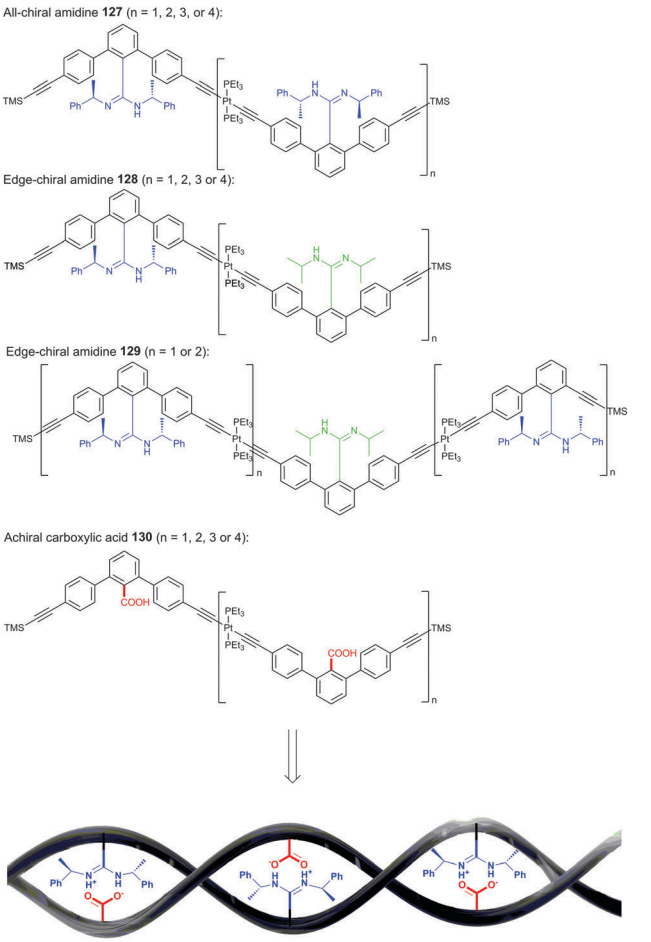

Scheme 14 Overview of the various amidine and carboxylic acid strands by Yashima and co-workers and their double helix formation.

or centre-chiral (**129**) composition, and their duplex formation with achiral carboxylate strands (**130**) were investigated (Scheme 14). Using ^{1}H NMR, UV/Vis, cold spray ionisation (CSI) MS and CD spectroscopy, it was shown that duplexes are formed between the all-chiral amidine strands **127** and the complementary carboxylic acid strands **130**, whereby the handedness of the helix is determined by the enantiomer of the amidine used and the length of the oligomer, with opposite handedness seen between the 2-mers (n = 1) and the 4-/5-mers (n = 3,4). The authors also showed by CD spectroscopy that helices formed between the edge-chiral (**128**) or centre-chiral (**129**) amidine strands and the achiral carboxylic acid strands had a preferred handedness, suggesting that the single chiral monomer in the strand acts as a helical sense director and that the chirality is thus amplified through the helix. It was found that these duplexes are dynamic and that their chiroptical properties depend on solvent, temperature and oligomer length and sequence, with a larger chiral amplification effect for centre-chiral than for edge-chiral amidine strands, and the effect decreased with increasing length of the strands, as supported by ^{1}H NMR and CD spectra and molecular dynamics (MD) simulations.

Anion sensors and chemodosimeters

Many examples have already been given for the optical detection of anions (colorimetric or fluorescent), but few are highly selective for a specific anion. Bai and co-workers developed a colorimetric and ratiometric fluorescent fluoride sensor based on the desilylation reaction of organosilicon compound **131**.[73] The addition of F^- to a THF solution of **131** leads to a colour

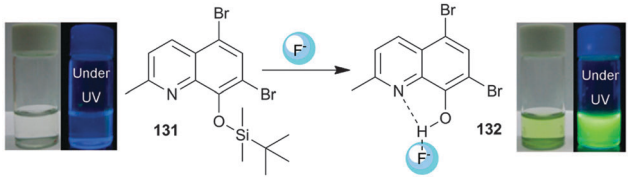

Fig. 23 Proposed mechanism of F^- sensing by **131**, with naked eye colour changes and under UV lamp fluorescent colour changes observed for **131** upon the addition of one mole equivalent of F^- (200 μM in THF). Reproduced with permission from *Chem. Commun.* 2011, **47**, 3957–3959. © Royal Society of Chemistry.

change from colourless to yellow-green and also the emission changes from modest blue to bright yellow-green (Fig. 23). UV/Vis titrations show that this colour change is due to a decrease of the 313 nm peak and the increase of the 363 nm and 410 nm peaks of the absorption spectra upon the addition of fluoride, while fluorescence studies show a decrease of the 403 nm peak and the emergence of a new peak at 520 nm, with the ratio of fluorescence intensity F_{520nm}/F_{403nm} exhibiting a linear change upon the addition of fluoride in the range 1–10 μM (ratiometric sensor). Furthermore, similar experiments with other anions, such as Cl^-, Br^-, OAc^-, NO_3^-, $H_2PO_4^-$, HSO_4^- and ClO_4^- show that F^- is the only anion that can induce these optical changes. The high selectivity and sensitivity for fluoride is attributed to the selective deprotection reaction by fluoride (forming **132**), followed by the formation of a hydrogen bond between F^- and the newly formed hydroxy group, resulting in a charge transfer interaction between F^- and the electron deficient sensor and altered emission properties. This mechanism of fluoride sensing was confirmed by ^1H NMR experiments, and UV/Vis and fluorescence studies on purified deprotected product **132**.

Duke and Gunnlaugsson have reported the synthesis of a highly selective dual colorimetric and fluorescent ICT-based anion sensor for fluoride (Scheme 15).[74] Compound **133** is based on a 1,8-naphthalamide skeleton in which the 3-position is functionalised with a 4-trifluoromethylphenylurea group. This system functions as a selective sensor for fluoride *via* a deprotonation mechanism at high fluoride concentration resulting in a dramatic enhancement in the absorption band at 327 nm and large changes within the ICT transition in the fluorescence emission spectrum of the compound in DMSO.

Singh and Kaur reported receptor **134** that can remove cyanide from water and from human serum through the formation of **135**.[75] Upon the addition of various anions (CN^-, F^-, OAc^-, $H_2PO_4^-$, Cl^-, Br^-, CO_3^{2-} and HCO_3^-) to a 1 : 1 water : ethanol solution of **134**, a colour change from light yellow to orange/red was only observed upon the addition of NaCN. Job plot and UV/Vis titrations show that

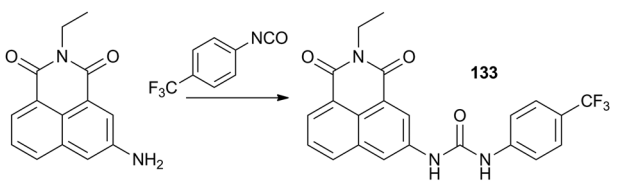

Scheme 15 Synthesis of anion sensor **133**.

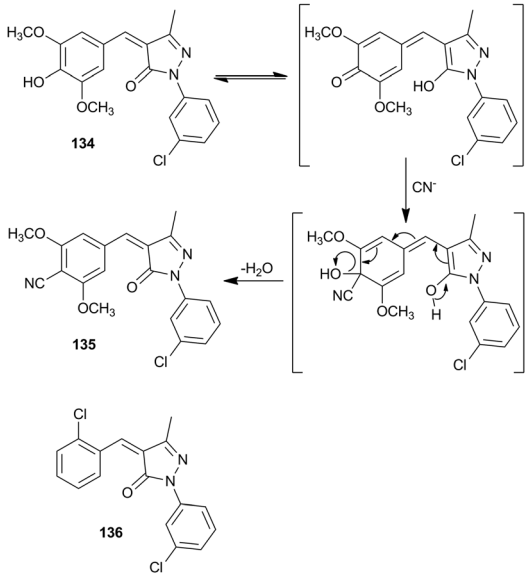

Scheme 16 Structure of compounds **134–136** and the proposed mechanism for the conversion of **134** into **135** by the addition of cyanide.

cyanide interacts with receptor **134** in a 1 : 1 stoichiometry with an association constant of $K_a = 10^6\ M^{-1}$. Compound **135** could be isolated from the mixture of cyanide and **134** and the authors propose, based on UV/Vis and ^1H NMR studies, that the reaction shown in Scheme 16 is responsible for this observation. This reaction mechanism requires the substitution of a phenolic OH by CN and this was confirmed as no response was seen when cyanide was added to the analogous compound **136** lacking the phenolic OH group. To show the generality of the cyanide sensing abilities of **134**, the UV/Vis studies were repeated in dry THF, dry MeCN, dry $CHCl_3$ and in 1 : 1 water : ethanol mixtures at various pHs (pH 2–7) and similar changes in colour and absorption spectra were observed upon the addition of CN^-. It was also shown that the presence of other anions or Fe^{3+} did not change the sensing ability towards CN^- in competitive binding studies. Furthermore, the authors additionally showed that **134** is able to sense CN^- in proteinaceous (and non-proteinaceous) human blood serum and that it is able to remove all CN^- anions from these media. The authors believe that this property, along with the presumed low toxicity of **134** (due to the similarity to the known drug trimethoprim) and ease of synthesis, makes **134** a potential commercial antidote for cyanide.

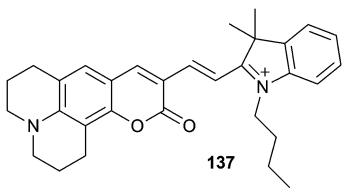

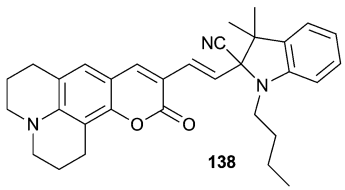

Lee, Kim and co-workers have reported coumarin derived receptor **137** that functions as a selective sensor for KCN.[76] UV/Vis and fluorescence measurements with potassium salts of F^-, Cl^-, Br^-, I^-, OAc^-, HSO_4^-, HPO_4^{2-}, HCO_3^-, NO_3^-, ClO_4^-, CN^- and SCN^- in 5 : 95 H_2O : MeCN showed that only the cyanide anion is able to induce a colour change from dark blue to yellow (naked-eye colorimetric sensor) and an increase in fluorescence intensity (turn-on fluorogenic sensor). ^1H NMR and FAB-MS experiments showed that the addition of CN^- to **137** results in the formation of **138**. Based on DFT and time-dependent DFT calculations, the authors suggest that this reaction of **137** with CN^- to produce **138** breaks the conjugation between the coumarin and the indole moiety, thereby disrupting the ICT in **137** and causing spectral changes in both absorbance and emission.

Calero *et al.* described the development of a quencher displacement assay (QDA) for anion sensing.[77] The conventional indicator displacement assay (IDA) was modified by attaching a fluorophore (**139**) and a separate metal cation receptor (**140**) to silica nanoparticles, generating a terpyridine–sulforhodamine-functionalised nanoparticle hybrid system, in order to achieve facile regeneration of the sensing material. The system works by first loading the terpyridine units with a metal cation, which quenches the fluorescence from the nearby sulforhodamine units. The anion to be sensed is then added and competes with the terpyridine units to bind the cation, and once the cations are displaced from the terpyridine units, the fluorescence signal is regenerated (Scheme 17). The authors believe that the possibility of utilising different coordination units and metal anion quenchers can make QDA's attractive for developing new chemosensors for anions.

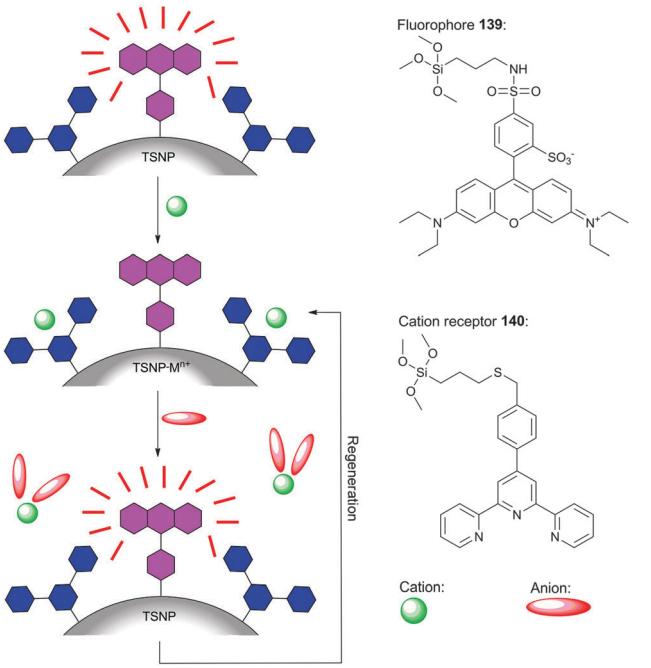

Scheme 17 Design concept of the anion quencher displacement assay (QDA) involving terpyridine–sulforhodamine functionalised nanoparticle (TSNP) and a metal ion quencher, along with the structure of fluorescent dye **139** (magenta) and cation receptor **140** (blue).

Table 3 Fluorescence response of **141** after 3 hour reaction with various alkylating agents (R–X) in CD_2Cl_2

R	X	F/F_0 enhancement
Me	I	49
Me	OTf	114
Et	I	29
Et	Br	89
Bn	Br	89
p-OMe Bn	Br	81
p-NO_2 Bn	Br	36
CH_2CH_2Ph	Br	99
$CH_2CH_2CH_2Ph$	Br	46
Propargyl	Br	61
$(CH_2)_2$–O–$(CH_2)_2$–O–CH_3	Br	45

Bull, Fossey and colleagues have developed a pyridine based sensor for alkyl halides.[78] Previous reports had shown that the conversion of **141** into **142** leads to a large fluorescence enhancement due to cation$\cdots\pi$ interactions in **142**.[79] Fluorescence titrations with MeI in CH_2Cl_2 showed that this property can be used to detect MeI with a detection limit of 1 nM. Additionally, the authors tested the sensing ability towards other alkyl halides by reacting them with **141** in CH_2Cl_2 under reflux for 3 hours and then measuring the fluorescence intensity (Table 3). A larger fluorescence enhancement was observed when triflate based alkylating agents were used rather than iodide based agents, presumably due to the heavy atom quenching effect of I^-. Furthermore, **141** also acts as a sensor for bromide based alkylating agents, but they required a longer reaction time (hours) compared to triflate/iodide based agents (seconds) before they can be accurately detected.

Catalysis

The link between anion binding and certain catalytic reactions has previously been suggested and reviewed, especially for thiourea based organocatalysts.[80] Jacobsen and co-workers have reported the first instance of an enantioselective thiourea anion binding catalyst with fluoride.[81] Pyridine derivatives have long been used to catalyse acyl transfer reactions and stabilisation of the acylpyridinium ion intermediate, *via* hydrogen bonding of the counterion to a specific hydrogen bond donor,

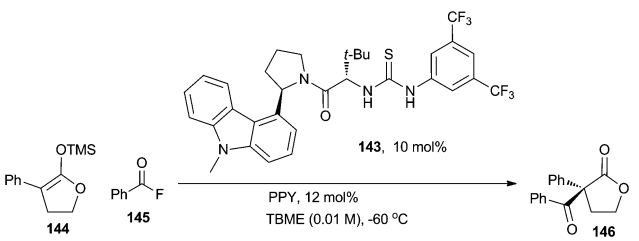

Scheme 18 Conversion of **144** into **146** catalysed by thiourea **143** and PPY.

could lead to increased reaction rates. Therefore, the authors investigated the enantioselective acylation of silyl ketene **144** with acyl fluorides using thiourea **143** and 4-pyrrolidinopyridine (PPY) catalysts and found that the reaction proceeds with a yield of 80% and an enantiomeric excess (ee) of 92% (Scheme 18). To test the substrate scope, a series of acylation reactions were performed with an assortment of benzoyl fluorides substituted with electron donating and electron withdrawing groups. *Meta*- and *para* substitutions were generally tolerated well, yet *ortho* substitutions resulted in inactivity. This observation, along with the fact that the reaction does not proceed in the absence of PPY or the thiourea catalyst, supports the concept of an acylpyridinium intermediate. Additionally, activation of **144** by fluoride is necessary for acylation to proceed, as it is observed that the use of benzoyl chloride does not generate the required product. This was attributed to the impressive hydrogen bond acceptor ability and silaphilicity of fluoride, allowing the enantioselective acylation process to move forward efficiently and afford the useful α,α-disubstituted butyrolactones, while only requiring low catalyst loadings.

Lin and Jacobsen have reported the use of arylpyrrolidino amido thioureas (**147a–f**) for the catalysis of enantioselective nucleophilic ring opening of episulfonium ions by indoles.[82] Initial optimisation of the catalysis conditions showed that arylpyrrolidino amido thioureas such as **147a–f** work best, that the episulfonium precursor should have a relatively non-nucleophilic leaving group and that sulfonic acids are required to co-catalyse the reaction rather than mineral acids (HCl). Furthermore, it was found that catalysts with a more extended aromatic substituent (**147b–f**) result in improved enantioselectivity. Based on this information and detailed kinetic analysis involving *in situ* infrared spectroscopy, structure–reactivity relationships and kinetic isotope effects, the authors propose a reaction mechanism as shown in Scheme 19, where the addition of indole is the rate- and enantioselectivity-determining step. The authors also propose that the transition state in this rate-determining step is stabilised by the thiourea catalyst through a number of interactions: (1) hydrogen bonding between the thiourea catalyst and the sulfonate anion – as confirmed by ^{1}H NMR titration of **147d** and dibenzylmethylsulfonium triflate in toluene-d_8; (2) hydrogen bonding between the indole NH and the amide oxygen of the catalyst – as suggested by the fact that *N*-methylindole results in poor enantioselectivity and by the linear relationship between reaction rate and indole NH acidity; (3) cation···π interactions between the arene in the catalyst and the episulfonium cation – as suggested by ^{1}H NMR experiments on the catalyst with a model sulfonium ion (dibenzylmethylsulfonium triflate) and the influence of the identity of the arene on the enantioselectivity.

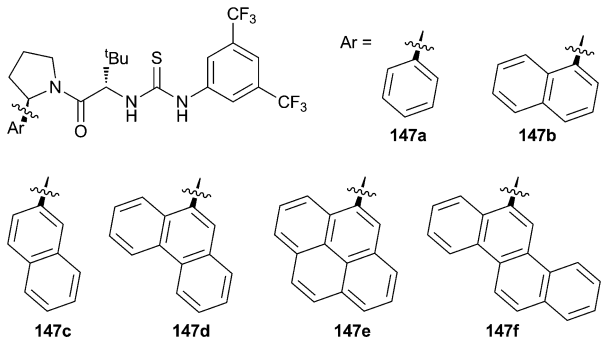

Jacobsen and co-workers have also shown that a combination of an achiral thiourea (**148**) and a chiral primary amine (**149** or a chiral aminothiourea) can be used to catalyse the intramolecular enantioselective [5+2] dipolar cycloaddition of **150** to **151** (Scheme 20).[83] The reaction proceeds with 58% yield and −85% ee. They hypothesised that the thiourea can encourage ionisation to the pyrylium ion *via* stabilisation of the counter anion prior to the cyclisation step, which was supported by the fact that **149** is virtually inactive in the absence of thiourea **148** (7% yield). Furthermore, the primary amine in **149** is also necessary for the catalytic reaction, as a tertiary amine analogue proved to be unreactive (in both the presence and absence of thiourea **148**). The authors propose a catalytic mechanism based on the initial condensation between the primary amine of **149**

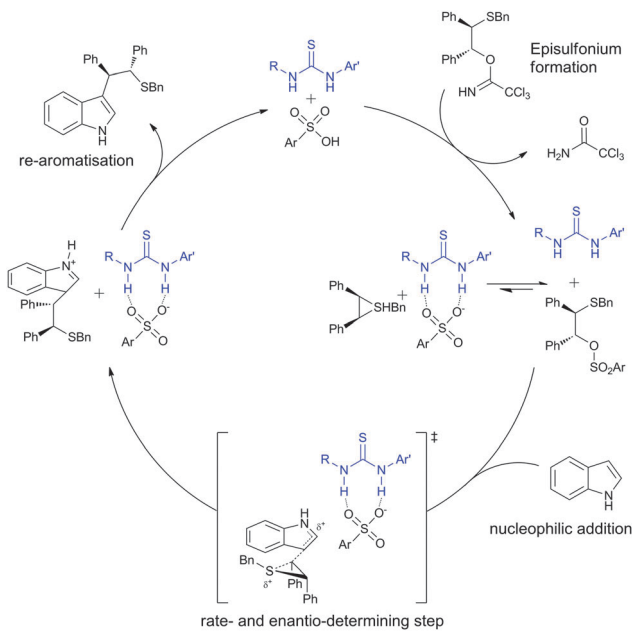

Scheme 19 Proposed catalytic cycle for thiourea catalysed ring-opening of episulfonium ions with indole; the catalyst (**147a–f**) is shown in blue.

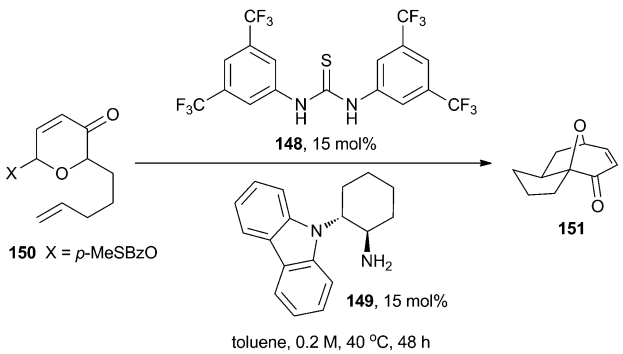

Scheme 20 Oxidopyrylium cycloaddition catalysed by **148** and **149**.

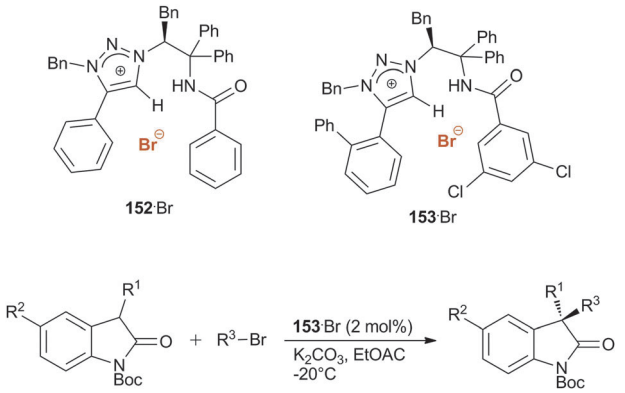

Scheme 21 Structure of catalysts **152**·Br and **153**·Br along with the alkylation of oxindole reaction that they catalyse.

and the ketone of the substrate, leading to a dienamine after tautomerisation, followed by hydrogen bond donor (**148**) mediated abstraction of *p*-MeSBzO to generate the pyrylium ion that can undergo an intramolecular cycloaddition.

Ooi and co-workers have reported the development of chiral 1,2,3-triazolium salts (such as **152**·Br) that function as cationic organocatalysts with anion recognition abilities.[84] The increased CH-acidity of the triazolium cation *versus* the simple 1,4-disubstituted 1,2,3-triazole unit means an increased anion binding capacity. X-ray crystallography of **152**·Cl showed that the combination of electrostatic interactions, CH···anion hydrogen bonding and a suitably positioned amide NH···anion hydrogen bond forms a structured and tightly bound ion pair. These hydrogen bonding interactions were further confirmed by comparison of the ^{1}H NMR spectra of **152** paired with various counter anions in CD_2Cl_2 at 298 K. The synthesised 1,2,3-triazolium salts were investigated for their potential to catalyse the enantioselective alkylation of 3-substituted oxindoles (Scheme 21). The combination of an *ortho*-biphenyl substituent and a 3,5-dichlorophenyl group into the amide moiety gave the most effective catalyst (**153**), giving a reaction yield of 99% with 97% ee. It was also established that this alkylation was best performed in ethyl acetate.

Transmembrane anion transport

The control of anion concentrations is crucial to cell survival and hence the development of small molecules that are capable of transporting anions across cellular membranes has recently received a great degree of attention, mainly due to their potential therapeutic advantage.[85–89] Prodiginines are small natural products that represent the most widely studied transmembrane chloride transporters due to their alleged anticancer activity.[90–92] The anion binding and transport properties of obatoclax (**154a**, a synthetic prodiginin that is currently in clinical trials as an anticancer drug) have been investigated by Quesada and co-workers, with the aim of discovering the mechanism of its anticancer activity.[93] Variations of the pyrrole substituents resulted in a series of compounds (**154a,b,c–157**) capable of transporting chloride and bicarbonate anions across synthetic POPC bilayers, *via* an antiport mechanism of transport. Compound **154b** showed the highest transport ability for the chloride–bicarbonate antiport process ($EC_{50,290s}$ = 0.18 μM). However, modification of the number of hydrogen bond donors present in the receptors leads to receptors with reduced transport activity (**155–157**). The active receptors were shown to possess *in vitro* cytotoxic activity against the small-cell lung cancer cell line GLC4. This anticancer activity was further investigated by *in vitro* acridine orange staining experiments performed on the same cell line and the active receptors were shown to de-acidify the lysosomes of the cell, thereby signalling an orange to green fluorescence change. Hoechst staining revealed apoptosis to be the mechanism of cell-death. As the *in vitro* anticancer activity of the compounds correlates well with their anion transport ability in liposomes, it is presumed that the change in intracellular pH induced by **154a–c** and **155–156** is due to bicarbonate transport facilitated by these receptors.

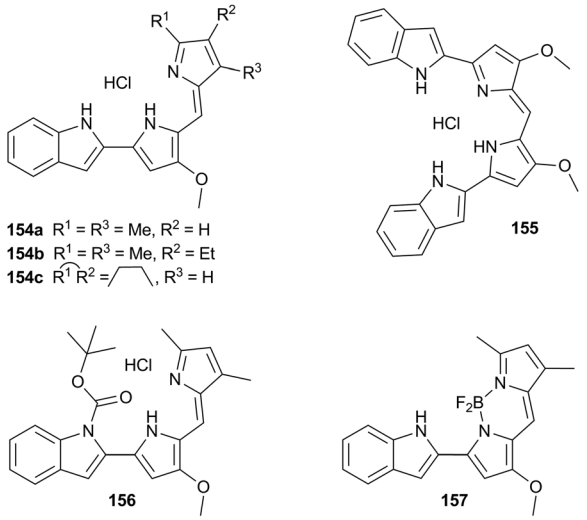

Quesada and co-workers have also focused on the study of transmembrane anion transport by a series of tambjamines (**158–163**), which are compounds structurally related to prodigiosin with proven anticancer and antimicrobial properties.[94] X-ray crystal structures of the HCl salts of **159** and **163** show a flat bicyclic core and hydrogen bond interactions between chloride and the tambjamine core. ^{1}H NMR titrations of the hydroperchlorate salts with TBACl in DMSO-d_6 suggest that these hydrogen-bonding interactions also persist in solution. Chloride ion selective electrode vesicle tests were used to determine the anion transport properties of the series and it was shown that novel receptor **163** is the most efficient transporter for chloride, promoting >90% chloride efflux after 5 minutes with a carrier loading of 0.2 mol% with respect to lipid. This receptor was also shown to promote chloride efflux at carrier loadings as low as 0.025 mol% with respect to lipid. On the other hand, tambjamine **159** was the worst transporter of the series, presumably due to its low lipophilicity. Variations of the ion selective electrode tests were able to support an anion exchange transport mechanism in synthetic vesicles. *In vitro* activity of the tambjamines was tested on small-cell lung cancer (GLC4) cells. Using acridine orange the

cell nuclei and cytoplasm fluoresced green (high pH), while some granular orange fluorescence was observed in the cytoplasm – a result of acidified lysosomes. In cells treated with tambjamine **163** the orange emission disappeared; a possible result of bicarbonate flux into the lysosome. The biological results correlate well with the synthetic transport tests and indicate the tambjamine family to be potential targets for drug development.

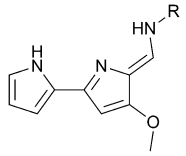

158 R = ^{i}Pr
159 R = Et
160 R = CH_2CH_2Ph
161 R = $C_{12}H_{25}$
162 R = Ph
163 R = *p*-^{t}BuPh

Gale and co-workers have shown that very simple compounds with urea and thiourea functionalities (**164–169**) can function as powerful chloride–bicarbonate antiporters at low concentrations without the need for pre-incorporation into phospholipid bilayers.[95] ^{1}H NMR titrations with various TBA salts in DMSO-d_6–0.5% water revealed that none of the six receptors interacts notably with nitrate but they do all bind chloride, the most noticeable being the interaction of indolyl urea **168** (K_a = 96 M^{-1}). Vesicle based transport assays showed that the urea based receptors do not promote the release of chloride from POPC vesicles, in both chloride–nitrate and chloride–bicarbonate antiport assays. On the other hand, phenylthiourea **165** showed moderate chloride release, whilst **167** and **169** effectively release chloride from within the synthetic vesicles ($EC_{50,270s}$ = 0.109 mol% and 0.029 mol% respectively for the chloride–nitrate assay). Experiments with 30 : 70 cholesterol : POPC liposomes demonstrated that the receptors function as anion carriers, as opposed to forming channels, and ^{13}C NMR experiments were used to directly confirm that the thiourea receptors are able to promote chloride–bicarbonate antiport. Additional experiments confirmed the remarkable transport activity of simple indolylthiourea **169**, which is able to antiport chloride/nitrate down to ratios of 1 : 25 000 transporter to lipid.

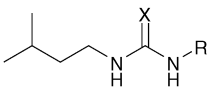

164 X = O, R = $(CH_2)_3CH_3$
165 X = S, R = $(CH_2)_3CH_3$
166 X = O, R = Ph
167 X = S, R = Ph
168 X = O, R = 7-indole
169 X = S, R = 7-indole

Gale and co-workers have also shown that simple bis-ureas of the form **170**, although more flexible than their mono-urea counterparts, are able to transport anions more effectively across lipid bilayers *via* a mobile carrier, antiport mechanism.[96] The basic modification of alkyl chain length of this type of receptor allows for tuneable anion transport activity as required. The increase in receptor flexibility with increasing alkyl chain length has no detrimental effect on transport activity; in fact the opposite is true with transport efficiency appearing to increase across the series until the optimum alkyl chain length is reached (n = 9). The receptor where n = 9 seems to strike the correct balance between enhanced membrane partitioning as a result of increased lipophilicity, and sufficient delivery capabilities through the aqueous media to the membrane, with supporting evidence being provided in the form of molecular dynamics simulations.

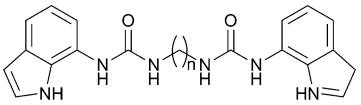

170 n = 4-12

A. P. Davis and co-workers have continued their work on cholapods, which have previously been shown to be very powerful anion receptors and transporters.[97] In 2011 they reported the development of smaller cholapod-like receptors based on a central *trans*-decalin system **171a–i**, which have the advantage of smaller molecular weights and decreased lipophilicity and are therefore more "drug-like" molecules.[98] ^{1}H NMR titrations showed a strong 1 : 1 interaction between the receptors and tetraethylammonium chloride, and extraction techniques were used to estimate binding affinities of >10^6 M^{-1}, with the introduction of electron withdrawing fluorinated aromatic groups leading to further increased affinities. The receptors were also assessed for anion transport abilities *via* fluorescent lucigenin assays after pre-incorporation of **171a–i** into POPC vesicles. The results demonstrated that the *trans*-decalin based receptors are effective chloride, and presumably nitrate, transporters with more electron deficient aromatic rings leading to enhanced transport ability – in accordance with the binding results. Furthermore, the introduction of a long octyl substituent (**171g–i**) results in an increased transport ability of the receptor. The most active of which, **171i**, was effective at concentrations as low as 1 : 250 000 receptor to lipid. This may be a consequence of positioning the decalin favourably within the membrane or promoting the movement of the decalin from one face of the membrane to the other during the transport processes.

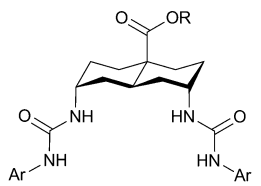

171a R = Me, Ar = Ph
171b R = Me, Ar = *p*-(CF_3)Ph
171c R = Me, Ar = *m*-$(CF_3)_2$Ph
171d R = Et, Ar = Ph
171e R = Et, Ar = *p*-(CF_3)Ph
171e R = Et, Ar = *m*-$(CF_3)_2$Ph
171g R = Octyl, Ar = Ph
171h R = Octyl, Ar = *p*-(CF_3)Ph
171i R = Octyl, Ar = *m*-$(CF_3)_2$Ph

Jeong and colleagues have prepared a series anion receptors (such as **172–176**) with differing side chains that possess cavities with convergent urea and hydroxyl hydrogen bond donor groups, mimicking the hydrogen bonding mode of StClC (serovarty-phimurium chloride channel).[99] The binding mode of these receptors was confirmed by X-ray analysis, with the bound chloride anion shown to form four hydrogen bonds with the receptor. ^{1}H NMR anion binding analysis in 1% H_2O : CD_3CN showed that receptors with chloride substituents on the phenyl rings have increased association constants, with the strongest binding observed for receptor **176** (K_a = 17 000 M^{-1} ± 12). Receptor **176** was also shown to be the most effective transporter of the series by lucigenin fluorescence assays. This receptor has strong electron withdrawing substituents to encourage hydrogen bonding interactions with the anion and also possesses lipophilic side chains to allow for easy

passage through the lipophilic POPC membrane. Mechanistic investigations of the anion transport process were also conducted and revealed that such receptors function *via* an antiport mechanism.

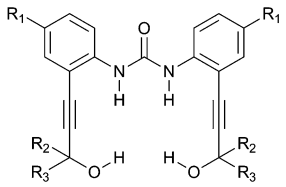

172 R^1 = ^{t}Bu, R^2 = R^3 = Me
173 R^1 = (C=O)-O-$(CH_2)_3CH_3$, R^2 = R^3 = Me
174 R^1 = Cl, R^2 = R^3 = Me
175 R^1 = Cl, R^2 = R^3 = Et
176 R^1 = Cl, R^2 = Me, R^3 = ^{i}Bu

Gale and-coworkers have previously shown that the addition of fluorinated substituents on tripodal tris-ureas and tris-thioureas can greatly enhance the transmembrane anion transport ability in vesicles and *in vitro* cell studies.[100] Building on these results, the same group has investigated a series of fluorinated indole, alkyl, and phenyl-substituted mono-ureas and mono-thioureas (*e.g.* **177–184**) for their ability to promote anion transport across synthetic phospholipid bilayers.[101] Both chloride–nitrate and chloride–bicarbonate antiport processes were studied using standard POPC phospholipid vesicle model systems. The overall results indicate that fluorinated receptors exhibit greater transport activity than their unfluorinated counterparts – in accordance with increased *c*log*P*. Receptor **180** proved to be the most active receptor, facilitating chloride–nitrate antiport at receptor loadings as low as 1 : 20 000 receptor to lipid, which corresponds to an $EC_{50,270s}$ value of just 0.016 mol%. The presence of a CF_3 group increased anion affinity in all cases, and also increased lipophilicity sufficiently to enhance transport rates across the board, presumably by favouring partitioning of the receptor into the lipophilic phase. *In vitro* ionophoric activity of the active compounds was tested in A375 melanoma cells, employing the technique of acridine orange staining. After exposure to compound **180** all orange fluorescence disappeared and only green fluorescence was observed, indicating an increase in pH of previously acidic organelles by acidification of the cell cytoplasm. Subsequent studies using Hoechst 33342 staining of the same cell line showed that this reduction in cellular pH can damage cells and is able to encourage apoptosis of cancer cells.

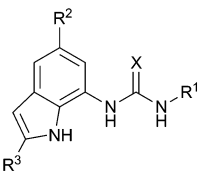

177 X = O, R^1 = Hexyl, R^2 = R^3 = H
178 X = S, R^1 = Hexyl, R^2 = R^3 = H
179 X = O, R^1 = Hexyl, R^2 = CF_3, R^3 = ^{n}Bu
180 X = S, R^1 = Hexyl, R^2 = CF_3, R^3 = ^{n}Bu
181 X = O, R^1 = Ph, R^2 = R^3 = H
182 X = S, R^1 = Ph, R^2 = R^3 = H
183 X = O, R^1 = *p*-CF_3Ph, R^2 = R^3 = H
184 X = S, R^1 = *p*-CF_3Ph, R^2 = R^3 = H

The majority of small-molecule anion transporters employ urea or thiourea based anion binding motifs, but concerns have been raised about the potential toxicity of thioureas. For this reason, Davis, Gale and co-workers compared the lipid bilayer anion transport capability of thiourea isosteres, such as receptors **185–187** based on the guanidine motif, to simple thiourea **188**.[102] Single crystal X-ray diffraction analysis of **185** and **186** showed that the guanidine subunit hydrogen atoms adopt the *trans* arrangement while the thiourea hydrogen atoms in thiourea **188** adopt the *cis* arrangement. ^{1}H NMR Job plot analysis (DMSO-d_6–0.5% water) indicated a 1 : 1 binding model for all receptors with a variety of anions. In all cases the receptors bind most strongly with sulfate anions. Chloride ion selective electrode tests with unilamellar POPC vesicles were used to test for anion transport abilities. At 2 mol% carrier loading (with respect to lipid) receptors **185** and **187** showed minimal chloride efflux (5% at 270 s), whilst receptor **186** gave a chloride efflux of 29%, comparable to thiourea **188** which shows 30% chloride efflux, and it was found that a chloride–nitrate antiport mechanism is the most likely reason for the observed chloride efflux. It was also reported that the addition of the cationophore valinomycin results in significantly enhanced anion transport for all receptors (*e.g.* receptor **186** increases from 29% to 58% chloride efflux). This enhancement was attributed to valinomycin bound potassium cations in the membrane either stabilising the anion–receptor complex in the membrane, or enhancing the extraction rate of anions from the aqueous phase into the membrane phase. These initial results suggest that hydrogen bonding thiourea isosteres may be optimised for anion binding and transport.

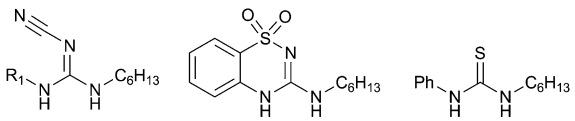

185 R_1 = C_6H_5
186 R_1 = C_6F_5
187
188

This indication of a dual host system was further investigated by the same group.[103] Taking lead from work where separate

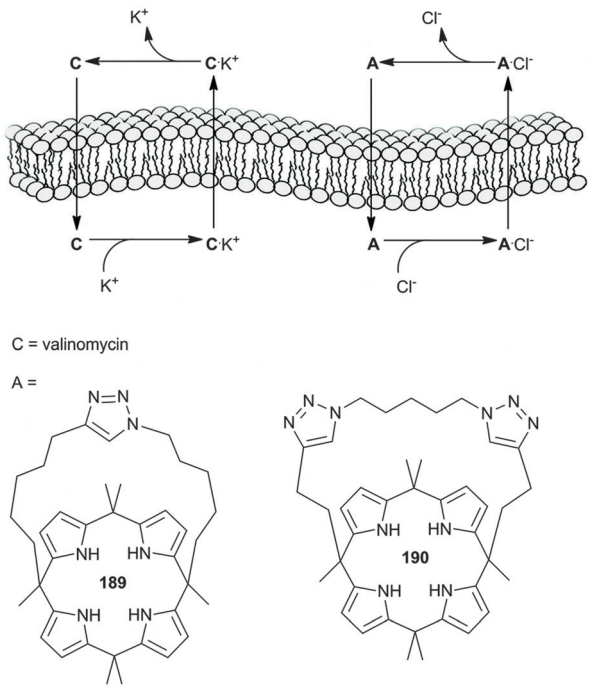

Scheme 22 Design concept of the dual host approach to co-transport of KCl by cation transporter C (valinomycin) and anion transporter A (**189** or **190**).

anion and cation receptors can be used to extract metal salts from aqueous to organic media, they wondered if the same tactic could be used to co-transport metal salts across POPC lipid bilayers, utilising synergistically coupled cationic and anionic uniport processes (Scheme 22). Using lucigenin fluorescence assays they were able to determine that triazole-strapped calix[4]pyrroles **189** and **190**, when added together with the known potassium cation transporter valinomycin, are able to significantly increase the internal vesicular concentration of chloride anions, more so than when valinomycin or the triazole-strapped calixpyrrole are added separately. This evidence supports the proposed K^+/Cl^- co-transport mechanism.

Gale and co-workers continued to improve on transport efficiency by small molecules and reported the first example of the use of squaramides **191–193** for transmembrane anion transport.[104] This investigation showed that squaramide based compounds outperform urea and thiourea analogues when it comes to transmembrane anion transport by nearly one order of magnitude, presumably a result of the increased strength of the anion binding interaction. Receptor **193**, for example, gave a chloride association constant of K_a = 643 M^{-1} and an $EC_{50,270s}$ value for chloride–nitrate antiport of 0.01 mol% with respect to lipid (compared to K_a = 41 M^{-1} and an $EC_{50,270s}$ = 0.16 mol% for the analogous thiourea), and was the most active transporter of the tested series. All transporters tested were shown to function by a mobile carrier mechanism, as opposed to channel formation, as indicated by U-tube experiments. Since the introduction of the squaramides motif reduces the receptors' lipophilicity, it seems that the squaramide motif is a good target for future development of potent anion transporters.

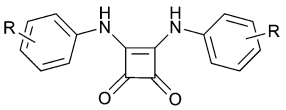

191 R = H
192 R = 4-CF_3
193 R = 3,5-CF_3

Bahmanjah, Zhang and Davis have investigated the use of monoacylglycerols **194–197** for chloride transport.[105] It was suggested that the 1,2-diol unit would provide a good anion binding region whilst the C3-acyl chains would give the compound sufficient lipophilicity to pass through a phospholipid membrane. Furthermore, the addition of an extra hydrogen bond donor to the head group and/or fluorination of the tail group would improve transport capabilities. Lucigenin fluorescence tests on vesicles pre-incorporated with **194–197** showed that monoacylglycerol **194** is able to promote chloride influx, but when the 1,2-diol unit was substituted for additional acylglycerol units (**195**) transport activity was lost, confirming the importance of the diol for transport activity. Substituting an amide NH at the C3 position resulted in increased anion affinity, as confirmed by ^{1}H NMR titrations in both $CDCl_3$ and CD_3CN, as well as increased transport efficiency (**196**, EC_{50} = 0.076 mM). This enhancement in transport efficiency was amplified even further upon fluorination of the acylglycerol tail (**197**, EC_{50} = 0.011 mM), and the group were able to confirm an antiport mechanism of transport for this class of compound.

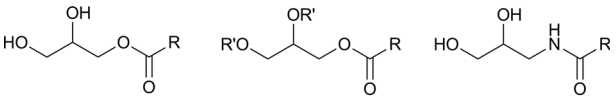

194 R = $(CH_2)_{16}CH_3$
195 R = $(CH_2)_{16}CH_3$, R' = $C(O)(CH_2)_{16}CH_3$
196 R = $(CH_2)_{16}CH_3$
197 R = $(CF_2)_6CF_3$

Matile and co-workers aimed to maximise atom efficiency of anion transporters by employing halogen bond functionalities (*e.g.* **198–204**).[106] These are considered the hydrophobic equivalent of hydrogen bonds, and hence do not require the same level of overcompensation to counteract the hydrophilic binding sites. DFT calculations revealed that chloride anions could be encapsulated by up to 6 molecules of **199**, forming a hydrophobic "shell", and that the anion binding interactions reduce upon replacement of **199** with water, indicating that the binding process is reversible and useful for anion transport processes. Furthermore, defluorination of the receptor or replacement of the iodine for bromine gives weaker halogen bonding. The crystal structure of **199** in the presence of KCl and 18-crown-6 confirms that at least 2 halogen bonds form between a chloride anion and the receptors (Fig. 24). HPTS fluorescence assays were used to determine the chloride transport efficiency of **199** and revealed an EC_{50} = 21.6 μM with a Hill coefficient of n = 4.7, consistent with the computational results for the halogen bonded capsules. The longer chain receptor **200** (EC_{50} = 3.07 μM) was a better transporter due to its increased ability to fully encapsulate the anion. At the other end of the scale trifluoroiodomethane **198** is a relatively poor yet still detectable transporter, and with only one carbon is the smallest possible organic ion transporter.

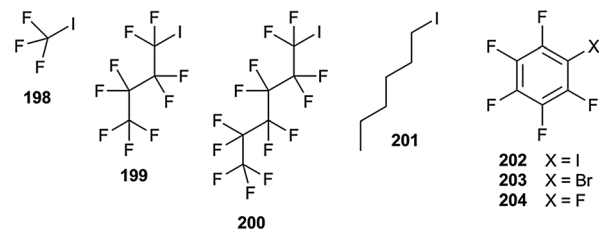

198 **199** **200** **201** **202** X = I **203** X = Br **204** X = F

Matile and co-workers have also investigated a series of ditopic calix[4]arene receptors **205–208** with a single-point variation, allowing them to probe the contributions of hydrogen bonds,

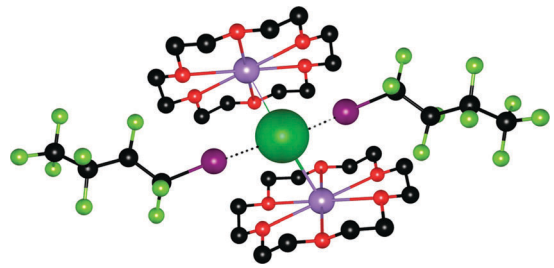

Fig. 24 Section of the crystal structure of chloride bound to 2 molecules of **199** and potassium counterions bound to 18-crown-6; hydrogen atoms are omitted for clarity and halogen bonds are shown by dashed lines, with the anion in spacefill and the receptors in ball-and-stick.

anion–π interactions and halogen bonds to anion transport.[107] The benefit of ditopic receptors is that they can co-transport ion pairs thereby avoiding temporary separation of charge. These receptors bind TMA (tetramethylammonium) counter cations in the upper rim of the calix[4]arene, while substitutions at the lower rim allow for anion binding. The group used pH sensitive HPTS (8-hydroxy-1,3,6-pyrenetrisulfonate) assays to establish that this class of receptors is able to antiport chloride–hydroxide. The overall process occurs *via* the combination of chloride–TMA and hydroxide–TMA symport actions. Binding of TMA in the upper rim is essential to the function of these transporters, as in tests with different counter cations no transport was observed. Single mutation from **205** to **206** resulted in the total loss of transport activity, whilst mutation to **207** partially restored the transport activity. ^{19}F NMR in dry acetone-d_6 shows evidence of detectable anion binding in receptor **206** (but not in **205** and **207**), hence it is suggested that the disruption in transport activity is a result of excessive binding by halogen bonding. Weakening of the halogen bond by mutation from **206** to **208** increased the transport ability more than 30 times, suggesting that **208** can transport chloride–hydroxide using halogen bonding if the halogen bond is weak enough.

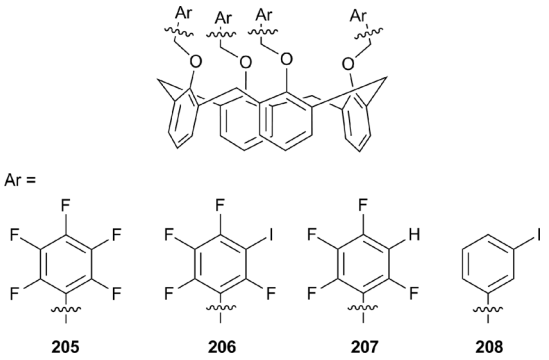

205 **206** **207** **208**

Matile and co-workers have also recently published work on self-sorting dimerisation.[108] Dimerisation and self-sorting are known to be key events associated with the function of photosystems and anion transporters, and the group has therefore introduced *cis*-core naphthalenediimides (NDIs) with only one free chiral π-surface (*e.g.* **209–211**) as a means to direct self-assembly into dimers. NMR studies ($CDCl_3$ at room temperature) provided evidence of dimerisation into heterodimers composed of pairs of enantiomers at high monomer concentrations. It was established that alternate self-sorting efficiency dropped with increasing π-acidity; a result of the increasing strength of π,π-contacts in the core. The most π-acidic NDIs (**211**) showed the highest level of self-sorting ability. These compounds showed a wide range of self-sorting ability, from complete self-sorting with less π-acidic species to no self-sorting with more π-acidic species, and alternate self-sorting somewhere in the middle. In terms of anion transport ability, the highest activity in HPTS transport assays was observed in systems where the π-acidity is intermediate and where the fewest number of dimers are detectable (various stereoisomers of **210**). In the reported sulfoxide series the transport activities are reported to increase with increasing Hill coefficients.

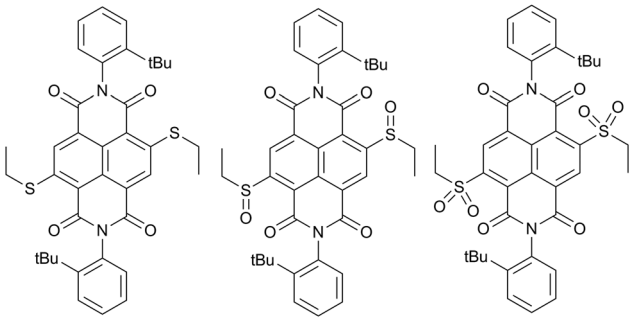

209 (3 stereoisomers) **210** (6 stereoisomers) **211** (2 stereoisomers)

The use of small molecule mobile carriers is just one approach towards transmembrane anion transport. Gokel and co-workers reported the formation of lipid bilayer channels from branched-chain pyrogallol[4]arenes, which assemble into nanotubes or bilayers.[109] Compound **212** crystallises as nanotubes formed by the stacking of two or more hexameric units interlocked by the branched pentyl side chains, while compound **213** crystallises as a head-to-head bilayer with a thickness of ~17.6 Å.[110] The authors postulate that when hexamers of **212** penetrate into the lipid bilayer, they reassemble into the nanotubular arrangement, encouraged by the interaction of the pentyl side chains and the fatty acid acyl chains of the lipid. It is suggested that two hexameric units stacked upon each other would form a channel and the lateral movement of these hexamer units of **212** over one another would "gate" the opening and closing of the nanotube, ready for ion transport. This gating was experimentally observed in an asolectin membrane by using planar lipid bilayer conductance studies, which also reveal a pore size of ~17 Å in the membrane, corresponding well to the dimensions of the hexameric units seen in the crystal structure of **212** (18 Å × 20 Å).

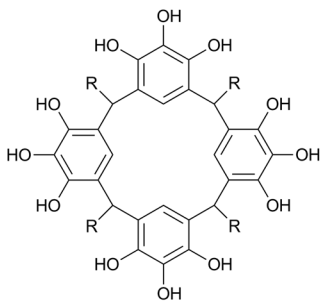

212 R = $CH(CH_2CH_3)_2$
213 R = $CH(CH_2CH_2CH_3)_2$

Building on their work on the use of isophthalamides as anion transporters,[111] Gokel and co-workers have also illustrated the use of tris-arenes based on isophthalic acid and 2,6-dipicolinic acid (**214–221**) for transport of plasmid DNA into ampicillin resistant *E. coli*.[112] Transformation experiments using 2.6 kb plasmids showed isophthalamides with OCH_3 (**214**) and H (**215**) substituents give an enhancement in transformation of 2.3- and 2-fold respectively compared with DMSO and water controls, while the Cl (**216**) and CN (**217**) substituted

species were less effective than the controls. In fact the CN substituted compound appeared to totally suppress transformation. The results for the 2,6-dipicolinic acid derivatives (**218–221**) follow the same trend as for the isophthalic acid derivatives, with the only major difference being that the CN substituted compound shows reduced activity without total suppression of transformation. Tests using 20 kb plasmids illustrate how OCH_3 and H substituted tris-arenes can dramatically enhance transformation up to 10- and 8-fold respectively, which is remarkable considering that increased plasmid size usually hinders transformation. The authors theorise that the tris-arenes bind individually to the phosphate residues of the DNA backbone, encapsulating the DNA in a hydrophobic "coat", which can be transported across the lipid bilayer by passive diffusion.

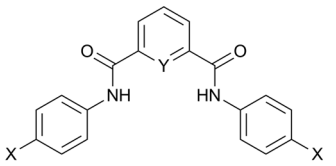

214 X = OCH_3, Y = CH
215 X = H, Y = CH
216 X = Cl, Y = CH
217 X = CN, Y = CH
218 X = OCH_3, Y = N
219 X = H, Y = N
220 X = Cl, Y = N
221 X = CN, Y = N

Yao, Yang and colleagues have continued their work on the electrophysical properties and potential function of **222**,[113] which has previously been shown to form channels in liposomes.[114] The group used single-channel patch clamp techniques to confirm the formation of channels in HEK 293 living cells and showed that 1 μmol of **222** is enough for the small molecule to self-assemble into chloride ion channels within the membrane. Subsequent whole-cell patch clamp recordings showed that compound **222** induces a large increase in current relative to the control experiments. By varying the size of the counter cation it was possible to confirm that the increase in whole-cell current was due to chloride channel formation. Channel selectivity was tested by measuring reverse cell potentials when the extracellular chloride was replaced with different anions, including fluoride, bromide, iodide and nitrate. The activity sequence was as follows $F^- < Cl^- < Br^- < I^- < NO_3^-$. The group were also able to show that compound **222**, once pre-incorporated into plasma membranes of cystic fibrosis airway epithelial cells, can increase the chloride permeability of such cells with damaged CFTR (Cystic Fibrosis transmembrane conductance regulator) channels; a significant step towards therapeutic use of this compound in the treatment of channelopathies such as cystic fibrosis.

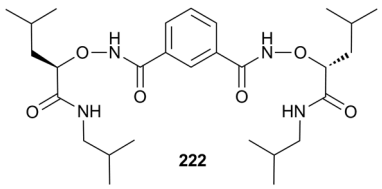

222

Conclusions

The years 2011 and 2012 have seen many advances in the area of supramolecular chemistry of anionic species and related subjects. The use of "unconventional" interactions to bind anions, such as CH hydrogen bonding, halogen bonding and anion···π interactions, has become increasingly popular. Additionally, more research has been devoted to employing the lessons learned from pure anion binding studies into real-world applications, such as sensing, catalysis and the medicinal use of transmembrane anion transport, and we can anticipate that this research field will continue to grow in the coming years.

Acknowledgements

We thank the EPSRC for funding (CJEH (EP/J009687/1) and LEK). NB thanks the University of Southampton and A*STAR for a postgraduate scholarship. ILK thanks the University of Southampton for a teaching assistantship. PAG thanks the Royal Society and the Wolfson Foundation for a Royal Society Wolfson Research Merit Award.

Notes and references

1 C. Caltagirone and P. A. Gale, *Chem. Soc. Rev.*, 2009, **38**, 520–563.
2 P. A. Gale, *Chem. Soc. Rev.*, 2010, **39**, 3746–3771.
3 P. A. Gale, *Chem. Commun.*, 2011, **47**, 82–86.
4 M. Wenzel, J. R. Hiscock and P. A. Gale, *Chem. Soc. Rev.*, 2012, **41**, 480–520.
5 C. Bazzicalupi, A. Bencini, C. Giorgi, B. Valtancoli, V. Lippolis and A. Perra, *Inorg. Chem.*, 2011, **50**, 7202–7216.
6 C. Bazzicalupi, A. Bencini, S. Puccioni, B. Valtancoli, P. Gratteri, A. Garau and V. Lippolis, *Chem. Commun.*, 2012, **48**, 139–141.
7 A. Bencini, C. Coluccini, A. Garau, C. Giorgi, V. Lippolis, L. Messori, D. Pasini and S. Puccioni, *Chem. Commun.*, 2012, **48**, 10428–10430.
8 M. A. Hossain, S. A. Kang, J. A. Kut, V. W. Day and K. Bowman-James, *Inorg. Chem.*, 2012, **51**, 4833–4840.
9 M. B. Nielsen, J. O. Jeppesen, J. Lau, C. Lomholt, D. Damgaard, J. P. Jacobsen, J. Becher and J. F. Stoddart, *J. Org. Chem.*, 2001, **66**, 3559–3563.
10 S. S. Andersen, M. Jensen, A. Sorensen, E. Miyazaki, K. Takimiya, B. W. Laursen, A. H. Flood and J. O. Jeppesen, *Chem. Commun.*, 2012, **48**, 5157–5159.
11 C. J. Serpell, J. Cookson, D. Ozkaya and P. D. Beer, *Nat. Chem.*, 2011, **3**, 478–483.
12 S. R. Beeren and J. K. M. Sanders, *J. Am. Chem. Soc.*, 2011, **133**, 3804–3807.
13 C. N. Carroll, B. A. Coombs, S. P. McClintock, C. A. Johnson II, O. B. Berryman, D. W. Johnson and M. M. Haley, *Chem. Commun.*, 2011, **47**, 5539–5541.
14 C. N. Carroll, O. B. Berryman, C. A. Johnson, L. N. Zakharov, M. M. Haley and D. W. Johnson, *Chem. Commun.*, 2009, 2520–2522.
15 J. M. Engle, C. N. Carroll, D. W. Johnson and M. M. Haley, *Chem. Sci.*, 2012, **3**, 1105–1110.
16 Y. P. Zhou, M. Zhang, Y. H. Li, Q. R. Guan, F. Wang, Z. J. Lin, C. K. Lam, X. L. Feng and H. Y. Chao, *Inorg. Chem.*, 2012, **51**, 5099–5109.

17 D. M. Jessen, A. N. Wercholuk, B. Xiong, A. L. Sargent and W. E. Allen, *J. Org. Chem.*, 2012, **77**, 6615–6619.
18 M. J. Kim, H. W. Lee, D. Moon and K. S. Jeong, *Org. Lett.*, 2012, **14**, 5042–5045.
19 R. M. Duke, T. McCabe, W. Schmitt and T. Gunnlaugsson, *J. Org. Chem.*, 2012, **77**, 3115–3126.
20 J. Krishnamurthi, T. Ono, S. Amemori, H. Komatsu, S. Shinkai and K. Sada, *Chem. Commun.*, 2011, **47**, 1571–1573.
21 Z. W. Yang, B. A. Wu, X. J. Huang, Y. Y. Liu, S. G. Li, Y. N. Xia, C. D. Jia and X. J. Yang, *Chem. Commun.*, 2011, **47**, 2880–2882.
22 R. Custelcean, P. V. Bonnesen, N. C. Duncan, X. H. Zhang, L. A. Watson, G. Van Berkel, W. B. Parson and B. P. Hay, *J. Am. Chem. Soc.*, 2012, **134**, 8525–8534.
23 P. G. Young, J. K. Clegg, M. Bhadbhade and K. A. Jolliffe, *Chem. Commun.*, 2011, **47**, 463–465.
24 C. D. Jia, B. A. Wu, S. G. Li, X. J. Huang, Q. L. Zhao, Q. S. Li and X. J. Yang, *Angew. Chem., Int. Ed.*, 2011, **50**, 486–490.
25 S. G. Li, C. D. Jia, B. Wu, Q. Luo, X. J. Huang, Z. W. Yang, Q. S. Li and X. J. Yang, *Angew. Chem., Int. Ed.*, 2011, **50**, 5720–5723.
26 S. G. Li, M. Y. Wei, X. J. Huang, X. J. Yang and B. Wu, *Chem. Commun.*, 2012, **48**, 3097–3099.
27 B. Wu, C. D. Jia, X. L. Wang, S. G. Li, X. J. Huang and X. J. Yang, *Org. Lett.*, 2012, **14**, 684–687.
28 A. Rostami, C. J. Wei, G. Guerin and M. S. Taylor, *Angew. Chem., Int. Ed.*, 2011, **50**, 2059–2062.
29 P. Sokkalingam, J. Yoo, H. Hwang, P. H. Lee, Y. M. Jung and C.-H. Lee, *Eur. J. Org. Chem.*, 2011, 2911–2915.
30 P. Sokkalingam, D. S. Kim, H. Hwang, J. L. Sessler and C.-H. Lee, *Chem. Sci.*, 2012, **3**, 1819–1824.
31 S. Fukuzumi, K. Ohkubo, Y. Kawashima, D. S. Kim, J. S. Park, A. Jana, V. M. Lynch, D. Kim and J. L. Sessler, *J. Am. Chem. Soc.*, 2011, **133**, 15938–15941.
32 S. K. Kim, G. I. Vargas-Zúñiga, B. P. Hay, N. J. Young, L. H. Delmau, C. Masselin, C.-H. Lee, J. S. Kim, V. M. Lynch, B. A. Moyer and J. L. Sessler, *J. Am. Chem. Soc.*, 2012, **134**, 1782–1792.
33 H. Maeda, Y. Bando, K. Shimomura, I. Yamada, M. Naito, K. Nobusawa, H. Tsumatori and T. Kawai, *J. Am. Chem. Soc.*, 2011, **133**, 9266–9269.
34 H. Maeda, K. Naritani, Y. Honsho and S. Seki, *J. Am. Chem. Soc.*, 2011, **133**, 8896–8899.
35 H. Maeda and Y. Terashima, *Chem. Commun.*, 2011, **47**, 7620–7622.
36 H. Maeda, K. Kinoshita, K. Naritani and Y. Bando, *Chem. Commun.*, 2011, **47**, 8241–8243.
37 J.-m. Suk, V. R. Naidu, X. Liu, M. S. Lah and K.-S. Jeong, *J. Am. Chem. Soc.*, 2011, **133**, 13938–13941.
38 J.-m. Suk, D. A. Kim and K.-S. Jeong, *Org. Lett.*, 2012, **14**, 5018–5021.
39 J.-i. Kim, H. Juwarker, X. Liu, M. S. Lah and K.-S. Jeong, *Chem. Commun.*, 2010, **46**, 764–766.
40 Q.-Y. Cao, T. Pradhan, S. Kim and J. S. Kim, *Org. Lett.*, 2011, **13**, 4386–4389.
41 P. Das, A. K. Mandal, M. K. Kesharwani, E. Suresh, B. Ganguly and A. Das, *Chem. Commun.*, 2011, **47**, 7398–7400.
42 N. Ahmed, B. Shirinfar, I. Geronimo and K. S. Kim, *Org. Lett.*, 2011, **13**, 5476–5479.
43 K. P. McDonald, Y. Hua, S. Lee and A. H. Flood, *Chem. Commun.*, 2012, **48**, 5065–5075.
44 Y. Hua, R. O. Ramabhadran, J. A. Karty, K. Raghavachari and A. H. Flood, *Chem. Commun.*, 2011, **47**, 5979–5981.
45 Y. Hua, R. O. Ramabhadran, E. O. Uduehi, J. A. Karty, K. Raghavachari and A. H. Flood, *Chem.–Eur. J.*, 2011, **17**, 312–321.
46 K. P. McDonald, R. O. Ramabhadran, S. Lee, K. Raghavachari and A. H. Flood, *Org. Lett.*, 2011, **13**, 6260–6263.
47 A. Caballero, N. G. White and P. D. Beer, *Angew. Chem., Int. Ed.*, 2011, **50**, 1845–1848.
48 A. Caballero, F. Zapata, N. G. White, P. J. Costa, V. Félix and P. D. Beer, *Angew. Chem., Int. Ed.*, 2012, **51**, 1876–1880.
49 M. G. Chudzinski, C. A. McClary and M. S. Taylor, *J. Am. Chem. Soc.*, 2011, **133**, 10559–10567.
50 M. Giese, M. Albrecht, T. Krappitz, M. Peters, V. Gossen, G. Raabe, A. Valkonen and K. Rissanen, *Chem. Commun.*, 2011, **48**, 9983–9985.
51 S. Guha, F. S. Goodson, L. J. Corson and S. Saha, *J. Am. Chem. Soc.*, 2012, **134**, 13679–13691.
52 C. L. D. Gibb and B. C. Gibb, *J. Am. Chem. Soc.*, 2011, **133**, 7344–7347.
53 X. M. He and V. W. W. Yam, *Org. Lett.*, 2011, **13**, 2172–2175.
54 H. C. Gee, C. H. Lee, Y. H. Jeong and W. D. Jang, *Chem. Commun.*, 2011, **47**, 11963–11965.
55 M. A. Tetilla, M. C. Aragoni, M. Arca, C. Caltagirone, C. Bazzicalupi, A. Bencini, A. Garau, F. Isaia, A. Laguna, V. Lippolis and V. Meli, *Chem. Commun.*, 2011, **47**, 3805–3807.
56 M. Mameli, M. C. Aragoni, M. Arca, M. Atzori, A. Bencini, C. Bazzicalupi, A. J. Blake, C. Caltagirone, F. A. Devillanova, A. Garau, M. B. Hursthouse, F. Isaia, V. Lippolis and B. Valtancoli, *Inorg. Chem.*, 2009, **48**, 9236–9249.
57 C. R. K. Glasson, J. K. Clegg, J. C. McMurtrie, G. V. Meehan, L. F. Lindoy, C. A. Motti, B. Moubaraki, K. S. Murray and J. D. Cashion, *Chem. Sci.*, 2011, **2**, 540–543.
58 C. R. K. Glasson, G. V. Meehan, J. K. Clegg, L. F. Lindoy, P. Turner, M. B. Duriska and R. Willis, *Chem. Commun.*, 2008, 1190–1192.
59 R. A. Bilbeisi, J. K. Clegg, N. Elgrishi, X. de Hatten, M. Devillard, B. Breiner, P. Mal and J. R. Nitschke, *J. Am. Chem. Soc.*, 2012, **134**, 5110–5119.
60 Y. R. Hristova, M. M. J. Smulders, J. K. Clegg, B. Breiner and J. R. Nitschke, *Chem. Sci.*, 2011, **2**, 638–641.
61 I. A. Riddell, M. M. J. Smulders, J. K. Clegg, Y. R. Hristova, B. Breiner, J. D. Thoburn and J. R. Nitschke, *Nat. Chem.*, 2012, **4**, 751–756.
62 H.-Y. Gong, B. M. Rambo, E. Karnas, V. M. Lynch, K. M. Keller and J. L. Sessler, *J. Am. Chem. Soc.*, 2011, **133**, 1526–1533.

63 H.-Y. Gong, B. M. Rambo, E. Karnas, V. M. Lynch and J. L. Sessler, *Nat. Chem.*, 2010, **2**, 406–409.
64 A. S. Singh and S.-S. Sun, *Chem. Commun.*, 2011, **47**, 8563–8565.
65 L. M. Hancock, L. C. Gilday, N. L. Kilah, C. J. Serpell and P. D. Beer, *Chem. Commun.*, 2011, **47**, 1725–1727.
66 N. H. Evans, H. Rahman, A. V. Leontiev, N. D. Greenham, G. A. Orlowski, Q. Zeng, R. M. J. Jacobs, C. J. Serpell, N. L. Kilah, J. J. Davis and P. D. Beer, *Chem. Sci.*, 2012, **3**, 1080–1089.
67 A. V. Leontiev, C. J. Serpell, N. G. White and P. D. Beer, *Chem. Sci.*, 2011, **2**, 922–927.
68 M. Chas, G. Gil-Ramírez and P. Ballester, *Org. Lett.*, 2011, **13**, 3402–3405.
69 M. Chas and P. Ballester, *Chem. Sci.*, 2012, **3**, 186–191.
70 V. Valderrey, E. C. Escudero-Adán and P. Ballester, *J. Am. Chem. Soc.*, 2012, **134**, 10733–10736.
71 J.-F. Ayme, J. E. Beves, D. A. Leigh, R. T. McBurney, K. Rissanen and D. Schultz, *Nat. Chem.*, 2012, **4**, 15–20.
72 H. Ito, M. Ikeda, T. Hasegawa, Y. Furusho and E. Yashima, *J. Am. Chem. Soc.*, 2011, **133**, 3419–3432.
73 Y. Bao, B. Liu, H. Wang, J. Tian and R. Bai, *Chem. Commun.*, 2011, **47**, 3957–3959.
74 R. M. Duke and T. Gunnlaugsson, *Tetrahedron Lett.*, 2011, **52**, 1503–1505.
75 P. Singh and M. Kaur, *Chem. Commun.*, 2011, **47**, 9122–9124.
76 H. J. Kim, K. C. Ko, J. H. Lee, J. Y. Lee and J. S. Kim, *Chem. Commun.*, 2011, **47**, 2886–2888.
77 P. Calero, M. Hecht, R. Martinez-Manez, F. Sancenon, J. Soto, J. L. Vivancos and K. Rurack, *Chem. Commun.*, 2011, **47**, 10599–10601.
78 W. Chen, S. A. Elfeky, Y. Nonne, L. Male, K. Ahmed, C. Amiable, P. Axe, S. Yamada, T. D. James, S. D. Bull and J. S. Fossey, *Chem. Commun.*, 2011, **47**, 253–255.
79 I. Richter, J. Minari, P. Axe, J. P. Lowe, T. D. James, K. Sakurai, S. D. Bull and J. S. Fossey, *Chem. Commun.*, 2008, 1082–1084.
80 Z. Zhang and P. R. Schreiner, *Chem. Soc. Rev.*, 2009, **38**, 1187–1198.
81 J. A. Birrell, J.-N. Desrosiers and E. N. Jacobsen, *J. Am. Chem. Soc.*, 2011, **133**, 13872–13875.
82 S. Lin and E. N. Jacobsen, *Nat. Chem.*, 2012, **4**, 817.
83 N. Z. Burns, M. R. Witten and E. N. Jacobsen, *J. Am. Chem. Soc.*, 2011, **133**, 14578–14581.
84 K. Ohmatsu, M. Kiyokawa and T. Ooi, *J. Am. Chem. Soc.*, 2011, **133**, 1307–1309.
85 A. P. Davis, D. N. Sheppard and B. D. Smith, *Chem. Soc. Rev.*, 2007, **36**, 348–357.
86 J. T. Davis, O. Okunola and R. Quesada, *Chem. Soc. Rev.*, 2010, **39**, 3843–3862.
87 S. Matile, A. Vargas Jentzsch, J. Montenegro and A. Fin, *Chem. Soc. Rev.*, 2011, **40**, 2453–2474.
88 G. W. Gokel and N. Barkey, *New J. Chem.*, 2009, **33**, 947–963.
89 P. A. Gale, *Acc. Chem. Res.*, 2011, **44**, 216–226.
90 J. T. Davis, in *Topics in Heterocyclic Chemistry*, ed. P. A. Gale and W. Dehaen, Springer, New York, 2010, vol. 24, pp. 145–176.
91 J. L. Seganish and J. T. Davis, *Chem. Commun.*, 2005, 5781–5783.
92 R. Pérez-Tomás, B. Montaner, E. Llagostera and V. Soto-Cerrato, *Biochem. Pharmacol.*, 2003, **66**, 1447–1452.
93 B. DíazdeGreñu, P. I. Hernández, M. Espona, D. Quiñonero, M. E. Light, T. Torroba, R. Pérez-Tomás and R. Quesada, *Chem.–Eur. J.*, 2011, **17**, 14074–14083.
94 P. I. Hernandez, D. Moreno, A. A. Javier, T. Torroba, R. Perez-Tomas and R. Quesada, *Chem. Commun.*, 2012, **48**, 1556–1558.
95 N. J. Andrews, C. J. E. Haynes, M. E. Light, S. J. Moore, C. C. Tong, J. T. Davis, W. A. Harrell Jr and P. A. Gale, *Chem. Sci.*, 2011, **2**, 256–260.
96 C. J. E. Haynes, S. J. Moore, J. R. Hiscock, I. Marques, P. J. Costa, V. Felix and P. A. Gale, *Chem. Sci.*, 2012, **3**, 1436–1444.
97 P. R. Brotherhood and A. P. Davis, *Chem. Soc. Rev.*, 2010, **39**, 3633–3647.
98 S. Hussain, P. R. Brotherhood, L. W. Judd and A. P. Davis, *J. Am. Chem. Soc.*, 2011, **133**, 1614–1617.
99 Y. R. Choi, M. K. Chae, D. Kim, M. S. Lah and K.-S. Jeong, *Chem. Commun.*, 2012, **48**, 10346–10348.
100 N. Busschaert, M. Wenzel, M. E. Light, P. Iglesias-Hernández, R. Pérez-Tomás and P. A. Gale, *J. Am. Chem. Soc.*, 2011, **133**, 14136–14148.
101 S. J. Moore, M. Wenzel, M. E. Light, R. Morley, S. J. Bradberry, P. Gomez-Iglesias, V. Soto-Cerrato, R. Perez-Tomas and P. A. Gale, *Chem. Sci.*, 2012, **3**, 2501–2509.
102 M. Wenzel, M. E. Light, A. P. Davis and P. A. Gale, *Chem. Commun.*, 2011, **47**, 7641–7643.
103 S. J. Moore, M. G. Fisher, M. Yano, C. C. Tong and P. A. Gale, *Chem. Commun.*, 2011, **47**, 689–691.
104 N. Busschaert, I. L. Kirby, S. Young, S. J. Coles, P. N. Horton, M. E. Light and P. A. Gale, *Angew. Chem., Int. Ed.*, 2012, **51**, 4426–4430.
105 S. Bahmanjah, N. Zhang and J. T. Davis, *Chem. Commun.*, 2012, **48**, 4432–4434.
106 A. V. Jentzsch, D. Emery, J. Mareda, S. K. Nayak, P. Metrangolo, G. Resnati, N. Sakai and S. Matile, *Nat. Commun.*, 2012, **3**, 905.
107 A. Vargas Jentzsch, D. Emery, J. Mareda, P. Metrangolo, G. Resnati and S. Matile, *Angew. Chem., Int. Ed.*, 2011, **50**, 11675–11678.
108 N.-T. Lin, A. Vargas Jentzsch, L. Guenee, J.-M. Neudorfl, S. Aziz, A. Berkessel, E. Orentas, N. Sakai and S. Matile, *Chem. Sci.*, 2012, **3**, 1121–1127.
109 S. Negin, M. M. Daschbach, O. V. Kulikov, N. Rath and G. W. Gokel, *J. Am. Chem. Soc.*, 2011, **133**, 3234–3237.
110 O. V. Kulikov, M. M. Daschbach, C. R. Yamnitz, N. Rath and G. W. Gokel, *Chem. Commun.*, 2009, 7497–7499.
111 C. R. Yamnitz, S. Negin, I. A. Carasel, R. K. Winter and G. W. Gokel, *Chem. Commun.*, 2010, **46**, 2838–2840.
112 J. L. Atkins, M. B. Patel, M. M. Daschbach, J. W. Meisel and G. W. Gokel, *J. Am. Chem. Soc.*, 2012, **134**, 13546–13549.
113 B. Shen, X. Li, F. Wang, X. Yao and D. Yang, *PLoS One*, 2012, **7**, e34694.
114 X. Li, B. Shen, X.-Q. Yao and D. Yang, *J. Am. Chem. Soc.*, 2007, **129**, 7264–7265.